Ordre N° :……

Serial N° :……

People's Democratic Republic of Algeria

Ministry of Higher Education and Scientific Research

University of El Oued

Faculty of Nature Sciences and Life

Department of Cellular and Molecular Biology

Master's Thesis

Submitted in Fulfillment of the Requirements for Degree of an Academic Master (LMD)

Field: Biological Sciences

Specialization: Applied Biochemistry

Nano-Bio Interfaces: Studying Protein on Polymer-Derived Nanoparticles for the Development of Bee Venom-ZnO Nanoparticles Using Collagen as a Novel Nanotherapeutic Strategy for Burn Repair in Rats

Presented by: **BEKAKRA Kheloud** **GUETTOUTA Zeneb**

LEMGHEDEM Hanene **MAMMADI Zakia**

Defended on [14/06/2026], in the presence of the Examination Committee:

Name	Rank	Affiliation	Role
Pr. TOUMI Ikram	Prof	University of El Oued	President
Pr. DEROUICHE Samir	Prof	University of El Oued	Supervisor
Dr. BOULARES Islam	M.A.B	University of El Oued	Co- Supervisor
Dr. ZEGHIB Khaoula	M.C. A	University of El Oued	Examiner

Academic Year: 2025-2026


بسم الله الرحمن الرحيم
١٤٣٨

إهـــــــــداء

قال تعالى: ﴿وَآخِرُ دَعْوَاهُمْ أَنِ الْحَمْدُ لِلَّهِ رَبِّ الْعَالَمِينَ﴾

الحمدُ لله الذي بنعمته تتمّ الصالحات، وبفضله تُدرك الغايات، وبلطفه تُذلّل الصعوبات، وبتوفيقه تتحقق الأمنيات، والصلاة والسلام على سيدنا محمدٍ خير البريات.أحمدُ الله عزّ وجلّ الذي وفّقني لإتمام هذا العمل، وأمدّني بالصبر والثبات في مسيرتي الدراسية وما كان من صواب فمن الله، وما كان من نقص فمن نفسي.

أهدي هذا العمل أولًا إلى أبي الحبيب

إلى من كان لي وطنًا حين ضاقت الأيام، وسندًا حين مالت الحياة، إلى من حمل عني تعب الطريق بصبره ودعواته وحنانه ،أبي مهما كتبتُ من كلمات فلن توفيك حقك، فأنت النعمة التي أحمد الله عليها دائمًا، وهذا النجاح ثمرة تعبك وإيمانك بي.حفظك الله وأطال في عمرك و أدامك سندًا.

إلى أمي الغالية

دفء الروح ونور الحياة، إلى قلبها الذي احتواني ودعواتها التي كانت تفتح لي أبواب الخير، أمي وجودك راحة لا تُوصف اللهم احفضها وارزقها الصحة والعافية

إلى أختي الوحيدة

رفيقة العمر وسندي الدائم، شكرًا لدعمك ونصحك وحضورك في كل مراحل حياتي. حفظكِ الله لي دائمًا.

إلى إخوتي

عزوتي وسندي بعد الله، شكرًا لكل محبة ودعم صادق. وفقكم الله لكل نجاح وسعادة

إلى زوجة أخي الغالية

شكرًا لطيب قلبكِ وجميل حضوركِ، كنتِ إضافة محبة لعائلتنا.

إلى أخي وابني أنس

أمير البيت، شكرًا لروحك الجميلة وقربك الذي يملأ البيت فرحًا حفضك الله وبارك لنا فيك

إلى صغيرَي القلب محمد الطاهر وأشرف

أنتما بهجة البيت ونوره اللهم احفضهم بعينك التي لا تنام واجعلهما قرة عين لأهلهما

إلى رفيقات الدرب حنان زينب وزكية

حنان رفيقة الروح قبل الطريق يا من كنت في ايامي الجميلة والصعبة حضورا يشبه الطمأنينة، زينب روح لطيفة تركت أثرًا جميلًا لا يُنسى صداقتك من الأشياء الثمينة التي رزقني الله بها ، زكية خير صدفة جمعتني بها الأيام كنت الحضور الذي يخفف عني ثِقل الأيام، وجودك كان من نعم الله ،جعلكن الله من سعداء الدنيا والاخرة

إلى أستاذي الفاضل، البروفيسور درويش سمير

شكرًا لعلمك وتوجيهاتك وصبرك، فقد كان لإشرافك أثر كبير في إخراج هذا العمل في صورته العلمية الرصينة وفقك الله وبارك لك في اعمالك

إلى أستاذتي الدكتورة بولعراس إسلام

لم تكوني مجرد داعمة علمية، بل كنتِ سندًا حقيقيًا في كل تفاصيل هذا العمل. بحرصكِ، واهتمامكِ، وصبركِ معنا، وبكلماتكِ التي كانت تبعث فينا الطمأنينة حين يزدحم القلق، كان وجودكِ فارقًا لا يُنسى ،شكرًا لأنكِ كنتِ قريبة منّا علميًا وإنسانيًا، ولكل لحظة دعم وتوجيه وإخلاص بذلتِه معنا ،فجزاكِ الله عني خير الجزاء، وجعل ما قدمتِه في ميزان حسناتكِ

إلى معلمي بالضياف يوسف

من علّمني الحرف وشدّ على يدي لأمسك القلم بثقة، لك مني عظيم الامتنان وجميل الدعاء.

إلى أخوالي، وإلى كل من أحبني بصدق ودعا لي بالخير... أهديكم ثمرة هذا الجهد بكل حب ووفاء.

والحمدُ لله أولًا وآخرًا، ظاهرًا وباطنًا **خلود**

إهـــــــــداء

بسم الله الرحمن الرحيم

الحمد لله الذي بنعمته تتمّ الصالحات، والذي أنار دربي بالعلم ومنحني القوة لأواصل الطريق رغم كلّ الصعوبات

إلى أبي الغالي

إلى سندي الأول ومصدر قوتي، إلى من علّمني أن النجاح يُصنع بالصبر والعمل، وكان دعاؤه الدائم يرافق خطواتي ابي العزيز، أهديك ثمرة جهدي اعترافًا بجميل عطائك الذي لا توفيه الكلمات

إلى عمي العزيز

إلى من كان لي أبًا ثانيًا وسندًا ثابتًا في حياتي، إلى من منحني دعمه واهتمامه دون انتظار مقابل ،لك مني كل الامتنان والتقدير، وأهديك هذا العمل عرفانًا بمكانتك الكبيرة في قلبي

إلى أمي الغالية... وإلى كل من كانت لي أمًا بقلبها وحنانها، إلى من غمرنني بالمحبة والرعاية

وكان دعاؤهن ودفؤهن سندًا لي في مختلف مراحل حياتي، لكُنَّ جميعًا أقدّم أسمى معاني الشكر والامتنان

إلى أخواتي الغاليات واخي

إلى من كنَّ لي سندًا ودفئًا ورفيقات درب في كل تفاصيل حياتي، شاركنني الفرح وخففن عني ثقل الأيام، ومنحنني قوةً أستمد منها الصبر والأمل، لكم في القلب محبة لا تُوصف وامتنان لا يُنسى، أهديكم هذا العمل وفاءً لمكانتكمّ التي لا تُقدَّر بثمن

إلى صديقاتي

للواتي رافقنني في هذا الإنجاز، إلى خلود، الأقرب إلى قلبي ورفيقة روحي التي كانت لي حضورا دافئا حين شعرت بالوحدة وإلى زينب، التي قرّبتنا الأيام فصارت الصداقة بيننا أجمل وإلى زكية، التي كان حضورها لطيفًا ومضيفًا للبهجة والدعم

إلى من كان لدعمه وتشجيعه أثرٌ جميل في مسيرتي

لك مني امتنانٌ صادق، وأهدي هذا العمل تقديرًا لأثرٍ لا يُنسى

إلى أستاذي المؤطر ، البروفيسور سمير درويش

إلى من كان قدوةً ومثالًا يُحتذى به ومصدر إلهامٍ وفخرٍ في مسيرتي العلمية، لك مني خالص التقدير والامتنان على توجيهك ودعمك القيّم

إلى أستاذتي الدكتورة بولعراس إسلام

إلى من شاركتنا الجهد والتعب، وكانت حاضرةً معنا في كل مرحلة بعطائها وتفانيها، تجمع بين روح الدعم العلمي وقرب الصديقة ،لك مني خالص الامتنان والتقدير على حضوركِ المؤثر وعطائكِ الذي ترك أثرًا عميقًا في هذا الإنجاز

أخيرا الى نفسي إلى من تعثرت أكثر من مرة، لكنها في كل مرة اختارت أن تنهض من جديد دون أن تتخلى عن طريقها أهديكِ هذا الإنجاز لأنكِ لم تستسلمي، ولأنكِ واصلتِ السير رغم السقوط والتعب، حتى وصلتِ

حنان

إهـــــــــداء

قال تعالى" وَكانَ فَضلُ اللهِ عَليكَ عَظيمًا" فواللهِ ما وُفِّقت لخيرٍ إلا بفضل الله... وما يُسِّرت لنفع إلا بفضل الله
وما كانتِ النيّةُ طوالَ هذا المسيرِ إلا ابتغاءَ وجهِ الله، فاللهمَّ تقبّل هذا السعي، وبارك ثماره، واجعل فيه الخَيرَ والنفعَ والأجرَ المبارك.

إلى بؤرة النور التي عبرت بي نحو الأمل والأماني الجميلة و اتسع قلبه ليحتوي حلمي حين ضاقت الدنيا فروّض الصعاب من أجلي وسار في حلكة الدرب ليغرس معاني النور والصفاء في قلبي وعلمني معنى أن نعيش من أجل الحق والعلم لنضل أحياء حتى لو فارقت اروحنا أجسادنا، إلى بطلي ، إلى من لم يبخل عليّ يومًا بعطائه ودعمه فوجودك كان القوة التي دفعتني لأواصل الطريق بثبات أبي الغالي ، أنارك الله كما أنرتَ حياتي حبًّا وأمانًا وقد أرضاني الله فيك يا أبتي فهلا رضيت عني ♡

وإلى التي تمتهن الحب وتغزل الأمل في قلبي عصفورا يرفرف فوق ناصية الحلم فتبقى روحي متلألأة ومشرقة .ما وصلتُ إليه اليوم بعد فضل الله إلا بدعواتك أمي ،وصبركِ،وإيمانكِ الدائم بي.أطال الله عمركِ في الخير،وجعلني دائمًا سببًا لفخركِ وسعادتكِ ♡

إلى أخواتي عائشة ,جبارية ,سالمة,وفاء ;إيمان ;أميرة وإتصاروامل إلى إخوتي عبد الله وعبد الرحمن

رفقاء الدرب ووحشة الطرقات شكرا لأنكم جزءا من هذا الإنجاز دعواتي أن يحفظكم الله لي دائمًا ، إخوةً وسندًا وعمرًا جميلًا .

الى كل أولاد وبنات اعمامي وعماتي الدين كانو بمثابة اخوتي

إلى أبناء أختي ساجد و آيات صغار قلبي أهديكم تخرجي اليوم لترونه غدا بفطنة وتفخرون بالحبيبة التي تلي أمكم ♡

إلى أعمامي الغوالي نصر،عمارة،عبد الكريم وبوبكر بارك الله لي فيكم كنتم السند بعد والدي، والقوة التي أشعر معها دائمًا بالأمان. شكرًا لكل موقفٍ صادق أسأل الله أن يحفظكم ويديم عزكم

إلى خالي العزيز . .صالح. .وزوجته إلى من كان له الفضل في أن يفتح لي أبواب التعلم والتطور، ويمنحني فرصة لأتقدم في مجالي بثقة وإصرار.لك مني كل الامتنان والتقدير، فبك بدأت خطواتي الأولى نحو الأفضل.

إلى جدتاي أطال في أعماركن رافقتني دعواتكن حتى الوصول شكرا لكن عزيزتي حفيدتكما

إلى جميع أفراد عائلتي فردا فردا أهديكم تخرجي و دعواتي أن لا يحرمني حبكم والطمأنينة الخالصة بجواركم ♡

إلى زوجات أعمامي اللاتي كنا لي خمس أمهات بعد أمي بارك الله في أعماركن هاهي ابنتكم اليوم تقطف ثمار جهودها.

إلى من خفّفوا ثقل الأيام بوجودهم، وجعلوا للحياة طعمًا أبهى، بنات خالي عبير، عائشة، مرام ، علياء وزمردة و ابنه عمّار

إلى صديقاتي مروى، صبرين، كنزة، إسراء وإكرام .ر. وبثينة .د. شكرا لكل دعم صادق لكل مرة راهنتم فيها على انتصاري شكرا لكل دعوة رافقتموني بها

ألى رفيقات رحلتي في تخصصي حنان وخلود شكرا على تلك الأيام التي لا تنسى إلى كل لحظة تشاركنا فيها الألم والأمل آنسني بكن الله طول العمر

إلى شريكات الرحلة خلود وحنان و زكية كنتم أجمل الرفاق وخير السند طوال المسير وأفضل الأصدقاء دمتن ودام عطاؤكن فلولا فضل الله ثم أنتن لما اختتم هذا الإنجاز

إلى أنيسة روحي إكرام نصفي الثاني وصاحبة المواقف غاليتي وأختي التي لم تلدها أمي أهديك تخرجي الذي تعلمي حذافير مشقته وفرحه

أهدي نجاحي هذا إلى مؤطري وأستاذي الفاضل الدكتور يوسف حمدي ، من حمل في قلبه روح الأب ومنحنا من علمه ونبله ما يضيء الطريق، أنت المثال الأسمى الذي نتعلم منه قبل أن نتعلم منهجًا. شكراً لأنك كنت دائمًا سندًا ومنارة لا تنطفئ .

إلى أستاذتي الفاضلة،العملة النادرة؛ الدكتورة بوطاس اسلام التي كانت عونًا لنا وخففت عنا مشقة الطريق، مؤطرتي وقدوتي وملهمتي، والسند الذي نلجأ إليه بعد الله. لكِ كل الامتنان والتقدير على عطائكِ النبيل وجهودكِ القيّمة.

وإلى كل من أعاننا بعون الله في مشقة الطريق شكرا لكم جميعا وبارك الله في أعماركم ♡

زينب

إهـــــــــداء

بسم الله الرحمن الرحيم

قال الله تعالى: **﴿ وَ مَا تَوْفِيقِي إِلَّا بِاللَّهِ ﴾**

الحمدُ للهِ حبًّا وشكرًا وامتنانًا، على أعوامٍ من السعي والصبر ختمها اللهُ بفرحةِ الإنجاز وتوَّجها بالنجاح

إلى أعظم رجل في الكون، إلى من دعمني بلا حدود ممتنة لأن الله اصطفاك أبا لي

أبي حفظكَ الله

إلى أجمل نعم الله في حياتي، إلى من أضاءت دعواتها دربي ملاكي قوتي وسندي

أمي رعاكِ الله

إلى مصدر الحب ونعمة الأيام الجميلة، ومصدر قوتي ودعمي الدائم في كل وقت أدامكم الله سندا وفرحا يملئ أيامي

إخوتي وأخواتي وزوجة أخي الأعزاء

إلى من لها مكانة خاصة في قلبي إلى التي لم تغب على البال أسال الله أن يتغمَّدها بواسع رحمته

فقيدتي أختي رحِمكِ الله

إلى من تطيبُ الحياة بقربهم، وكانوا جزءًا من كلِّ لحظةٍ جميلةٍ في حياتي

أفراد عائلتي الكبيرة

إلى من شاركنني التعب خطوة خطوة رفيقاتي في هذا الطريق، كنتنَّ مثالا للإخلاص والتعاون وبكنَّ كان الطريق أخف وأجمل

خلود زينب و حنان

إلى من كان لنا قدوةً مشرقة في مسيرتنا العلمية، وجعل من العلم رسالةً ومن الأخلاق عنوانًا لها أستاذي ومؤطِّري بارك الله لك في أعمالك وزادك من واسع علمه

البروفيسور درويش سمير

إلى أستاذتي ومؤطِّرتي الدكتورة الجميلة، التي كانت سندًا ودعمًا في كل خطوة من هذه الرحلة، سيبقى فضلكِ محفورًا في ذاكرتنا، وستبقى كلماتكِ وتشجيعاتكِ من أجمل ما رافق مسيرتنا العلمية. جزاكِ الله عنا خير الجزاء، وبارك لكِ في علمكِ وعملكِ

الدكتورة بولعراس إسلام

إليكم أهدي ثمرة جهدي.... بحث تخرّجي هذا، راجيةً من الله أن يجعل فيه ثمرةَ تعبٍ وخيرًا ونفعًا، وأن يطيل أعماركم ويديمكم سندًا وفخرًا لي

زكيّة

Acknowledgement

At the outset of this work, we would like to express our deepest gratitude to Almighty Allah for His infinite blessings and for granting us the patience, perseverance, and strength necessary to accomplish this dissertation. Without His grace and guidance, this work would not have been possible.

We would like to extend our sincere appreciation and profound respect to our supervisor, Professor Derouiche Samir, for his invaluable guidance, insightful advice, and continuous support throughout the course of this research. His patience, encouragement, and scientific expertise played a fundamental role in the successful completion of this study.

We are equally indebted to Dr. Boularras Islam, whose constant support, academic guidance, and exemplary professionalism greatly contributed to our research journey. Her dedication and encouragement have been a true source of inspiration.

We also wish to express our sincere gratitude to the distinguished members of the examination committee for accepting to evaluate this dissertation and for their constructive comments and valuable suggestions, which significantly enhanced the quality of this work.

Our special thanks are addressed to the laboratories of El Wifak Clinic, Dr. Khelifi Ammar, the hospital department at the university pole, and the laboratory technician Mr. Ben Khalifa Aymen for their generous collaboration and for providing the necessary facilities and favorable conditions to carry out the experimental part of this research.

We would also like to acknowledge the Faculty of Natural and Life Sciences at University of Martyr Hamma Lakhdar El Oued, as well as Mrs Goubi Sanaa, laboratory engineer Mrs. Chrit Mouna, and engineer Mr. Khennoufa Omar, for the scientific environment, technical assistance, and facilities they provided, which greatly facilitated the completion of this work under optimal conditions.

Furthermore, we extend our appreciation to all members of the university community and to everyone who offered us support, encouragement, and assistance throughout this academic journey, especially the administration of the Faculty of Exact Sciences.

Finally, we express our deepest love and gratitude to our families and friends, whose unwavering support, prayers, and encouragement accompanied us throughout every stage of this journey and motivated us to achieve this accomplishment.

To all those who contributed, directly or indirectly, to the realization of this work, we extend our heartfelt thanks and sincere appreciation.

Abstract

This study aimed to biosynthesize a nanotherapeutic product for enhancing experimental wound healing in rats. Zinc oxide nanoparticles (ZnO NPs) were synthesized using natural collagen as a reducing and stabilizing agent and further bio-conjugated with bee venom to produce a nanomaterial with potential therapeutic applications. Using standard analytical methods and protocols, Collagen extracted from chicken feet exhibited characteristic UV–Visible absorption peaks between 210–280 nm and typical FTIR amide bands confirming its purity and protein structure. ZnO NPs-BV were successfully synthesized and characterized using UV–Visible spectroscopy, FTIR, scanning electron microscopy (SEM), energy-dispersive X-ray (EDX) analysis, and X-ray diffraction (XRD). The rate of immobilized proteins was also quantified, and their biological activities were assessed, including antioxidant, anti-inflammatory, antibacterial, and ultraviolet (UV) protective effects. For the *in vivo* evaluation, 20 female Wistar albino rats were divided into four equal groups (n = 5): a healthy control group, an untreated burn group, and two treatment groups topically treated with 1% ZnO NPs-BV cream and 1% silver sulfadiazine cream, respectively. Cutaneous burns were induced under chloroform anesthesia using a 1.2 cm diameter electric soldering iron applied for 3 seconds. Treatments were applied every other day for three weeks, and wound healing was monitored macroscopically alongside the assessment of hematological, biochemical, and oxidative stress parameters, as well as histological examination of skin and spleen tissues. The results showed the formation of nanoparticles with a characteristic hexagonal crystalline structure and an average size of 33.4 nm, with effective immobilization of bee venom proteins. Results of *in vitro* biological evaluation demonstrated that ZnO NPs-BV possessed notable anti-inflammatory activity in both protein denaturation and RBC membrane stabilization assays. Antioxidant assays (DPPH and FRAP) indicated an important free radical scavenging and reducing power. Additionally, ZnO NPs-BV exhibited notable photoprotective activity, with performance comparable to that of the commercial sunscreen formulation. Antibacterial testing revealed concentration-dependent activity, with the strongest inhibition observed against *Pseudomonas aeruginosa*, and *Staphylococcus aureus*. For *in vivo* results, the experimental wounds applied to rats resulted in skin and spleen tissue abnormalities, abnormalities in hematological and biochemical parameters, as well as a disturbance in the oxidative stress balance.The group treated with ZnO NPs-BV demonstrated a marked acceleration in burn wound healing compared to the untreated group, evidenced by improved wound contraction and restoration of skin tissue architecture, along with reduced inflammatory markers and improved

serum iron, albumin levels, and oxidative stress balance. Histological analysis further confirmed a clear improvement in the structural organization of both skin and spleen tissues. In conclusion, these findings suggest that ZnO NPs-BV exhibits a promising and safe therapeutic effect by reducing oxidative stress, enhancing tissue repair, accelerating burn wound healing, and restoring tissue function

Keywords: ZnO NPs-BV, Burns, Collagen, Bee venom, Oxidative stress, Wound healing.

الملخص

هدفت هذه الدراسة إلى التخليق الحيوي لمنتج علاجي نانوي بهدف تعزيز التئام الجروح التجريبية لدى الجرذان. تم تحضير جسيمات أكسيد الزنك النانوية (ZnO NPs) باستخدام الكولاجين الطبيعي كعامل مختزل ومثبت، ثم تم اقترانها حيويًا بسمّ النحل لإنتاج مادة نانوية ذات تطبيقات علاجية محتملة. وباستخدام الطرق والبروتوكولات التحليلية القياسية، أظهر الكولاجين المستخلص من أرجل الدجاج قمم امتصاص مميزة في مطيافية الأشعة فوق البنفسجية–المرئية (UV–Visible) ضمن المجال 210–280 نانومتر، بالإضافة إلى حزم الأميد المميزة في تحليل الأشعة تحت الحمراء بتحويل فورييه(FTIR) ، مما أكد نقاوته وبنيته البروتينية. وقد تم بنجاح تخليق وتوصيف جسيمات أكسيد الزنك النانوية المحملة بسمّ النحل (ZnO NPs–BV) باستخدام مطيافيةUV–Visible ، وFTIR، والمجهر الإلكتروني الماسح(SEM) ، وتحليل الأشعة السينية المشتتة للطاقة(EDX) ، وحيود الأشعة السينية .(XRD) كما تم تحديد نسبة البروتينات المثبتة على الجسيمات النانوية، وتقييم أنشطتها البيولوجية المختلفة، بما في ذلك النشاط المضاد للأكسدة، والمضاد للالتهاب، والمضاد للبكتيريا، والواقي من الأشعة فوق البنفسجية. أما بالنسبة للتقييم داخل الجسم الحي، فقد تم تقسيم 20 جرذة ألبينو ويستار أنثى إلى أربع مجموعات متساوية (5 حيوانات في كل مجموعة): مجموعة شاهدة سليمة، ومجموعة حروق غير معالجة، ومجموعتا علاج تم فيهما التطبيق الموضعي لكريم يحتوي على 1% من ZnO NPs-BV وكريم سلفاديازين الفضة بتركيز 1% على التوالي. وقد أُحدثت الحروق الجلدية تحت تخدير الكلوروفورم باستخدام مكواة لحام كهربائية بقطر 1.2 سم طُبقت على الجلد لمدة 3 ثوانٍ. وتم تطبيق العلاجات يومًا بعد يوم لمدة ثلاثة أسابيع، مع متابعة التئام الجروح ظاهريًا، إلى جانب تقييم المؤشرات الدموية والكيميائية الحيوية ومؤشرات الإجهاد التأكسدي، بالإضافة إلى الفحص النسيجي لأنسجة الجلد والطحال.أظهرت النتائج تكوّن جسيمات نانوية ذات بنية بلورية سداسية مميزة ومتوسط حجم بلغ 33.4 نانومتر، مع تثبيت فعّال لبروتينات سمّ النحل على سطحها.وأظهرت نتائج التقييم البيولوجي خارج الجسم الحي أن جسيمات ZnO NPs–BV تمتلك نشاطًا ملحوظًا مضادًا للالتهاب في كل من اختبار تمسخ البروتين واختبار تثبيت غشاء كريات الدم الحمراء. كما بينت اختبارات النشاط المضاد للأكسدة (DPPH) و(FRAP) قدرة مهمة على اصطياد الجذور الحرة والاختزال. بالإضافة إلى ذلك، أظهرت جسيمات ZnO NPs–BV نشاطًا وقائيًا ضوئيًا ملحوظ مع اداء مماثل لاداء تركيبة واقي الشمس التجاري. كما كشف اختبار النشاط المضاد للبكتيريا عن فعالية تعتمد على التركيز، حيث سُجل أقوى تثبيط ضد بكتيريا الزائفة الزنجارية (*Pseudomonas aeruginosa*) والمكورات العنقودية الذهبية(*Staphylococcus aureus*) أما نتائج الدراسة داخل الجسم الحي، فقد أظهرت أن الحروق التجريبية المطبقة على الجرذان تسببت في حدوث اضطرابات في أنسجة الجلد والطحال، واختلالات في المؤشرات الدموية والكيميائية الحيوية، إضافة إلى اضطراب في توازن الإجهاد التأكسدي.وقد أظهرت المجموعة المعالجة

بـ ZnO NPs-BV تسارعًا ملحوظًا في التئام الحروق مقارنة بالمجموعة غير المعالجة، تجلى في تحسن انكماش الجروح واستعادة البنية النسيجية الطبيعية للجلد، مع انخفاض المؤشرات الالتهابية وتحسن مستويات الحديد والألبومين في المصل واستعادة التوازن التأكسدي. كما أكد التحليل النسيجي حدوث تحسن واضح في التنظيم البنيوي لكل من أنسجة الجلد والطحال. وفي الختام، تشير هذه النتائج إلى أن جسيمات أكسيد الزنك النانوية المحملة بسمّ النحل (ZnO NPs-BV) تمتلك تأثيرًا علاجيًا واعدًا وآمنًا، من خلال تقليل الإجهاد التأكسدي، وتعزيز إصلاح الأنسجة، وتسريع التئام الحروق، واستعادة الوظائف النسيجية.

الكلمات المفتاحية: جسيمات أكسيد الزنك النانوية المحملة بسمّ النحل (ZnO NPs-BV)، الحروق، الكولاجين، سمّ النحل، الإجهاد التأكسدي، التئام الجروح.

ABBREVIATIONS LIST

[$K_3Fe(CN)_6$]: Potassium ferricyanide

ABTS: ABTS radical scavenging assay

ACD: Allergic contact dermatitis

BSA: Bovine serum albumin

BV: Bee venom

COX: Cyclooxygenase

DLS: Dynamic light scattering

DMSO: Dimethyl sulfoxide

DNA: Deoxyribonucleic acid

DPPH: 1,1-diphenyl-2-picrylhydrazyl

DTNB: Dithio-bis-2-nitrobenzoic acid

EDS: Energy dispersive X-ray spectroscopy

EDTA: Ethylenediaminetetraacetic acid

EDX: Energy dispersive X-ray

$FeCl_3$: Ferric chloride

FESEM: Field emission scanning electron microscopy

FRAP: ferric reducing antioxidant power

FTIR: Fourier transform infrared spectroscopy

Gly: Glycemia

GPx: Glutathione peroxidase

GSH: Reduced Glutathione

GSSG: Glutathione disulfide

H_2O_2: Hydrogen peroxide

H_3PO_4: Orthophosphoric acid

H_3PO_4: Phosphoric acid

HCl: Hydrochloric acid

HCT: Hematocrit

HRTEM: High-resolution transmission electron microscopy

IC_{50} : Half maximal inhibitory concentration

IL-1 : Interleukin-1

IL-6 : Interleukin-6

IL-10: Interleukin-10

JCPDS: Joint committee on powder diffraction

MAPKs: Mitogen-activated protein kinases

MB: Methylene blue

MCD: Mast cell degranulation

MDA: Malondialdehyde TBA

MDR: Multi-drug resistant

NaCl: Sodium chloride

NaOH: Sodium hydroxide

NBT: Nitro blue tetrazolium

NF-κB: Nuclear factor kappa B

NH_2: Amino group

NPs: Nanoparticles

PBS: Phosphate Buffered Saline

PLA_2: Phospholipase A_2

PLB: Phospholipase B

PLT: Platelets

RBCs: Red blood cells

ROS: Reactive oxygen species

Rpm: Revolutions per minute

SEM: Scanning electron microscope

SOD: Superoxide dismutase

SPF: Sun Protection Factor

TAC: total antioxidant capacity

TBARS: Thiobarbituric acid reactive substances

TBS: Tris-buffered saline

TCA: Trichloroacetic acid

TG/DTA: Thermogravimetric analysis / differential thermal analysis

TGF-β: Transforming growth factor beta

TLRs: Toll-like receptors

TLR 2: Toll-like receptor 2

TLR 4: Toll-like receptor 4

TNB: 2-nitro-5-mercocapturic acid

TNF-α: Tumor necrosis factor alpha

UV-VIS: Ultraviolet-visible spectroscopy

VEGF: Vascular Endothelial Growth Factor

WBCs: White blood cells

XPS:X-ray photoelectron spectroscopy

XRD: X-ray diffraction

ZnO NPs : Zinc oxide nanoparticles

HLA-DR: Human leukocyte antigen – DR isotype

($O2^{\bullet -}$): Superoxide anion radical

COX-2: Cyclooxygenase-2

IGF-1: Insulin-like growth factor 1

GATA-1: GATA binding protein 1

LDL: Low-density lipoprotein

RDW: Red cell distribution width

MCV: Mean corpuscular volume

MCH: Mean corpuscular hemoglobin

MCHC: Mean corpuscular hemoglobin concentration

FIGURES LIST

TABLES LIST

SUMMARY

Introduction

Introduction

Burn injuries are considered one of the leading causes of trauma and continue to represent a serious public health issue due to their high global incidence and mortality rates. According to the World Health Organization, burns are responsible for approximately 180,000 deaths annually (Afetor et al., 2024). They result from the exposure of the skin to various thermal sources, with the type and severity of injury varying accordingly (Warby & Maani, 2023). Burns are among the most common and painful injuries and, in severe cases, may lead to permanent disability or even death (Bhatia et al., 2016).

The primary management of burns involves several therapeutic interventions, including cooling of the affected area, fluid resuscitation, and support of vital functions such as respiration and ventilation, in addition to surgical intervention when required (Żwierełło et al., 2023). Silver sulfadiazine is widely used in the treatment of burn wounds because of its antimicrobial efficacy (Bhatia et al., 2016), while opioids are commonly administered for pain relief associated with these injuries. However, prolonged use of these treatments may be associated with several adverse effects (Markiewicz-Gospodarek et al., 2022). Cases of resistance to silver sulfadiazine, as well as nephrotoxicity and leukopenia, have been reported, which limits its long-term application on extensive wounds (Bhatia et al., 2016). Furthermore, repeated opioid use may contribute to the development of hyperalgesia, thereby emphasizing the need for safer and more effective therapeutic alternatives (Markiewicz-Gospodarek et al., 2022).

Bees are considered insects of significant commercial and medical importance, and they have existed since the Cretaceous period of the Mesozoic era (Sadek et al., 2024). Various bee products, including honey and bee venom, have been used for thousands of years, with their therapeutic properties being mentioned in several religious texts, including the Holy Quran (Wehbe et al., 2019). Bee venom, also known as apitoxin, has gained considerable attention in the medical field due to its diverse biological properties, as it exhibits anti-inflammatory, antioxidant, antifungal, antiviral, and antimicrobial effects. These combined properties contribute to enhancing and accelerating the wound healing process (Kurek-Górecka et al., 2020).

Nanotechnology is considered one of the fastest-developing technologies worldwide and is often described as the industrial revolution of the twenty-first century. Numerous research, development, and manufacturing processes have been adopted globally to produce safer and more efficient nanomaterials for various applications, and consequently, the terms nanotechnology,

nanoscience, and nanomaterials have become widely used not only in scientific research but also in everyday life (Khan et al., 2025). In this context, zinc oxide nanoparticles (ZnO NPs) are regarded as promising inorganic compounds that have attracted considerable attention in recent years due to their many advantages, including low production cost, ease of synthesis, high biocompatibility, and low toxicity, making them suitable for numerous scientific and medical applications (Karam & Abdulrahman, 2022; El-Khawaga, 2025). Furthermore, green synthesis or eco-friendly production of these nanoparticles has gained increasing interest as an alternative to conventional chemical and physical methods while maintaining nanoparticle quality and functional properties (Imath et al., 2025), as this approach relies on biological synthesis using bioactive molecules, particularly proteins, along with other plant-derived compounds extracted from plants or microorganisms that effectively contribute to the reduction and stabilization of nanoparticles (Hameed et al., 2023).

This work aims to biosynthesize a nanotherapeutic product based on zinc nanoparticles loaded with bee venom, and to evaluate its effectiveness in accelerating burn healing and improving skin tissue regeneration, by studying its physical and chemical properties and its biological efficacy against bacteria, inflammation and oxidative stress for enhancing experimental wound healing in rats. In order to achieve this objective, this work was divided into two main parts:

***In vitro* part:** involves the extraction of collagen from chicken feet and its use as a green reducing agent for the synthesis of zinc nanoparticles associated with bee venom. It also includes the physicochemical quantitative and qualitative characterization of the obtained nanocomposite, as well as the evaluation of its biological activity.

***In Vivo* part:** it was dedicated to studying the therapeutic efficacy of bee venom-loaded zinc oxide nanoparticles (ZnO NPs-BV) in accelerating the healing of experimental burns, through the evaluation of their effects on hematological and biochemical parameters as well as histological changes, and by comparing them with conventionally treated and untreated groups in laboratory rats.

First part

Bibliographic Synthesis

Chapter I

Skin

I. Skin and Importance

The skin forms a natural barrier that protects the body from external factors, encompassing physical, chemical, and microbial components, in addition to important immune functions **(Chen et al., 2025)**. The skin is composed of multiple layers **(Brito et al.,2024)**, each with specific roles; these layers not only provide protection but also contribute to the regulation of body temperature, enable the sensation of touch, heat, and pain, and maintain internal homeostasis. Together, these layers work to ensure the body's safety and the continuity of its vital functions **(Mirzayev, 2025)**.

II. Skin Structure

II.1. Epidermis

The epidermis, the outermost layer of the skin, provides a waterproof barrier and plays a key role in determining skin tone. **(Lopez-Ojeda et al., 2022)**. It is an avascular layer composed primarily of keratinocytes, along with other specialized cells including pigmented cells, immune cells such as Langerhans cells, and sensory cells like Merkel cells. In thin skin, the epidermis is organized into four layers: the stratum basale, stratum spinosum, stratum granulosum, and stratum corneum. In contrast, thick skin consists of five layers, including all the previously mentioned layers plus the stratum lucidum, which is located between the stratum granulosum and the stratum corneum **(Lotfollahi, 2024)**.

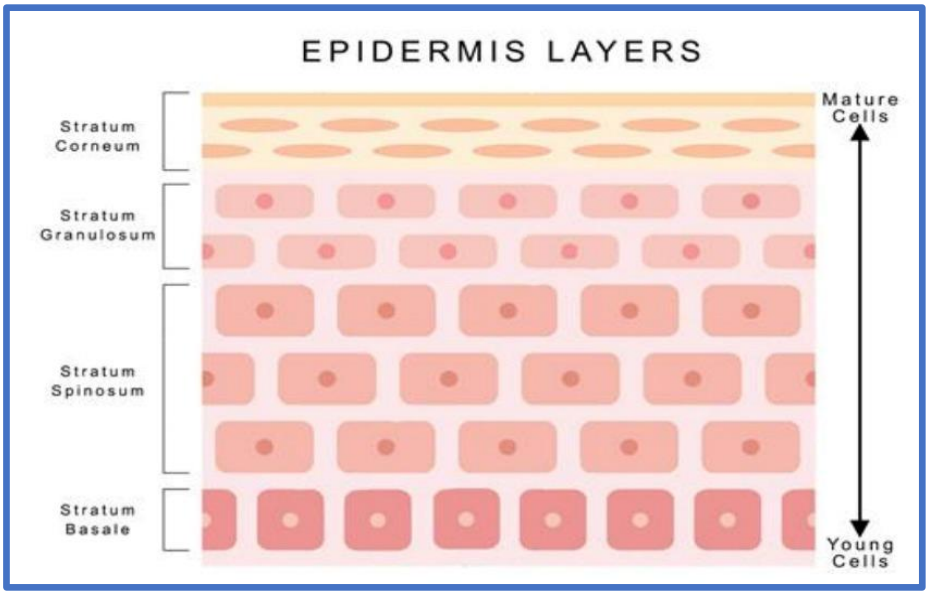

Figure 01: Details of epidermis layers' structure **(Kasolang et al., 2020)**

II.2. Dermis

Beneath the epidermis lies the dermis, a thicker layer that plays a crucial role in both the structure and function of the skin **(Zhang et al., 2024)**. It contains blood vessels and nerves that nourish and support the epidermis, as well as an abundant extracellular matrix (ECM) produced by fibroblasts. The dermis also houses various cell types and complex structures, including vasculature, nerves, and sweat glands **(Hosseini et al., 2022; Weng et al., 2020)**. Structurally, it is divided into two main regions: a superficial papillary layer composed of loose connective tissue rich in blood vessels and fibroblasts that contribute to wound healing, and a deeper reticular layer made up of dense connective tissue that provides tensile strength and elasticity to the skin due to the presence of collagen and elastin fibers **(Lotfollahi, 2024; Bonham et al., 2020)**.

II.3. Hypodermis (Subcutaneous Layer)

The hypodermis is located beneath the dermis and connects the skin to muscles and bones. which is also known as the hypodermis or superficial fascia. **(Moghaddam et al., 2023)**. It mainly consists of adipose tissue that provides cushioning and insulation, in addition to loose connective tissue rich in blood vessels **(Lotfollahi, 2024)**. It plays a major role in skin mobility and flexibility however, some of its functions decline with aging **(Lopez-Ojeda et al., 2022)**.

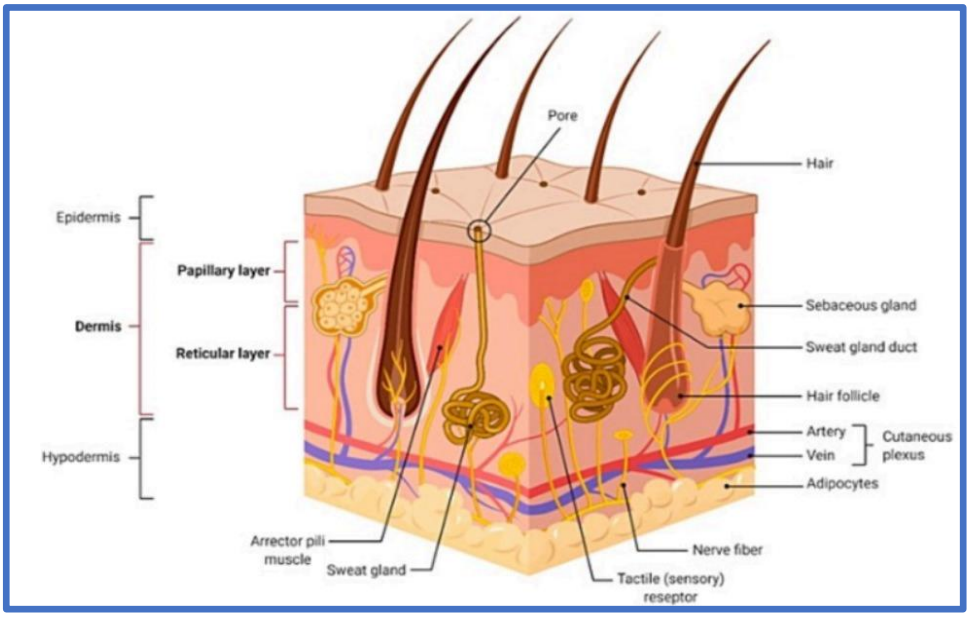

Figure 02: the three main layers of human skin: epidermis, dermis, and hypodermis **(Moghaddam et al., 2023)**

III. Skin Functions

III.1. Temperature Regulation

The skin plays a vital role in maintaining body temperature through multiple mechanisms including insulation, control of heat loss through radiation, convection, and conduction, vasoregulation where vasodilation promotes heat loss and vasoconstriction preserves body heat, evaporation, and piloerection which assists in insulation **(Gerasymchuk et al., 2023)**. Temperature regulation occurs through the modulation of blood flow to near surface regions of the skin and through the release of sweat **(Madhvapathy et al., 2022**). The skin helps regulate body temperature by sweating to cool the body down when it overheats and by shivering creating "goose bumps" when it is cold, with shivering closing the pores and tiny hairs standing on end to trap warm air **(Drahansky et al., 2012)**.

III.2. Immune Surveillance and Defense

The skin carries out vital cutaneous immune surveillance, involving the synthesis and release of pro-and anti-inflammatory mediators, including cytokines, chemokines, and trophic factors, as well as the antimicrobial activity of sebum **(Gerasymchuk et al., 2023)**. The skin provides immunological functions offering resistance to microorganisms and noxious external agents **(Madhvapathy et al., 2022**). Additionally, the skin participates in defense mechanisms against infections and pathogenic phenomena **(Rostkowska et al., 2023)**.

III.3. Metabolic Function

The skin participates in metabolic processes by producing vitamin D when exposed to ultraviolet radiation **(Madhvapathy et al., 2022)**, and it also participates in some hormonal and metabolic functions **(Gerasymchuk et al., 2023)**. that are essential for maintaining overall body health **(Chen et al., 2025)**.

III.4. Sensory Function

The skin contains specialized nerve receptors that allow the body to sense touch, pressure, vibration, pain, and temperature (heat or cold). These receptors help humans detect environmental hazards and protect themselves from injuries or harmful conditions **(Baker et al., 2023)**.

III.5. Wound Healing and Tissue Regeneration

The skin is characterized by its continuous ability to regenerate epidermal cells and promote wound healing, and to restore the skin barrier after injuries, thus maintaining tissue integrity and the continuity of vital skin functions **(Chen et al., 2025) (Gerasymchuk et al., 2023)**.

III.6. Secretion and Excretion

The skin contributes to the elimination of water, salts, and some waste products through perspiration. Sebaceous glands secrete sebum, which keeps the skin smooth and prevents dryness, thus enhancing skin protection and maintaining its health **(Baker et al., 2023)**.

III.7. Absorption and Transport Functions

The skin facilitates absorption of gases and medications through transcellular diffusion and performs absorption (resorption) activities **(Madhvapathy et al., 2022) (Rostkowska et al., 2023)**. It also facilitates the transport of respiratory gases and nutrients between skin layers and to and from the skin surface **(Gerasymchuk et al., 2023)**.

III.8. Physical and Chemical Protection

The skin is the first line of defense against harmful stimuli such as physical and chemical trauma, microorganisms, radiation, and oxidative stress **(McKnight et al., 2022).** The stratum corneum provides mechanical strength, reduces the effects of ultraviolet radiation, contributes to regulating skin hydration, and, along with lipids, forms a barrier that prevents water loss and the entry of irritants **(Baker et al., 2023).**

IV. Skin Diseases

Skin diseases represent a major global public health concern, affecting nearly one-third of the world's population **(Flohr & Hay, 2021)**.

IV.1. Infectious Skin Diseases

❖ Impetigo

Impetigo is a highly contagious, superficial bacterial infection of the epidermis that primarily affects children, although individuals of any age may be affected. It typically manifests as erythematous lesions covered with characteristic yellowish crusts, often accompanied by itching and sometimes pain **(Colebrook & Pradhan., 2025; Hartman-Adams et al., 2014)**.

❖ **Ringworm**

Tinea, commonly known as ringworm, refers to a group of superficial fungal infections caused by dermatophytes, including Epidermophyton, Microsporum, and Trichophyton. These fungi infect keratinized tissues such as the skin, hair, and nails. The classification of tinea infections depends on the affected body site, such as tinea pedis (feet), tinea corporis (body), tinea capitis (scalp), and tinea cruris (groin) **(Rathi et al., 2025; Mosam et al., 2023)**.

❖ **Herpes Simplex**

Herpes simplex virus (HSV) is a common human pathogen comprising two types: HSV-1 and HSV-2 **(Tayyar& Ho, 2023)**. It is responsible for recurrent infections, including oral and genital herpes. HSV-1 is mainly associated with oral and ocular lesions, whereas HSV-2 is more frequently linked to genital infections **(Mancini et al., 2025)**.

IV.2. Inflammatory and Autoimmune Diseases

❖ **Allergic Contact Dermatitis**

Allergic contact dermatitis (ACD) is a significant dermatological condition characterized as a type IV hypersensitivity reaction **(Tramontana et al., 2023)**. It develops through two main stages: sensitization and elicitation, contributing to its considerable public health impact **(Aristizabal-Torres, 2025)**.

❖ **Atopic Dermatitis**

Atopic dermatitis is a chronic, relapsing inflammatory skin disorder associated with impaired epidermal barrier function, leading to the development of eczematous lesions **(Talamonti et al., 2021)**.

❖ **Psoriasis**

Psoriasis is a chronic immune-mediated autoimmune disease characterized by erythematous plaques covered with silvery scales, commonly affecting extensor surfaces. It affects approximately 2–3% of the global population **(Christensen et al., 2023; Lada et al., 2022)**.

IV.3. Skin Disorders Related to Sebaceous Glands

- **Rosacea**

Rosacea is a chronic inflammatory skin condition with a multifactorial etiology, involving dysregulation of innate immunity, neurovascular alterations, oxidative stress, and microbiome imbalance **(Andrusiewicz, 2025)**.

- **Acne**

Acne vulgaris is a common chronic inflammatory disorder of the pilosebaceous unit, characterized by lesions such as comedones, papules, and pustules **(Layton et al., 2025)**.

IV.4. Chronic or Serious Skin Diseases

- **Skin Cancer**

Skin cancer encompasses a heterogeneous group of malignancies and is among the most prevalent cancers worldwide. It is broadly categorized into melanoma and non-melanoma types **(Apalla et al., 2017**). Melanoma arises from abnormal proliferation of melanocytes, whereas non-melanoma skin cancers, including basal cell carcinoma and squamous cell carcinoma, originate from epidermal keratinocytes **(Roky et al., 2025)**.

- **Vitiligo**

Vitiligo is a common depigmenting disorder caused by the progressive loss of melanocytes, affecting the skin, hair, and mucous membranes **(Ismail et al., 2025)**. Clinically, it presents as well-defined depigmented patches and may be associated with whitening of hair **(Joge et al., 2022)**.

V. Skin Injury

V.1. Wounds and Abrasions

Wounds and abrasions are forms of skin damage that compromise its structural integrity. Wounds involve disruption of the skin and may extend to deeper tissues, leading to impairment of the protective barrier **(Nagle et al., 2023)**. In contrast, abrasions are superficial injuries limited to the epidermis and do not penetrate deeper layers, making them generally less severe **(Wu., 2017)**.

V.2. Ulcer

An ulcer is characterized by a significant and deep loss of skin or mucosal tissue, typically resulting from chronic or continuous damage. It is commonly associated with inflammation and delayed tissue repair **(Senthelal et al., 2024)**.

V.3. Burns

Burns are injuries that damage the skin barrier, particularly the epidermal layer, leading to disruption of its protective function **(Shpichka et al., 2019)**. This damage can impair both local and systemic immune responses, thereby increasing susceptibility to microbial invasion and infection **(Roy et al., 2024)**.

VI. Causes of Burns

VI.1. Thermal Injuries

Thermal burns occur when the skin comes into contact with heat sources such as hot liquids, flames, heated objects, or friction **(Sood et al., 2020**). This exposure leads to cellular and tissue damage, which triggers localized inflammation and significant pain **(Zwierełło et al., 2023)**.

VI.2. Chemical burns

Chemical burns result from exposure to harmful substances, including household cleaning products, acids, and alkaline materials chemical burns these agents can penetrate the skin and cause severe tissue destruction, even when the exposed area appears limited **(Pelizzo et al., 2025)**.

VI.3. Electrical Injuries

Electrical injuries are complex and potentially severe forms of trauma caused by contact with low- or high-voltage electrical currents **(Bernal et al., 2018).** The extent of damage is influenced by factors such as current type, duration of exposure, and tissue resistance, and these injuries may lead to deep burns, extensive tissue damage, and systemic complications **(Zemaitis et al., 2025).**

VI.4. Radiation Burns

Radiation burns arise from exposure to different types of radiation, including alpha, beta, and gamma rays **(Karmaker et al., 2021)**. Alpha particles do not penetrate the skin but can be

hazardous if inhaled or ingested. Beta particles typically cause superficial skin damage, whereas gamma rays penetrate deeply into tissues and may affect critical organs such as the lungs and bone marrow. These burns can also result in acute radiation syndrome and other systemic effects **(Alshammari et al., 2024).**

VII .Burns Degrees

VII.1. Superficial Burns

Superficial (first-degree) burns are limited to the epidermis, the outermost layer of the skin **(Singh et al., 2018)**. They typically present with a pink to red appearance, are dry, lack blister formation, and are associated with mild to moderate pain. Healing generally occurs within 5 to 10 days without leaving scars **(Warby & Maani, 2023)**.

VII.2. Second-Degree Burns

Second-degree burns extend into the dermis and are characterized by blister formation, increased pain, and a higher risk of scarring **(Abazari et al., 2022)**. Management of these burns requires more advanced care, including proper wound cleansing, frequent dressing changes, and the use of topical agents to enhance healing and reduce the risk of infection **(Manzoor et al., 2024)**.

VII.3. Third-Degree Burns (Full-Thickness Burns)

Third-degree burns involve complete destruction of the dermal layer. Due to damage to nerve endings, these burns are often painless despite their severity **(Dhupa, 2020)**. They typically require surgical intervention, except in cases where the affected area is very small **(Azam et al., 2024)**.

VII.4. Fourth-Degree Burns

Fourth-degree burns extend beyond the skin into deeper tissues, including muscles and bones **(Katt & Coyle, 2021)**. These severe injuries are often associated with localized necrosis and represent the most critical form of burn damage **(Markiewicz-Gospodarek et al., 2022)**.

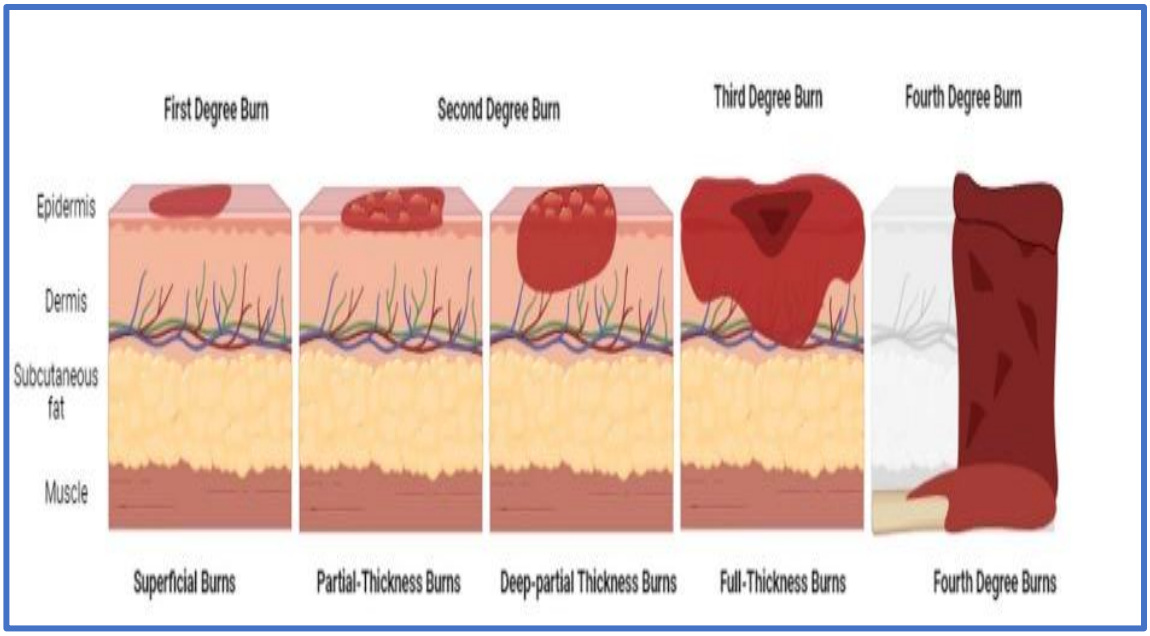

Figure 03: Classification of burn wounds on the basis of severity of damage to the skin **(Manzoor et al., 2024)**

VIII. Molecular and Microbial Complications of Burns

VIII.1. Role of Oxidative Stress in Burn Exacerbation

Oxidative stress plays a central role in the pathophysiology of burn injuries. Following a burn, shock can lead to tissue ischemia, which reduces blood flow and oxygen delivery to the affected areas. This imbalance between reactive oxygen species (ROS) and the body's antioxidant defenses results in the overproduction of free radicals, causing cellular and tissue damage. Consequently, oxidative stress worsens the post-burn condition by increasing tissue susceptibility to injury and impairing the natural healing process **(Markiewicz-Gospodarek, 2022; Chen et al., 2025)**.

VIII.2. Role of Bacteria in Burn Exacerbation

Thermal injuries compromise the skin's barrier function, facilitating microbial colonization and deeper tissue invasion **(Rowan et al., 2015)**. Burn wounds provide an ideal environment for pathogen proliferation due to nutrient availability and weakened local immunity, significantly raising the risk of infection. Bacterial infection is a key factor in aggravating burn outcomes, as it enhances inflammation, delays wound healing, and can lead to systemic complications. Multi-drug resistant (MDR) organisms, particularly Pseudomonas aeruginosa and Acinetobacter species, are

major contributors to burn wound infections due to their resistance to treatment and association with increased morbidity and mortality **(Roy et al., 2024)**.

IX. Early Burn Management

Limiting tissue damage and preventing systemic complications **(Nielson et al., 2017)**. The initial assessment involves determining the burn's severity, extent, and depth, stabilizing vital signs, and ensuring airway and circulatory support. Fluid resuscitation is critical to prevent hypovolemic shock caused by plasma loss and increased vascular permeability. Mild pain is typically controlled with non-opioid analgesics as needed. Prompt intervention improves survival rates and promotes optimal wound healing **(Markiewicz-Gospodarek et al., 2022)**.

IX.1. Wound Cleaning and Debridement

Thorough cleaning of burn wounds is essential to reduce infection risk and accelerate recovery **(Thomas et al., 2021)**. Necrotic or nonviable tissue is removed using surgical, mechanical, or enzymatic techniques, allowing healthy granulation tissue to form and decreasing microbial load. Effective debridement also enhances the efficacy of topical treatments and wound dressings **(Markiewicz-Gospodarek et al., 2022)**.

IX.2. Infection Control and Antimicrobial Therapy

Burn wounds, due to the compromised skin barrier, are highly susceptible to microbial colonization **(Ladhani et al., 2021)**. Topical antimicrobials such as 1% silver sulfadiazine and mafenide acetate are commonly applied, while systemic antibiotics (e.g., vancomycin or ceftriaxone/piperacillin-tazobactam) are indicated in cases of systemic infection. The primary goal is to prevent sepsis, a major contributor to mortality in burn patients **(Markiewicz-Gospodarek et al., 2022)**.

IX.3. Burn Dressings and Local Wound Care

Dressings are crucial for maintaining a moist healing environment, protecting the wound from contamination, and minimizing fluid loss **(Obagi et al., 2019)**. Hydrogel dressings provide pain relief and tissue soothing, hydrocolloid dressings promote granulation tissue formation, and silver-containing dressings (e.g., Acticoat®) help control bacterial infection. Dressing selection is based on the depth of the burn and the stage of wound healing **(Markiewicz-Gospodarek et al., 2022)**.

IX.4. Surgical Treatment and Skin Grafting

For deep burns, surgical intervention is required to excise damaged tissue and cover the wound with autologous skin grafts or synthetic substitutes **(Gacto-Sanchez, 2017)**. Early grafting reduces infection risk, accelerates re-epithelialization, and minimizes scarring and contracture formation **(Markiewicz-Gospodarek et al., 2022)**.

Chapter II

Bee Venom

I. Definition of Bee Venom

Bee venom (BV), also known as Apitoxin, is one of the main bioactive products of honeybees, produced in the venom glands of the worker bee belonging to the order Hymenoptera **(Devi et al., 2016)**. It is a complex natural mixture of biologically active compounds, primarily used as a defense mechanism that is secreted when the bee is threatened, aiming to protect the colony from predators and rivals **(Erdoğan et al., 2025; Grinn-Gofroń et al., 2025)**.

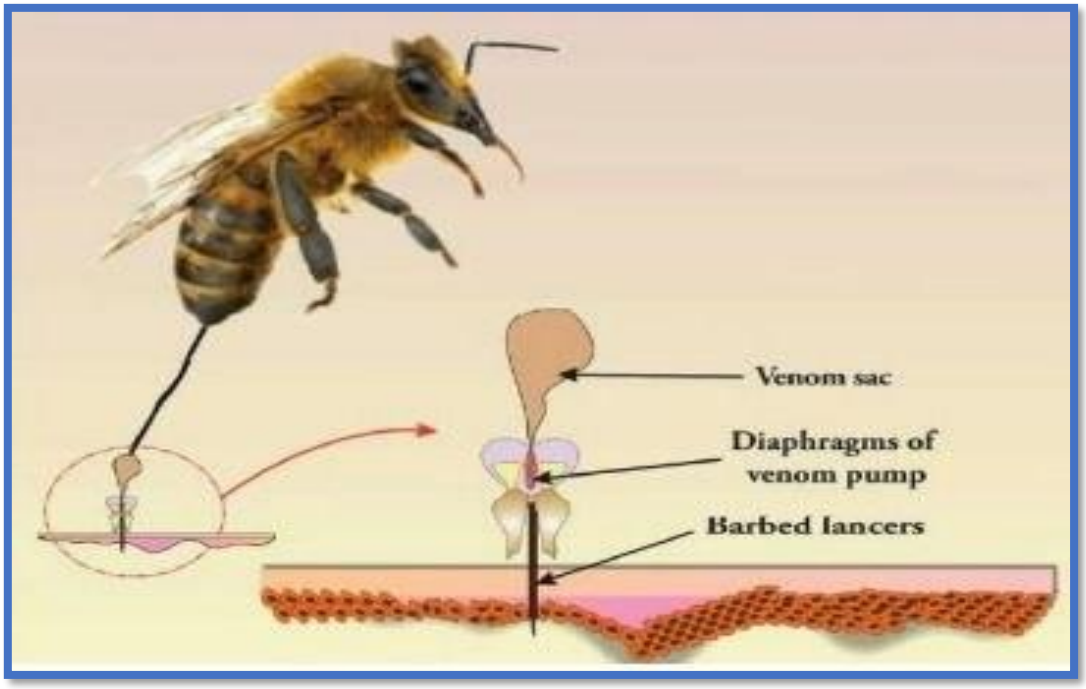

Figure 04: Venom gland of *Apis* mellifera **(Jaafar, & Albushabaa, 2025)**

II. Composition of Bee Venom

II.1. Melittin

Melittin, the principal component of bee venom, is one of the most extensively studied membrane-active peptides and consists of 26 amino acids. Its amphipathic nature enables it to be soluble in aqueous environments and to readily associate with various types of membranes, including artificial lipid bilayers **(Guha et al., 2021)**. Furthermore, it's a-helical structure, characterized by dual polarity, facilitates its interaction with lipid membranes and its ability to modulate multiple cellular signaling pathways, thereby playing a significant role in regulating inflammatory and immune. responses **(El Mehdi et al., 2022)**.

II.2. Apamin

Apamin, an 18-amino-acid peptide, makes up 2–3% of the total dry weight. It contains a disulfide bond between two cysteine residues, which provides it with a highly stable and cohesive chemical structure **(Tusiimire, 2016)**. Apamin has demonstrated potential benefits in combating atherosclerosis, treating heart failure, and improving neurological disorders **(Shi et al., 2022)**.

II.3. Phospholipase A_2 (PLA_2)

PLA, is the main enzyme in bee venom, accounting for approximately 10% of its dry weight. It catalyzes the hydrolysis of membrane phospholipids at the sn-2 position, producing lysophospholipids and unsaturated fatty acids that act as precursors for the synthesis of inflammatory mediators such as leukotrienes and prostaglandins **(Xu, 2018)**. This enzyme, together with melittin, contributes to cell membrane disruption and is considered the most important allergenic component of bee venom, making it a central factor in the venom's immune and inflammatory activity **(Gajski et al., 2024)**.

II.4. Mast Cell Degranulation Peptide

Peptide MCD is a low-molecular-weight peptide found in bee venom, known for its ability to stimulate mast cell degranulation, leading to the release of histamine and multiple inflammatory mediators that contribute to the venom's immune and inflammatory effects **(Ullah et al., 2023)**. Although it is considered a secondary component compared to melittin, phospholipase A and apamin, recent studies have shown that MCD peptide can exert anti-allergic and anti-inflammatory effects by modulating mast cell signaling pathways, opening new prospects for potential therapeutic applications in controlling inflammatory and allergic responses **(Sriwidodo et al., 2025)**.

II.5. Adolapin

Adolapin is a basic polypeptide composed of approximately 103 amino acids (11.5 kDa), accounting for only 1–5% of bee venom’s dry weight. It is less abundant and less extensively studied than melittin or phospholipase A_2 **(Nassar, 2022)**. Despite its low concentration, adolapin exhibits notable pharmacological properties, including anti-inflammatory, analgesic, and antipyretic activities. Its mechanism of action involves the inhibition of prostaglandin synthesis via cyclooxygenase (COX) inhibition, as well as the suppression of lipoxygenase and phospholipase

A_2 activities, thereby producing effects similar to those of nonsteroidal anti-inflammatory drugs **(Ullah et al., 2023; Supriya et al., 2025)**.

II.6. Other Enzymes and Peptides in Bee Venom

Bee venom contains secondary enzymes and peptides that contribute to its biological effects and cellular penetration **(Hossen et al., 2016)**. These include PLB, which catalyzes the hydrolysis of phosphoglycerides, and hyaluronidase, which creates openings in connective tissue to facilitate venom entry **(Silva de França & Tambourgi, 2023)**. The venom also contains small peptides such as secapin and tertipin, which exhibit anti-proteolytic and antimicrobial activities, contribute to increased pain sensitivity and tissue swelling, and help regulate the inflammatory response. Together, these components enhance the inflammatory and immune effects of bee venom and increase its overall biological activity **(Gajski, 2024)**.

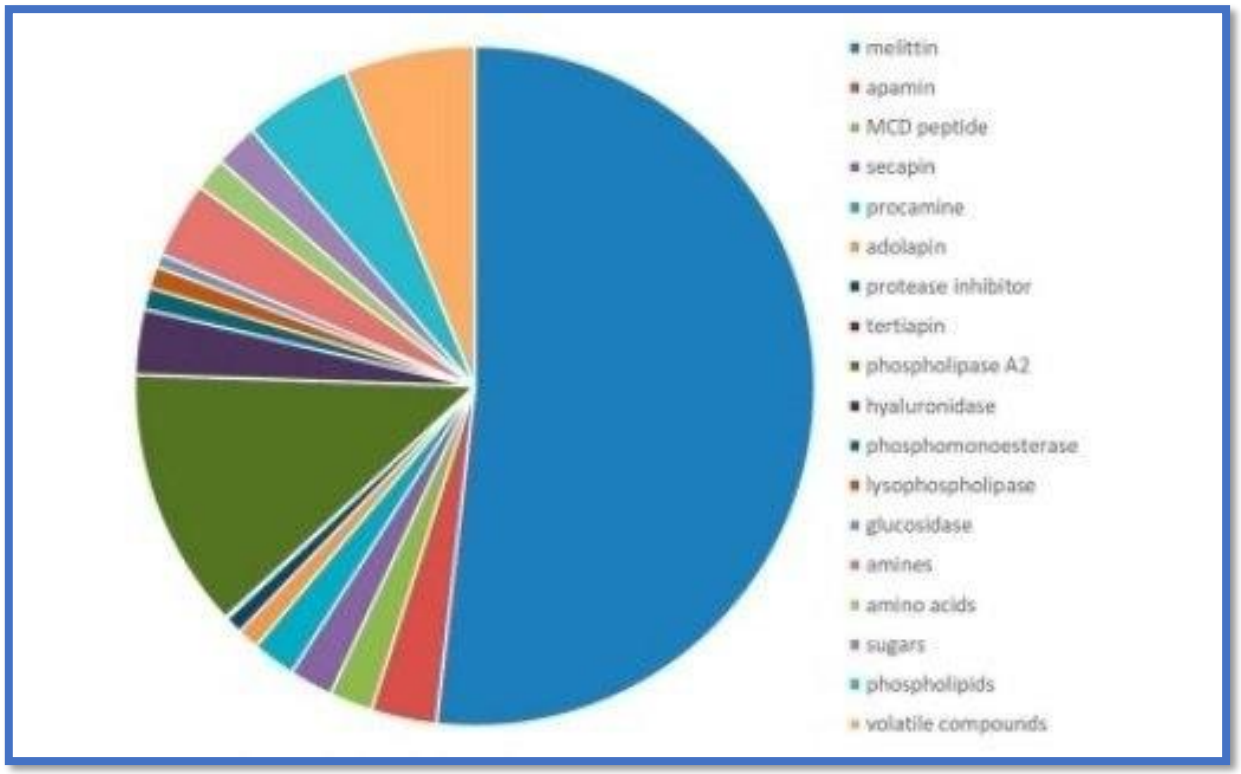

Figure 05: Composition of dry bee venom **(Jaafar, & Albushabaa, 2025)**

III. Biological Activities of Bee Venom

Bee venom therapy encompasses a variety of therapeutic approaches that rely on the use of bee venom and its bioactive components to treat various diseases **(Wehbe et al., 2019)**. It has been used in alternative medicine for more than 3000 years. The therapeutic effects of bee venom are attributed to its anti-inflammatory, antioxidant, antifibrotic, immunomodulatory, anticancer, and anti-apoptotic properties **(Abdelrahaman et al., 2025)**.

III.1. Antioxidant Activity

Bee venom (BV) is characterized by the presence of several bioactive compounds exhibiting antioxidant properties. This antioxidant activity is mainly associated with components such as melittin, phospholipase A_2, and apamin **(Carpena et al., 2020)**. These compounds contribute to reducing lipid peroxidation and enhancing the activity of antioxidant enzymes such as superoxide dismutase, thereby decreasing oxidative stress levels **(Li et al., 2015)**. Furthermore, bee venom contains additional antioxidant molecules, including phytol derivatives, which directly protect mammalian cells against damage induced by reactive oxygen species, supporting cellular integrity and survival **(Carpena et al., 2020)**.

III.2. Neuroprotective Activity

Bee venom demonstrates promising therapeutic potential in neurodegenerative diseases by reducing neuroinflammation caused by the activation of glial cells **(Ku et al., 2020)**. Its bioactive components, such as phospholipase A2 and apamin, contribute to anti-inflammatory effects and improvement of neurological functions **(Ong et al., 2015)**. Animal studies have shown that bee venom can reduce pain and enhance neurological performance in certain neurological disorders and chemotherapy-induced neuropathy, making it a potential therapeutic option for alleviating neuropathic pain and supporting neural function **(Bava et al., 2023)**.

III.3. Antimicrobial and Antiviral Activity

Bee venom exhibits strong activity against Gram-positive and Gram-negative bacteria, as well as certain viruses and fungi **(Isidorov et al., 2023)**. This effect is mainly attributed to melittin, a peptide capable of disrupting microbial cell membranes, leading to leakage of cellular contents and subsequent cell death **(Hong et al., 2019)**. Additionally, bee venom inhibits the formation of bacterial biofilms, making it a promising candidate for combating antibiotic resistance **(Stela et al., 2024)**.

III.4. Antidiabetic Activity

Diabetes mellitus is a common metabolic disorder characterized by elevated blood glucose and lipid levels, along with numerous associated complications **(Balaji et al., 2019)**. Melittin enhances insulin production by reducing pancreatic inflammation. Furthermore, melittin affects pancreatic cell membranes, facilitating the influx of calcium ions, which in turn stimulates pancreatic β-cells to secrete insulin **(Radwan et al., 2024; Ullah et al., 2023)**.

III.5. Wound Healing

Wound healing is a complex biological process that proceeds through four main phases: hemostasis, clot formation, inflammation, and cellular proliferation **(Duda et al., 2023)**. Studies have shown that bee venom (BV) enhances the healing process when applied topically or administered via subcutaneous injection, particularly by accelerating the hemostasis phase through the stimulation of growth factors such as TGF-β and VEGF. This makes it a promising therapeutic option, especially for patients with diabetes **(Sadek et al., 2024)**.

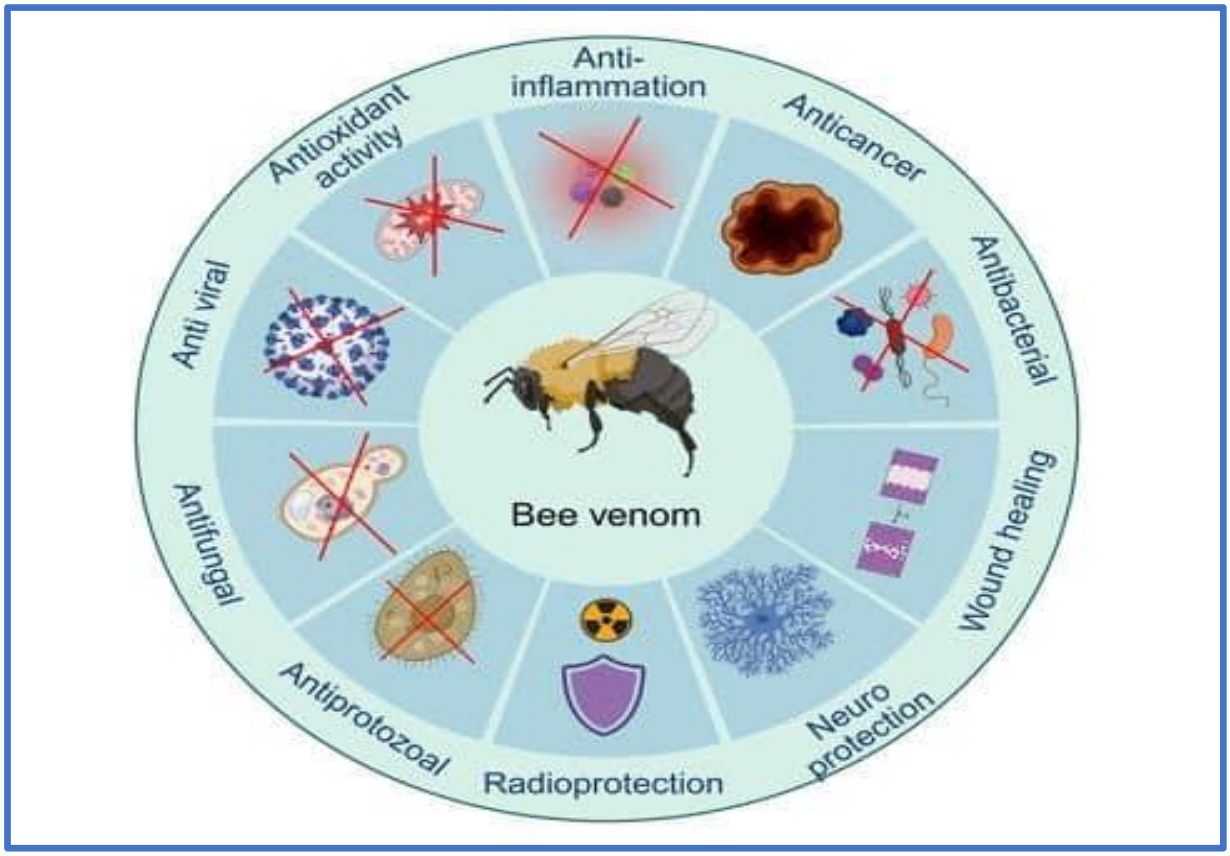

Figure 06: Biological activities of bee venom **(Sadek et al., 2024)**

IV. Toxicity of Bee Venom

Bee venom is considered a substance with therapeutic properties; however, its use is limited due to its potential toxicity and unpredictable effects **(Balaji et al., 2019)**. Studies indicate that a significant proportion of cases report adverse effects, particularly immune reactions and allergic responses resulting from hypersensitivity and dose concentration **(Khan et al., 2016)**. The toxicity of bee venom is primarily attributed to its active components, such as melittin and phospholipase A_2 (PLA_2), which act synergistically to disrupt cellular membranes, leading to hemolysis and increased cytotoxicity **(Carpena et al., 2020)**.

Toxic reactions may be classified as:

Immediate: including systemic manifestations such as hypotension and shock.

Delayed: potentially leading to multiple organ failure after several hours **(Marzano et al., 2016)**.

Although the lethal dose is estimated to be approximately 13.19 mg/kg, small amounts of venom may be fatal in certain individuals due to severe hypersensitivity. Early medical intervention (intravenous fluid resuscitation, blood transfusion, and dialysis) is essential to reduce complications and prevent the progression to severe conditions **(Stela et al., 2024)**

Chapter III

Nanotechnology

I. Nanotechnology

Nanoscience and nanotechnology represent rapidly advancing interdisciplinary fields that have attracted considerable scientific interest worldwide **(Malik et al., 2023).** The term nano originates from the Greek word nanos, meaning dwarf, and refers to materials engineered at the nanometer scale, typically ranging from 1 to 100 nanometers **(Reshma et al., 2025; Mohammed Saied et al., 2022).** At this nanoscale dimension, materials exhibit physicochemical properties that differ significantly from their bulk counterparts, including enhanced surface area, altered chemical reactivity, improved solubility, and unique optical, electrical, and magnetic characteristics **(Ma et al., 2024).** These distinctive properties enable nanomaterials to interact efficiently with biological systems and improve transport across cellular membranes, thereby expanding their technological and biomedical applications **(Guan et al., 2024).**

Nanotechnology has emerged as an innovative approach for addressing major challenges in healthcare, environmental protection, agriculture, and food science **(Ajaz et al., 2024)**. In medicine, nanoparticles are widely investigated for targeted drug delivery systems, diagnostic imaging, and cancer therapy **(Tiwari et al., 2023).** Environmental nanotechnology contributes to water purification, pollutant degradation, and sustainable resource management. In the food sector, nanomaterials are applied to improve food quality, safety, and shelf life through advanced packaging systems **(Biswas et al., 2022).** Furthermore, plant nanotechnology plays an important role in enhancing crop productivity, nutrient delivery, and stress resistance **(El-Saadony et al., 2023)**. Due to its capacity for precise material engineering and potential reduction of toxicity, nanotechnology is considered a key enabling technology for sustainable development across multiple scientific and industrial sectors **(Elzein, 2024).**

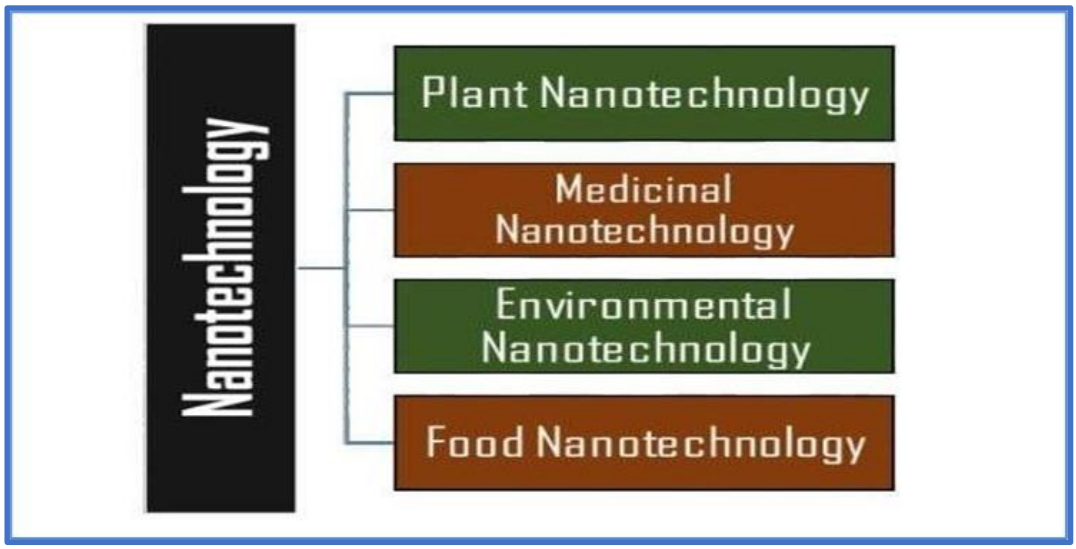

Figure 07 : Nanotechnology domains **(Ajaz et al., 2024)**

II. Nanoparticles

Nanoparticles (NPs) are defined as assemblies of atoms or molecules that may be of the same or different types. **(Szczyglewska et al., 2023)**. Their size typically ranges from 1 to 100 nm **(Joudeh & Linke., 2022)**. Nanoparticles exhibit significant diversity in their properties, such as chemical composition, size, and shape, and their behavior differs markedly from that of bulk materials at the nanoscale **(Abbas et al., 2024)**. The category of nanoparticles includes organic, inorganic, and carbon-based nanoparticles, depending on their origin, properties, shape, and size **(Prajapati et al., 2024).** Nanoparticles are of great importance due to their wide range of applications in various fields, including the environment, agriculture, biotechnology, biomedicine, and medicine. They are used in wastewater treatment **(Zahra et al., 2020)**, environmental monitoring **(Rassaei et al., 2011)**, as functional food additives **(Chen et al., 2023)**, and as antimicrobial agents **(Islam et al., 2022).**

In addition, their advanced properties, such as biocompatibility, anti-inflammatory and antibacterial activity, efficient drug delivery, high bioactivity, and tumor-targeting ability, have contributed to their increasing use in biotechnological and applied microbiological applications **(Altammar., 2023).**

Table 01: Properties of the nanomaterial and bulk material (**Ahire et al., 2022).**

Nanomaterial	Bulk material
Shows different properties at a small scale	Properties remain same
Chemically more reactive	Chemically less reactive
Large surface area	Small surface area
Lighter material	Heavier material
Faster in performance	Slower in performance
More energy efficient	Not energy efficient
Cheaper than bulk	Expensive

III. Type Nanoparticles

Based on composition, nanoparticles are broadly classified into carbon-based, organic, and metallic types.

III.1. Carbon-Based Nanomaterials

Carbon nanomaterials mainly consist of two primary groups, namely fullerenes and carbon nanotubes, in addition to other subtypes. These materials differ in terms of structure, size, and physicochemical properties **(Al-Harbi & Abd-Elrahman, 2025)**. They are characterized by their small dimensions, large surface area, and high electrical conductivity, along with unique properties that make them suitable for various applications **(Díez-Pascual, 2021)**. Due to these advantages, they have attracted increasing interest in the biomedical field **(Farahani et al., 2025)**, particularly as effective drug delivery carriers **(Swain et al., 2025)**.

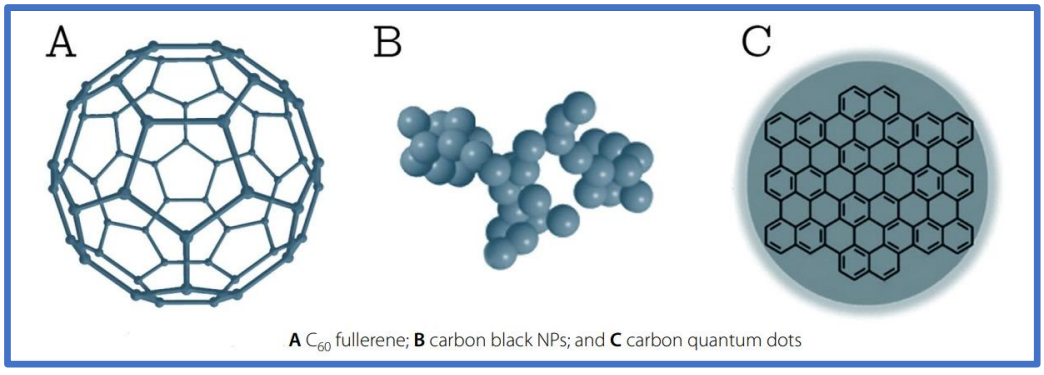

Figure 08: Different types of carbon-based NPs **(Joudeh & Linke, 2022)**

III.2. Metallic Nanoparticles

Metallic nanoparticles are composed entirely of metals and exhibit unique electrical properties due to the well-known localized surface plasmon resonance (LSPR) phenomenon. Nanoparticles such as gold, silver, and copper show strong light absorption in the visible region **(Salem et al., 2022)**. Owing to their enhanced properties related to small size, large surface area, and shape, these nanoparticles are widely used in various scientific applications **(Altammar, 2023)**.

III.3. Organic Nanoparticles

Organic nanoparticles are prepared from materials such as lipids and polymers and include various types, as illustrated in Figure A. Among the most prominent are micelles and liposomes, which possess a hollow spherical structure. These nanoparticles are characterized by low toxicity and biodegradability **(Alshammari et al., 2023),** Applications of organic nanoparticles depend on their various properties, and they are mainly used in the biomedical field, particularly in drug delivery and cancer therapy. **(Joudeh & Linke, 2022)**

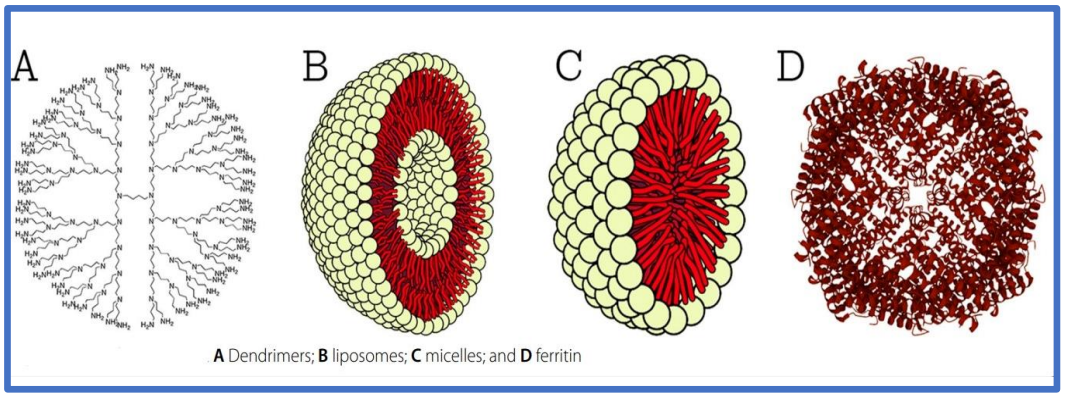

Figure 09: Types of organic NPs **(Joudeh & Linke, 2022)**

IV. General Method of Synthesis for Metal Oxide Nanoparticles

Two main strategies are used for the synthesis of nanoparticles, namely the top-down and bottom-up approaches **(Erdoğan & Özsoy, 2025)**. The top-down approach involves breaking down bulk materials into nanoscale structures using techniques such as electrical explosion, etching, deposition, and mechanical milling **(Bains et al., 2025)**. However, this method has several limitations, including high energy consumption, high operational costs, and large waste generation **(Kumar et al., 2024)**. It also requires harsh conditions such as high temperature and pressure and

may involve radiation exposure **(Antony Jose et al., 2025)**. In addition, it offers limited control over particle size and shape, which can affect uniformity and surface properties **(Bloch et al., 2021)**.

In contrast, the bottom-up approach builds nanoparticles from atoms or molecules and includes chemical and biological methods **(Jiang et al., 2022)**. Chemical methods are widely used due to their ability to produce highly pure nanoparticles with controlled properties **(Parveen et al., 2025)**. However, they are often costly and may generate toxic by-products, especially for biomedical applications **(John, 2025)**. They also require stabilizing agents to prevent aggregation, which increases cost and complexity **(Islam et al., 2022)**. Moreover, they are associated with environmental pollution and health risks due to toxic reagents **(Ying et al., 2022)**.

Physical methods are another Top-down/Bottom-up related strategy, including vapor–condensation, laser ablation, and mechanical milling. Although they produce high-purity nanoparticles, they suffer from high energy demand, expensive equipment, limited size control, and poor scalability **(Khan et al., 2022)**. To address these limitations, green synthesis has emerged as a promising Bottom-up alternative using natural resources such as plant extracts **(Gavilán et al., 2023)**. It reduces environmental impact, toxicity, and production cost while improving biocompatibility **(Yang et al., 2023)**.

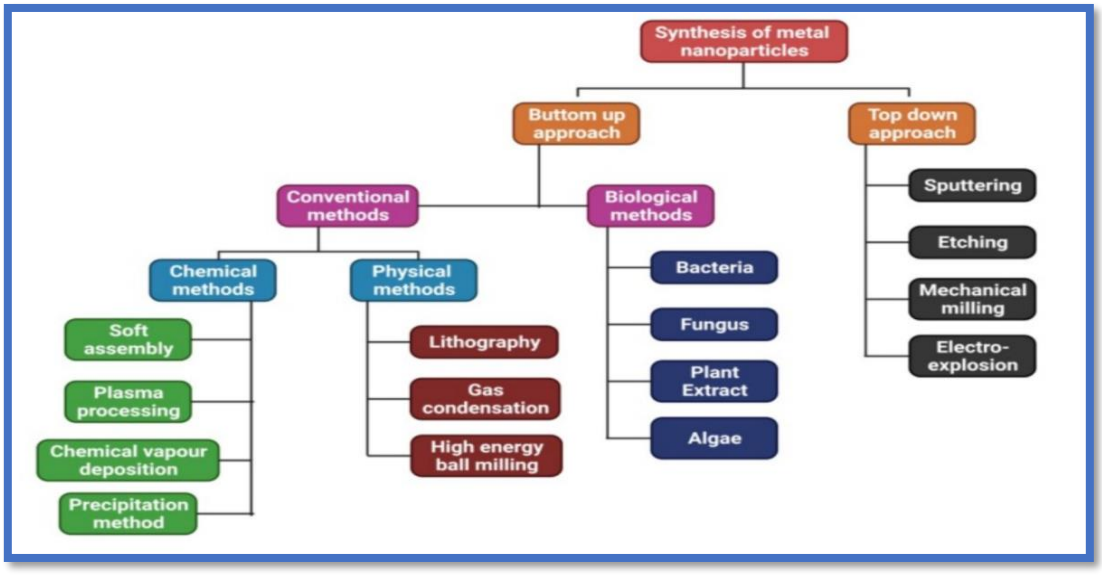

Figure 10: Classifications of nanomaterials based on dimensionality and chemical composition **(Islam et al., 2022)**

V. Zinc Oxide Nanoparticles (ZnO NPs)

Zinc oxide is an inorganic chemical compound widely used in everyday life. In recent years, the rapid advancement of nanotechnology has enabled the development of zinc oxide-based nanomaterials with novel properties **(Czyżowska & Barbasz, 2022)**. Zinc nanoparticles (ZnO NPs) exhibit a wide range of applications, as they are used in the food industry as supplements, incorporated into food packaging materials, and extended to medical applications, due to their antimicrobial properties **(Dkhil et al., 2020).** Zinc oxide nanoparticles (ZnO NPs), on the other hand, are distinguished by their efficient photocatalytic properties, along with enhanced stability, improved crystallinity, and fewer structural defects compared to bulk zinc oxide. These features make them more effective in the degradation of various substances, especially organic pollutants **(Chetehouna et al., 2020).**

VI. Green Synthesis of ZnO NPs

Nano-biotechnology, a newly emerging branch of nanotechnology (**El-Moslamy et al., 2023)**, has enabled the development of environmentally friendly strategies for nanoparticle synthesis. Among these, the green synthesis approach has gained significant attention, as it encompasses the use of natural materials such as plant extracts, bacteria, fungi, algae **(Swain et al., 2025),** as well as natural biopolymers that provide a low-cost and eco-friendly alternative, which act as bio-reductants and bio-stabilizers due to their richness in bioactive phytochemicals **(Vijayakumar & Vaseeharan, 2018)**.

Table 02: Green synthesis of ZnO nanoparticles using various biological sources

Type	Reducing agent	Precursor	Size	Shape	Characterization	Referens
Plant	*Grewia Flavescens*	Zn $(NO_3)_2.6H_2O$	20-30 nm	Spherical	UV-Vis spectroscopy, TGA/DTA, TEM, XRD, DLS, and FTIR	**(Sana et al., 2023)**
	Carica Papaya	Zn $(CO3COO)_2$. 6 H_2O	~21 nm	Spherical, semi-spherical, hexagonal, and rod-like	HRTEM, XPS, UV–Vis spectroscopy, FTIR, EDX, TEM, SEM, and XRD	**(Gaur et al., 2023)**
	Dysphania Ambrosioides	Zn $(NO_3)_2.6H_2O$	7-130 nm	Hexagonal prism, and quasis pherical	TG/DTA, HRTEM, FESEM, FTIR, EDS, TEM, and XRD	**(Álvarez-Chimal et al., 2022)**
	Punica Granatum	Zn $(CH3COO)_2$.$2H_2$	10-45 nm	Spherical, well arranged, and crystallographic	UV-Vis spectroscopy, EDX, SEM, TEM, XRD, and FTIR	**(Fouda et al., 2023)**
	Phyllanthus niruri (Phyllanthaceae)		25-61nm	Hexagonal wurtzite, quasi-spherical	FE-SEM, XRD	**(Wary et al., 2022)**
Bacteria	*Priestia Megaterium*	$ZnSO_4$	5.77-13.9 nm	Semi-sphere	HR-TEM, DLS, FTIR, EDX, spectroscopy	**(Ashour & Abd-Elhalim , 2024)**
	Streptomyces Baarnensis	$ZnSO_4.7H_2O$	< 12 nm	Spherical	HR-TEM, DLS, TEM FTIR, XRD ,UV-Vis spectroscopy	**(Kalaba et al.,2024)**
	Bacillus Subtilis	Zinc nitrate hexahydrate salt	38 ± 2 nm	Rod-shaped	UV-Vis, XRD, FTIR, TEM, SEM	**(Ewais et al.,2024)**
	Enterobacter Sp	Zinc sulfate	18.4 nm	Hexagonal structure	FTIR, TEM, XDR, UV-Vis	**(Elsilk ET AL., 2024)**

	Bacillus Paramycoides	$ZnSO_4$	4.37 nm	Hexagonal structure	UV-Vis spectroscopy, FTIR, TEM, XRD, DLS	**(El-Refai et al., 2024)**
Fungi	*Trichoderma Harzianum*	Zinc acetate Dihydrate [$Zn(CH_3.COO)_2.2H_2O$]	12-41 nm	Spherical, rod, andhexagonal shapes	UV-Vis spectroscopy, FTIR, EDX, SEM, XRD, DLS, HR-TEM	**(Mishra et al., 2025)**
	Arthrobotrys Oligospora	Zinc acetate	29.45-71.30 ı	Hexagonal wurtzite crystallir	UV-Vis spectroscopy, Raman spectroscopy, FTIR, SEM, XRD, TEM, EDAX	**(Gautam et al., 2025)**
	Fusarium oxysporum sp	Zn $SO_4.7H_2O$	15-80 nm	Highly crystalline Nature	FTIR, EDX, TEM, XRD, DLS	**(Salaheldin et al., 2024)**
Algae	*Sargassum Ilicifolium*	[$Zn(OAc)_2 \cdot 2H_2O$]	25.22 nm	Spherical	DLS, X-RD, and FE-SEM	**(Mardani-Talaee, 2025)**
	Padina pavonica	$Zn(NO_3)_2 \cdot 6H_2O$	16.34-22,88n	Spherical	MB, SEM, EDX, FTIR	**(Alprol et al., 2024)**
	Spirogyra Hyaline	zinc acetate (ZA) dihydrate and zinc nitrate (ZN) Hexahydrate	ZA 56 nm ZN 40 nm	Spherical	UV-Vis spectroscopy, FTIR, SEM, EDX, XRD	**(Hameed et al., 2023)**
Protein	Egg albumin		16 nm (XRD 10-20 (TEM) 8-22 (AFM)	Spherical, Hexagonal wurtzite	AFM, TEM, XRD	**(Ambika & Sundrarajan, 2015)**
	Proteinase K	$ZnSO4.7H_2O$	15-25 nm	Spherical	TEM, FTIR, XRD	**(Radwan et al., 2022)**

Recent research highlights the growing importance of green synthesis methods in the production of metal oxide nanoparticles, with zinc oxide nanoparticles (ZnO NPs) standing out among other metal oxides owing to their abundance, stability, electrical conductivity, piezoelectric properties, nontoxicity, and optical transparency **(Zeghoud et al., 2022)**. Moreover, ZnO NPs are highly attractive materials due to their remarkable features, including a large surface-to-volume ratio, high surface area, high catalytic efficiency, and good adsorption capacity **(Mutukwa et al., 2022)**. This eco-friendly approach relies on the bioactive compounds present in the extracts to facilitate the hydrolysis of zinc ions and ensure the stabilization of the synthesized nanoparticles **(Mahajan et al., 2025)**.

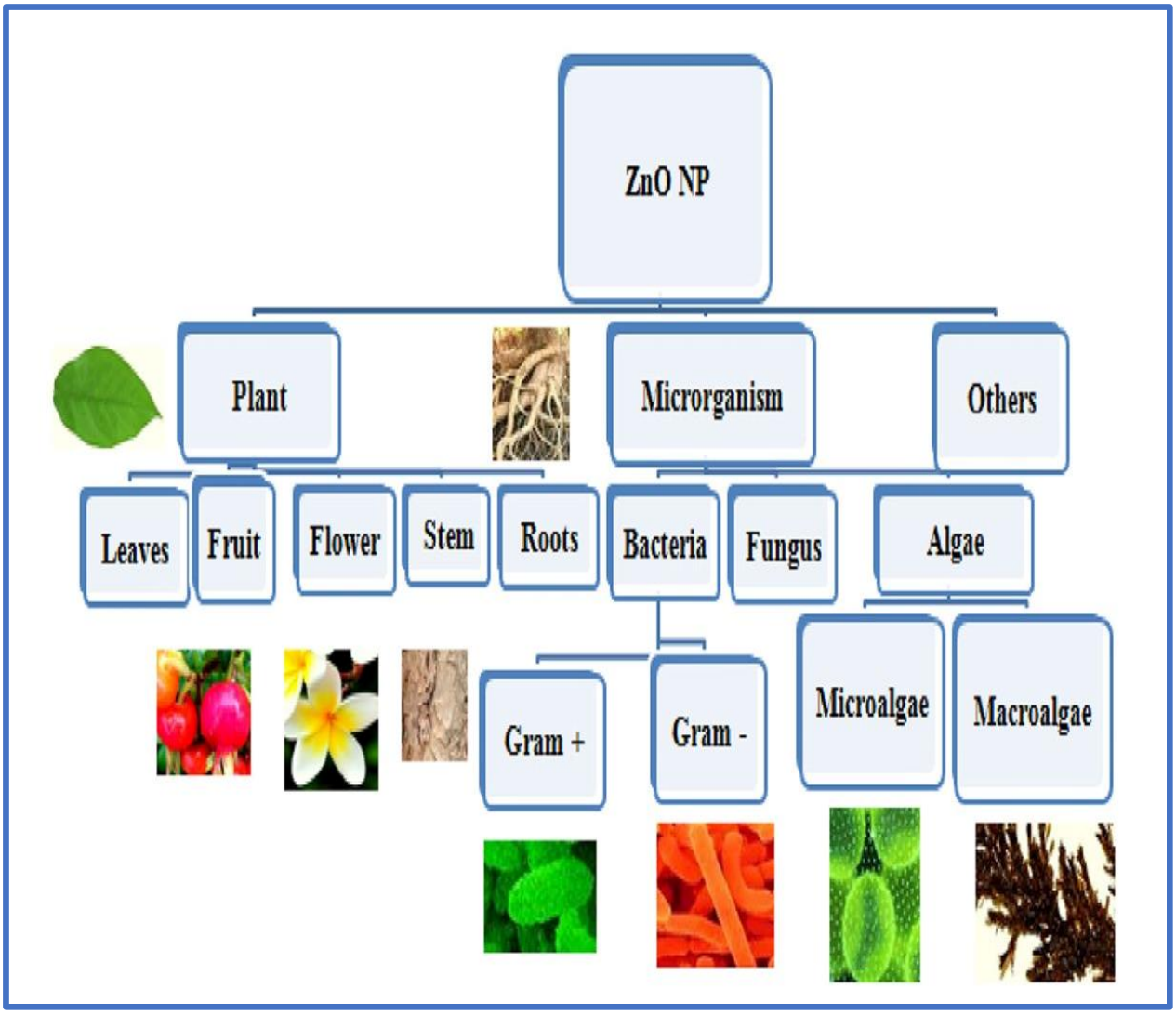

Figure 11: Zinc oxide nanoparticle synthesis by using different sources **(Jadoun et al., 2020)**

VII. Green Synthesis of Nanoparticles Using Biopolymers (Collagen)

The use of natural biopolymers in the green synthesis of nanoparticles has emerged as a modern, eco-friendly, and cost-effective approach compared with conventional physical and chemical synthesis methods **(Kabir, 2025)**. These biopolymers act as both reducing and stabilizing agents, enabling the production of stable nanoparticles with high biocompatibility **(Aouadi et al., 2024)**. Collagen, a natural fibrous structural protein rich in functional groups such as amino, hydroxyl, and carboxyl groups, represents an effective biomaterial for the biosynthesis of nanoparticles, particularly zinc oxide nanoparticles (ZnO-NPs) **(Mandal et al., 2022)**. It facilitates metal ion reduction and regulates nanoparticle growth. Collagen-based nanoparticles have demonstrated nanoscale sizes ranging from 20-50 nm, along with significant antibacterial activity and good biocompatibility, highlighting their promising applications in biomedical and antimicrobial fields **(Vijayakumar & Vaseeharan, 2018)**. The efficiency of green synthesis is influenced by several factors, including pH, temperature, biopolymer concentration, and reaction time, which collectively determine the size, morphology, and stability of the synthesized nanoparticles **(Ansari et al., 2023).**

VIII. Biomedical Applications

Zinc oxide nanoparticles (ZnO-NPs) are widely used due to their tunable properties, low toxicity, and good biocompatibility **(Mandal et al., 2022)**. They are especially suitable for targeted biomedical applications **(Islam et al., 2022)**. Their applications encompass anticancer activity, antioxidant and anti-inflammatory properties, antibacterial effects, antidiabetic potential, as well as roles in bioimaging and drug delivery systems **(Al-darwesh et al., 2024)**.

VIII.1. Anti-inflammatory Activity

Zinc oxide nanoparticles (ZnO-NPs) exhibit anti-inflammatory activity by reducing pro-inflammatory cytokines and demonstrating superior tissue penetration compared to larger particles **(Youssef et al., 2024)**. In Alzheimer's disease models, they significantly decreased inflammatory markers, indicating their efficacy in mitigating inflammation **(Chandrasekaran et al., 2022)**.

VIII.2. Antioxidant Activity

Zinc oxide nanoparticles (ZnO-NPs) exhibit antioxidant activity by scavenging reactive oxygen species (ROS) and reducing oxidative stress within cells, thereby helping to protect vital cellular components from damage **(Ramzan et al., 2022)**. Recent studies have confirmed their effectiveness in assays such as DPPH and ABTS **(Shnawa et al., 2024)**, with this activity depending on particle size and preparation method. Green synthesis enhances their efficiency due to the association with bioactive plant compounds **(Chemingui et al., 2022)**.

VIII.3. Antibacterial Activity

Zinc oxide nanoparticles (ZnO-NPs) exhibit promising antibacterial properties due to their large surface area and their ability to combat a wide range of diseases, making them a reliable therapeutic option in medical technology at both the micro and nano levels **(Helmy et al., 2023; Akinyemi et al., 2022)**. These nanoparticles affect cell wall morphology and integrity, disrupting normal cellular structure and functions. Additionally, ZnO-NPs demonstrate antibacterial activity through multiple mechanisms, including membrane disruption, DNA damage, enzyme inhibition, and mitochondrial impairment **(Lopez Venditti et al., 2025)**.

VIII.4 Anticancer Activity

In cancer therapy, they selectively target cancer cells by generating ROS, inducing apoptosis, DNA damage, and cell cycle arrest, and they can enhance chemotherapy and photodynamic therapy while also being useful in imaging and targeted delivery **(El-Aassar et al., 2021; Al-Shehaby et al., 2025; Anjum et al., 2021; Lebaka et al., 2025)**.

VIII.5. Antidiabetic Activity

Diabetes mellitus is a common chronic disease **(Liu et al., 2020)**. Inhibition of the α-amylase enzyme contributes to lowering blood glucose levels, although conventional drugs may cause side effects. Therefore, nanoparticles have emerged as a promising alternative, demonstrating antidiabetic activity **(Elankathirselvan et al., 2024)**, particularly zinc oxide nanoparticles, which enhance insulin production and increase glucose clearance **(Ramana et al., 2023)**.

VIII.6. Drug Delivery

In drug delivery, ZnO NPs act as efficient nanocarriers due to their high surface area, biocompatibility, and easy functionalization, enabling targeted, controlled, and pH-responsive drug release with reduced toxicity **(Mandal et al., 2022; Naser et al., 2023; Eren et al., 2024)**. They can also carry drugs, genes, proteins, and imaging agents and are used in theranostic systems for combined treatment and diagnosis **(Ezzat et al., 2025; Lebaka et al., 2025)**.

VIII .7. Bio-Imaging

Several studies have highlighted the importance of ZnO NPs in cellular imaging. These NPs can emit green fluorescence due to oxygen vacancies and other processes, facilitating the visualization of cancer cells via minimally invasive methods **(El-Saadony et al,.2024)**.

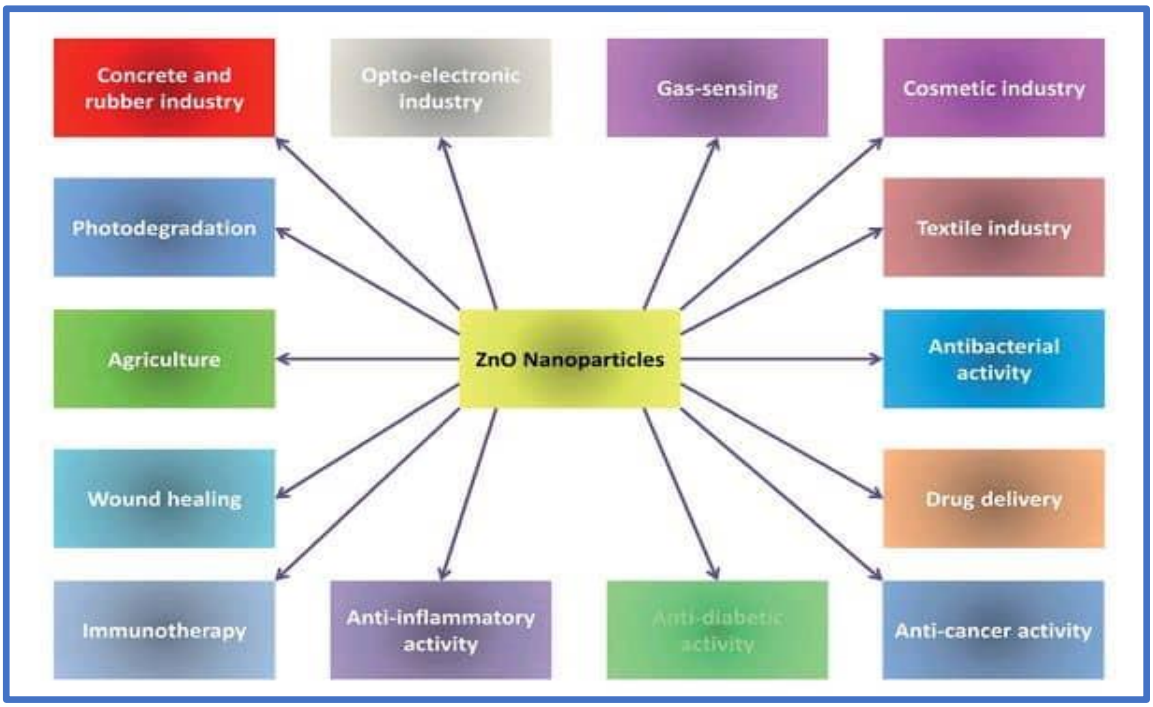

Figure 12: Applications of ZnO NPs **(Raha & Ahmaruzzaman., 2022).**

Second part

Experimental Part

Chapter I

Materials & Methods

I. Materials

I.1 . Biological Materials

I.1.1. Bee Venom

The purified, dried bee venom was purchased from a local beekeeper in Boumerdes Province, Algeria, specifically from the Jellabine area, in October 2025. The sample was stored in a cool, dark place at 4 °C.

I.1.2. Collagen

Collagen was extracted from chicken feet, collected in November 2025 from a poultry shop in Taghzout El Oued (Algeria), and transported to the laboratory under suitable conditions. The samples were thoroughly washed with water, the nails were removed manually, and then they were refrigerated.

I.2. Animals

I.2.1. Animals' Care

In this study, twenty female Albino Wistar rats at the age of 08 weeks old, weighing 148 ± 3.85 g sourced from the Institute Pasteur of Algiers. They were housed in cages within the animal room of the Department of Molecular and Cellular Biology at the Faculty of Nature and Life Sciences, Echahid Hamma Lakhdar-El-Oued University, Algeria. During a 15-day period of adaptation, the animals were carried under the same conditions of room temperature with a 12 h light/12 h dark cycle. Throughout the study, the rats were given free access to food and water.

I.2.2. Experimental Design

Following the period of adaptation, the rats were weighed, with weights ranging 166.25 ± 4.75 g. The animals were then divided into four groups each containing five rats.

- → **Group 1 (control group):** Healthy rats, without burn injury.
- → **Group 2 (Untreated group):** Burned rats, without treatment.
- → **Group 3 (ZnO NPs-BV group):** Burned rats treated with ZnO NPs-BV (Beevenox) 1 % cream.
- → **Group 4 (Sulfadiazine® group):** Burned rats treated with Sulfadiazine® 1 % cream.

In the experimental part of this study, all rats were first anesthetized with chloroform to minimize pain and stress. The experimental area on the back of the rats' necks was then shaved using a razor to ensure uniform skin erosion. Twenty-four hours after anesthesia and shaving, a standardized circular skin burn was induced using an electric soldering iron (1.2 cm diameter) applied for 3 seconds per rat, following a standardized protocol. Subsequently the burn, topical treatment was applied every other day for three weeks. One group was treated with ZnO NPs-BV cream, another with Sulfadiazine® 1% cream is used for the prevention and treatment of wound infections in patients with second- and third-degree burns, and a third group was left untreated. All animals were subjected to the same conditions and procedures to standardize the experimental conditions and ensure reliable comparison of results.

Throughout the treatment period, the wound was evaluated at the macroscopic level (size, morphology, color, and margin) and the body weights of the rats were monitored once per week.

I.2.3. Sacrifice, Blood Sampling and Tissues Collection

After a 16-hour fasting period, the rats were anesthetized with chloroform and sacrificed. Blood glucose levels were measured concurrently using a glucometer. Subsequently, blood samples were collected into EDTA-containing tubes for hematological analyses and into heparinized tubes for biochemical assays. Serum was separated by centrifugation at 1000 rpm for 5 minutes.

Following sacrifice, the target organs (liver, spleen, and skin) were excised, accurately weighed, and washed twice with physiological saline solution (0.9 % NaCl). The tissues were then stored at -20 °C until further use. for oxidative stress parameter analysis.

For histological examination, spleen and skin tissues were fixed in 10 % formaldehyde solution.

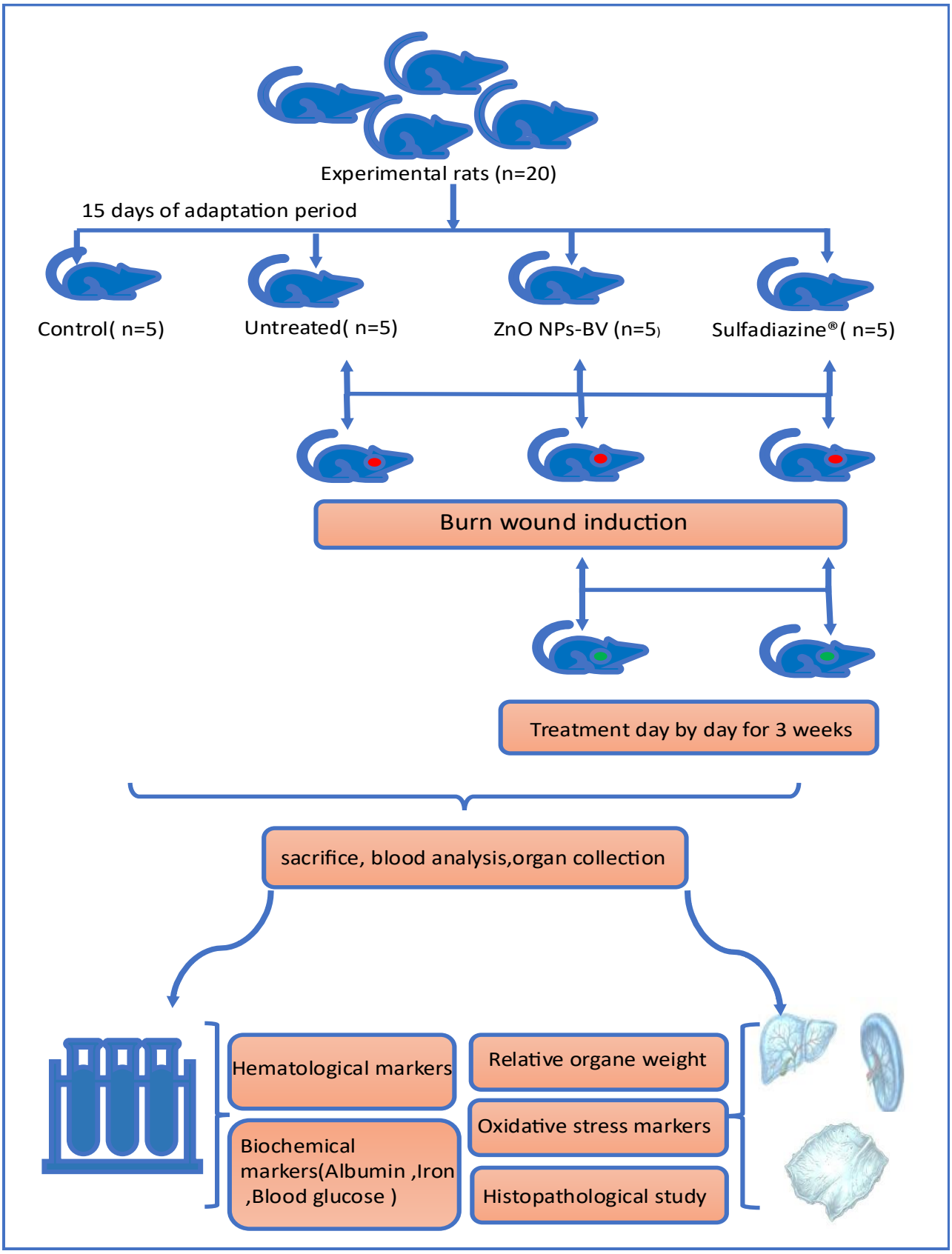

Figure 13: Experimental design of the study.

II. Methods

II.1. Preparation and Characterization of the Biomaterials Used in the Study

II.1.1. Collection and Storage of Bee Venom

The electric bee venom collection device, designed for use inside the hive, consists of a unit equipped with closely spaced wires connected to an electric current powered by lithium batteries. To ensure the purity and quality of the collected bee venom for human use, a glass plate covered with a shrinkable food-grade film is placed between the wires.

The electric bee venom collection device remains inside the hive for a period ranging from 8 to 12 hours. After this period, the device is carefully removed and transferred to a cool, shaded area. To prevent contamination, beekeepers wear masks and gloves during the collection process. The food-grade shrinkable film covering the glass plate is removed, and the dry venom deposited on the center of the plate is carefully scraped off using a sterilized scalpel. The collected dry venom is stored in glass containers and kept in a freezer, where it remains stable for at least two years.

Figure 14: Collection of bee venom by electrical stimulation **(original photo)**

II.1.2. Collagen

II.1.2.1. Extraction of Collagen

Collagen was extracted from chicken feet skin by acid-based extraction method. Collected chicken feet skin were washed with distilled water to remove all the adhering material and were dried in hot air oven. Demineralization of chicken feet skin was achieved by soaking in 0.2 N HCl for 90 min followed by washing with distilled water. Removal of non-collagenous protein was

achieved by treating with 0.1 M NaOH solution (scale to alkali solution ratio of 1:10 (w/v)) for 6 h at 4 °C under continuous stirring. Alkali treated were washed with cold water till neutral or slightly basic pH was reached. To extract soluble collagen, treated chicken feet skin were ground to a fine paste, extracted with 0.5 M acetic acid, The samples were washed using distilled water until neutral **(Chandraprabha et al., 2022)**. The third stage was extraction by hydro-extraction method. The extraction was carried out at 40 ^{o}C for 2 hours using a water bath shaker with a speed of 150 rpm. The ratio between chicken feet and distilled water was 1:2 (b/v). Extraction result was in the form of collagen solution, then the solution was dried with a freeze dryer to obtain dry collagen and the yield was calculated **(Suparno & Prasetyo., 2019).**

II.1.2.2. Characterization of Collagen

II.1.2.2.1. Visual Observation of Collagen

The extracted collagen was subjected to a preliminary characterization of its physicochemical properties. Its macroscopic characteristics, including color and texture, were evaluated by direct visual observation, while the pH value was determined using a calibrated digital pH meter under standard laboratory conditions.

II.1.2.2.2. UV-Visible Spectroscopy

Collagen was analyzed using a UV-Visible spectrophotometer (UV-Vis Spectrophotometer, JENWAY 6705) in the wavelength range of 200–800 nm to study absorption peaks associated with peptide bonds and side chains, and to evaluate its purity and structural integrity.

II.1.2.2.3. Fourier Infrared (FTIR) Spectroscopy

Collagen was characterized using Fourier-transform infrared spectroscopy (FTIR Spectrometer) in the wavenumber range of 4000–400 cm^{-1}, aiming to identify characteristic bands and analyze the secondary structure, thereby providing insight into the integrity of the triple-helical conformation.

II.1.3. Preparation and Characterization of ZnO NPs-BV

II.1.3.1. Biosynthesis of ZnO Nanoparticles

An aqueous zinc nitrate solution was mixed with an aqueous collagen solution, and the reaction mixture was continuously shaken on a Black Chiffon shaker incubator at 60°C for 4 hours, during which the pH was adjusted using NaOH. The resulting product was centrifuged and rinsed

with double-distilled water and ethanol, respectively, before being dried and stored in an amber-colored sample vial until use **(Djouadi & Derouiche, 2021).**

II.1.3.2. Preparation of Bee Venom–Coated ZnO Nanoparticles

ZnO nanoparticles (90%) were first dispersed in a suitable volume of distilled water and placed on a magnetic agitator to ensure uniform suspension. Bee venom solution (10%) was then added dropwise to the ZnO nanoparticle suspension under continuous stirring. The mixture was maintained under agitation for four hours to allow effective coating and interaction between the venom and ZnO nanoparticles. After incubation, the suspension was centrifuged for 20 minutes, and the supernatant (homogenate) was discarded. The resulting ZnO NPs-bee venom nanocomposite was then dried in an oven at 50°C and stored for further analysis.

II.1.3.3. Characterization of Venom-Zinc Nanocomposites

II.1.3.3.1. UV-Visible Spectroscopy

The sample was analyzed using a UV–Visible spectrophotometer (JENWAY 6705) over a wavelength range of 200–800 nm to investigate its optical properties and determine the maximum absorption wavelength (λ max), as well as to confirm the formation of zinc oxide nanoparticles (ZnO NPs).

II.1.3.3.2. Fourier Infrared (FTIR) Spectroscopy

This technique was employed to identify the functional groups and characteristic chemical bonds of the sample. The analysis was carried out using fourier transform infrared spectroscopy (Agilent Technologies) at a wavenumber frequency range from 4000 to 400 cm^{-1} and a resolution of 16 cm^{-1}.

II.1.3.3.3. Scanning Electron Microscopy (SEM)

Scanning Electron Microscopy (SEM) was used to determine the surface morphology, size and shape of the ZnO NPs.

II.1.3.3.4. Energy-Dispersive X-Ray (EDX)

Energy-dispersive X-ray (EDX) was employed to confirmed the presence of zinc elements in the nanoparticles and their chemical composition.

II.1.3.3.4. X-Ray Diffractometry (XRD)

An X-ray diffractometer (PROTO® AXRD Benchtop) was utilized to detect the chemical formula, crystallite structure, lattice parameters and crystallite size of ZnO NPs. The XRD was performed in the scaling angle (2θ) range of 10-80° with Cu Kα radiation (λ = 1.540593 Å). The crystallite size was determined using the Debye-Scherrer equation, which is written as $D = k \lambda/\beta \cos \theta$. The Scherrer constant (0.9-1), the X ray wavelength (1.540593 Å), the full-width half maximum (FWHM), and the Bragg angle (θ), both stated in radians, are the parameters that are taken into consideration by the formula. Using formula $1/(d^2) = (3/4)[(h^2+hk+k^2)/a^2]+(l^2/c^2)$, where d is the interplanar spacing and h, k, and l are the Miller indices, the lattice parameters a, b, and c were found.

II.1.4. Determination of Proteins

❖ **Principle**

The tissue proteins were determined according to a colorimetric method by a SHIMATZU type spectrophotometer using Coomassie blue as a reagent, which is reacted with the amine group (NH_2) of the proteins to form a blue complex. The appearance of the blue color reflects the degree of ionization of the acid medium and the intensity corresponds to the concentration of proteins. The absorption is measured at 595 nm **(Bradford, 1976).**

❖ **Preparation of Bradford's reagent**

- Dissolve 100 mg of Coomassie blue in 50 mL of ethanol (95%).
- Shake the mixture for 2 hours with a shaker away from light.
- Add 100 mL of orthophosphoric acid (H_3PO_4) (85%)
- Complete the volume to 1 liter with distilled water.
- Filter the solution obtained with filter paper.
- **Note**: This reagent is stable for 2 weeks at 4°C.

❖ **Procedure**

1. Take 40 µL of the protein solution.
2. Add 2 mL of Coomassie blue.
3. Shake and let to stand for 5 minutes.
4. Read the optical densities against the blank at 595 nm.

5. Compare the protein concentration in the tissues studied.

The protein concentration is determined by comparison with a standard range of bovine serum albumin (0.1-0.2-0.3-0.4-0.5-0.6-0.7-0.8-0.9-1 mg/mL) previously carried out under the same conditions.

II.1.5. Preparation of ZnO NPs-BV Cream (Beevenox)

The formulation was prepared using petroleum jelly (Vaseline®) as a base, with ZnO nanoparticles (ZnO NPs) as the active ingredient. A 1% solution of the active compound was prepared. The required amount of petroleum jelly (Vaseline®) was weighed and melted, after which the active compound was added. The mixture was subjected to ultrasonication for 30 minutes at 50 °C to ensure thorough homogenization, resulting in a homogeneous formulation suitable for topical application on burns. The preparation was stored in a cool, dry place.

II.2. In vitro Study

II.2.1. Biological Activities of ZnO NPs-BV

II.2.1.1. Anti-Inflammatory Activity

II.2.1.1.1. BSA Anti-Denaturation Assay

The study examined how ZnO NPs-BV could reduce inflammation by inhibiting protein denaturation. The experiment involved incubating 0.65 mL of 1% bovine serum albumin solution with 0.65 mL of various sample concentrations (5-25-50-100-150-200 µg/mL) at room temperature for 30 minutes. Subsequently, 0.01 mL of concentrated HCl was added, and the mixture was heated at 72 °C for 30 minutes. After cooling for ten minutes, the absorbance was measured at 660 nm. Diclofenac® served as the standard treatment **(Boulaares et al., 2024).**

The percentage inhibition of protein denaturation was determined using a specific formula:

$$Inhibition\ percentage\ \% = \left(\frac{A\ sample - A\ control}{A\ sample}\right) x\ 100 \qquad (1)$$

II.2.1.1.2. RBC Membrane Stabilization Assay

The hemolysis assay was conducted following the protocol outlined by **(Boulaares et al., 2024)**. Blood was collected in EDTA-containing tubes to prevent clotting, then centrifuged at 1000

rpm and 40 °C for 10 minutes. The supernatant was carefully extracted. The erythrocytes were then subjected to three additional 5-minute washes using 1X PBS (pH 7.4). The washed erythrocytes were stored at 4 °C and utilized within 6 hours for the hemolysis assay. A mixture of 0.05 mL of diluted erythrocyte suspension (0.1 mL erythrocytes + 0.9 mL 1XPBS) was combined with 0.1 mL of test samples (ZnO NPs-BV) or standard. A 0.1 mL of 1X PBS served as the negative control. The reaction mixture was incubated at 37 °C in a water bath for 60 minutes. Subsequently, 0.85 mL of 1X PBS was added to bring the reaction mixture volume to 1 mL. The mixture was then centrifuged at 300 rpm for three minutes to separate the supernatant. The hemoglobin content in the supernatant was quantified using a spectrophotometer at 540 nm. Diclofenac® was employed as the standard.

The formula for calculating the percentage inhibition of hemolysis remained unchanged:

$$Inhibition\ percentage\ \% = 100 - \left(\frac{A\ sample}{A\ control}\right) x\ 100 \qquad (2)$$

II.2.1.2. Antioxidant Activity

II.2.1.2.1. DPPH Free-Radical Scavenging Activity

The ability of samples to neutralize the 1,1-diphenyl-2-picrylhydrazyl DPPH radical was used to assess their antioxidant properties. Various concentrations of ZnO NPs-BV, and ascorbic acid were prepared. One milliliter of samples or antioxidant standards (serving as positive control reference compounds) was combined with one milliliter of DPPH in methanol (0.1 mM). A negative control was prepared without antioxidants. After a 30-minute incubation period, the mixture's absorbance was measured at 517 nm using a UV-visible spectrophotometer **(Singh et al., 2008).**

The following formula is used to calculate DPPH free-radical scavenging activity values :

$$Inhibition\ percentage\ \% = \left(\frac{A\ control - A\ sample}{A\ control}\right) x\ 100 \qquad (3)$$

II.2.1.2.2. Ferric Reducing Antioxidant Power FRAP

The reducing power of plant extract or nanoparticles was evaluated using the method outlined by **(Rahman et al., 2015).** Various concentrations of ZnO NPs-BV and ascorbic acid were

prepared. Each test tube contained 0.25 mL of antioxidant standards or samples, 0.625 mL of potassium buffer solution (0.2 M, pH=6.6), and 0.625 mL of 1% potassium ferricyanide [$K_3Fe(CN)_6$] solution. The reaction mixtures were then incubated in a water bath at 50 °C for 20 minutes to complete the reaction. Subsequently, 0.625 mL of 10% trichloroacetic acid (TCA) solution was added to each test tube. The entire mixture underwent centrifugation at 3000 rpm for ten minutes. Following this, 1.8 mL supernatant, 1.8 mL distilled water, and 0.36 mL of 0.1% ferric chloride ($FeCl_3$) solution were combined. A negative control was prepared without antioxidants. The absorbance of the resulting solution was measured at 700 nm.

The calculation of ferric reducing antioxidant power (FRAP) values is performed as follows:

$$Inhibition\ percentage\ \% = 100 - \left(\frac{A\ control}{A\ sample}\right) x\ 100 \qquad (4)$$

II.2.1.3 .Test of Sun Protection Factor

II.2.1.3.1. Samples Preparation

In this analysis, two products were used our ZnO NPs-BV product and Bariéderm-CICA® as standard. 0.1g of all samples was weighed, transferred to a 10 mL volumetric flask, diluted to volume with ethanol (Merck product, analytical grade), followed by ultrasonication for 5 min and then filtered through cotton, rejecting the ten first mL. A 1 mL aliquot was transferred to 10 mL volumetric flask and diluted to volume with ethanol.

II.2.1.3.2. Spectrophotometric Measurement and SPF determination

The absorption spectra of samples in solution were obtained in the range of 290 to 320 nm, every 5 nm. UV/Visible spectrophotometer, equipped with 1 cm quartz cell and a computer. Three determinations were made at each point using ethanol as a blank. SPF values were determined using UV spectrophotometry and the following equation:

$$SPF = CF\ x \sum_{290}^{320} EE\ (\lambda)\ x\ I\ (\lambda)\ x\ Abs\ (\lambda) \qquad (5)$$

Where EE: erythemal effect spectrum; I : solar intensity spectrum; Abs: absorbance of sunscreen product ; CF: correction factor (= 10). The values of EE x I are constants. and are showed in **Table 03**.

Table 03: Normalized product function used in the calculation of SPF .

Wavelength (nm)	EE X I (normalized)
290	0,0150
295	0,0817
300	0,2874
305	0,3278
310	0,1864
315	0,0837
320	0,0180
Total	1

(**Mbanga et al., 2014)**

II.2.1.4. Antibacterial Activity

Antibacterial activity was tested using the disk diffusion method. The disk diffusion test was performed on Mueller-Hinton agar plates against common Gram-negative (*Pseudomonas aeruginosa* ATCC 27853 and *Escherichia coli* ATCC 25922) and Gram-positive (*Staphylococcus aureus* ATCC 25923) bacteria to evaluate the antibacterial properties of ZnO NPs-BV. The bacteria were maintained on nutrient agar plates at 4°C. They were then incubated overnight at 37°C. A standard 0.5 mL McFarland bacterial suspension was prepared in sterile physiological water. The suspension was homogeneously dispersed onto the dry surface of Mueller-Hinton agar by wiping it three times with a cotton swab. Next, sterile paper discs (Watman No. 3), 6 mm in diameter, were impregnated with 20 µL of the solution (at concentrations of 5, 10, 20, and 40 mg/mL). The discs were dried in a clean environment before being placed on the inoculated agar surface. Discs impregnated with the preparative solvent (DMSO) were used as a control. All plates were incubated at 37°C for 24 hours. The antibiotics gentamicin and ampicillin were used as controls for all pathogens. After incubation, the diameter of the inhibition zone around each disc was measured in millimeters **(Chetehouna et al., 2023).**

II.3. *In Vivo* Study

II.3.1. Wound Area Measurement

The rats were anesthetized with chloroform prior to each measurement to ensure immobilization. The major and minor wound diameters were measured using a ruler on days 1, 8, 15, 19, and 22 of the study period. Digital photographs of the wounds were captured for documentation and subsequent analysis. Wound area was then calculated using the elliptical formula (Equation 6), as this method is widely applied for estimating circular and elliptical wound areas and provides greater accuracy compared with simple linear measurements **(Jørgensen et al., 2016).**

$$Wound\ Area\ Measurement\ (cm) = \pi\ x\ a\ x\ b \qquad (6)$$

Where a= major radius / b= minor radius.

II.3.2. Relative Organ Weight

To calculate a relative organ weight, **(Mossa et al., 2015)** utilized the following formula:

$$Relative\ organ\ weight\ \% = \left(\frac{Organ\ weight\ (g)}{Body\ weight\ (g)}\right) x\ 100 \qquad (7)$$

II.3.3. Hematological Parameters

The hematological parameters: (FNS) was performed by Mindray bc31s fns.

II.3.4. Biochemical Parameters

Determinations of biochemical parameters: Albumin, Serum iron, Fasting blood glucose measured using glucometer.

II.3.5. Oxidative Stress Parameters

II.3.5.1. Preparation of Homogenates

1 g of organ tissues was homogenized in a 9 mL tris buffer saline (TBS) solution at pH 7.4. The homogenates underwent centrifugation at 4000 x g for 20 minutes at 4°C, and the supernatant was obtained for assessing oxidative stress parameters **(Derouiche et al., 2024).**

$$GSH\ (nmol/mg\ of\ tissue) = \frac{(OD \times 1 \times 1.525)}{13133 \times 0.8 \times 0.5 \times mg\ of\ tissue} \quad (8)$$

II.3.5.2. Reduced Glutathione (GSH) Levels

The measurement of GSH levels was conducted using the methodology outlined by Ellman **(Weckbecker & Cory, 1988),** which relies on the formation of a yellow color when DTNB is introduced to substances containing sulfhydryl groups. The process involved combining (0.4 mL of tissue homogenate and 0.4 mL of buffer solution) with 0.2 mL of 0.25% salicylic acid, followed by centrifugation at 2500 g for 15 minutes. Subsequently, 0.5 mL of the resulting supernatant was mixed with 0.025 mL of 0.01 M DTNB and 1 mL TBS (pH 7.4). The absorbance was then measured at 412 nm. GSH concentrations were reported in nmol/mg of tissue, calculated using a specific equation.

$$MDA\ (nmol/mg\ of\ tissue) = \frac{OD\ sample}{1.53\ x\ 10^5 x\ mg\ of\ tissue} \quad (9)$$

II.3.5.3. Malondialdehyde (MDA) Levels

The measurement of MDA in the samples was conducted using the colorimetric method described by **(Yagi, 1976).** This technique measures the optical density of a pink complex formed when TBA reactive substances condense with MDA in an acidic, heated environment in the presence of TBA. The process involved combining 200 µL of homogenate samples with 800 µL of TBA reagent in a sealed glass test tube. The mixture was then heated in a water bath at 100 °C for 15 minutes, followed by cooling in cold water for 30 minutes. After releasing the gases produced during the reaction, the solutions were centrifuged at 3000 rpm for 5 minutes. The

supernatant's optical density (OD) was then measured at λ= 532 nm using a Jenwey spectrophotometer. The concentration of thiobarbituric acid reactive substances (TBARS) was determined using the molecular extinction coefficient of MDA (Ɛ = 1,53.105 M-1.cm-1) and the following equation:

II.3.5.4. Superoxide Dismutase (SOD) Activity

This study employed the SOD activity measurement technique developed by **(Beauchamp & Fridovich, 1971)**. The procedure involved combining 25 µL of sample with 500 µL (0,1 mM, 13 mM), 900 µL phosphate buffer solution (50 mM; pH 7.8), and 50 µL of NBT (75 µM) in test tubes. After a 5-minute incubation at 25°C, 25 µL of riboflavin (2 µM) was added, followed by a 20-minute incubation in a light box. The optical density was then measured at 560 nm. SOD activity was expressed in Unit/mg of tissue, with the percentage inhibition of NBT reduction by SOD calculated using the following equation:

$$Inhibition\ percentage\ (\%) = \frac{OD\ blanc\ - OD\ sample}{OD\ blanc}\ x\ 100 \quad (10)$$

Where 1 Unit of SOD corresponds to 50% inhibition.

II.3.6. Histological Study

After the rats were sacrificed, a histological examination was performed on the spleen and skin only, using one rat from each group. Following thorough washing, the organs were fixed in a 10% formaldehyde solution. The samples were then dehydrated through a graded ethanol series after paraffin embedding. Subsequently, thin sections of 3 µm thickness were prepared using a microtome. The sections were mounted on glass slides and stained with hematoxylin and eosin (H&E). Finally, the slides were observed and analyzed under a light microscope at magnifications of 10× and 40×.

II.3.7. Statistical Analysis

The obtained values were represented as mean ± standard error mean (SEM). The statistical evaluation is carried out using the student's T-test for comparison between our experimental groups. All data in this study were examined by Minitab 13.0 software. $P < 0.05$ indicates a statistically significant difference.

Chapter II

Results & Discussion

I. Results

I.1. Preparation and Characterization of the Biomaterials Used in the Study

I.1.1. Extraction and Characterization of Collagen

I.1.1.1. Visual Observation of Collagen

The extracted collagen exhibited a pure white color and a viscous, gel-like consistency. The pH value of the extract was 5.87, indicating a slightly acidic medium, which is consistent with the nature of collagen obtained using acid-based extraction methods. These physical and chemical characteristics reflect the quality of the extract and its suitability for research and biological applications.

Figure 15: Visual Appearance of Collagen

I.1.1.2. UV-Visible Spectroscopy of Collagen

The UV-Vis absorption spectra, as shown in **Figure 16**, revealed absorption spectra in the range of 210 to 240 nm, and multiple absorption spectra at 228, 241, and 244 nm. This is attributed to the purity of the extracted collagen. The document also indicated the presence of an absorption spectrum at 262 and 250 nm, falling within the range of 250-280 nm, which corresponds to the aromatic amino acids that make up the collagen extracted from chicken feet.

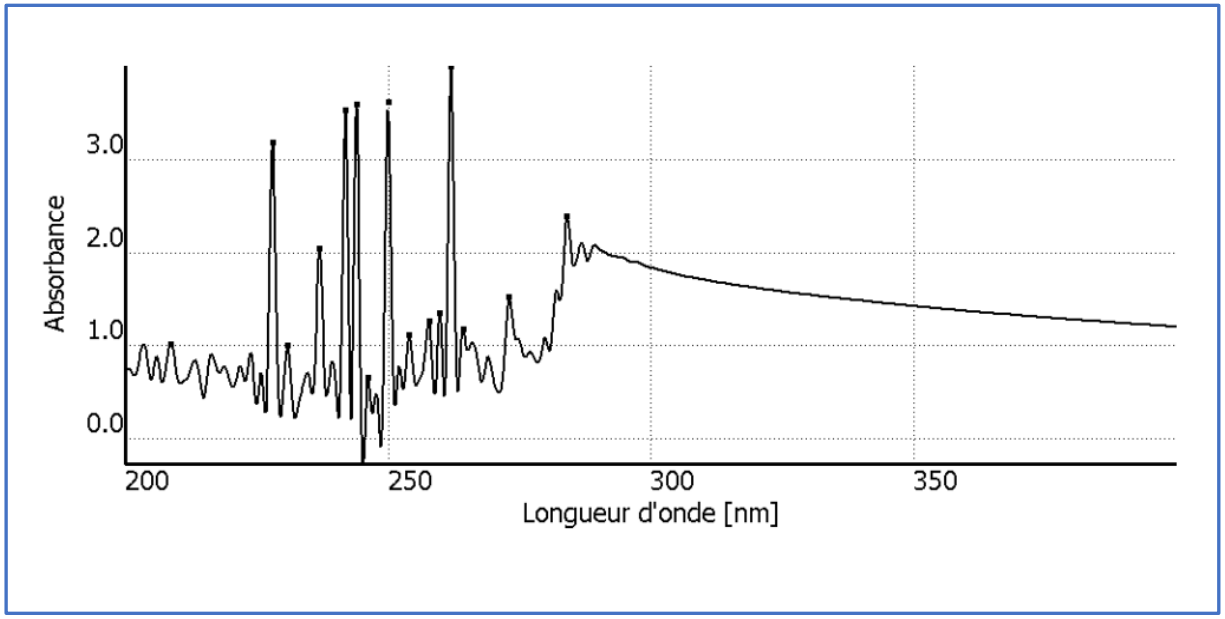

Figure 16: UV-Vis spectra of collagen

I.1.1.3. FT-IR Spectroscopy of Collagen

Fourier transform infrared spectroscopy of chicken feet collagen (**Figure 17)** showed characteristic peaks of amide A, B, I, II, III at 3300, 2924, 1640, 1520 and 1240 cm^{-1} respectively.

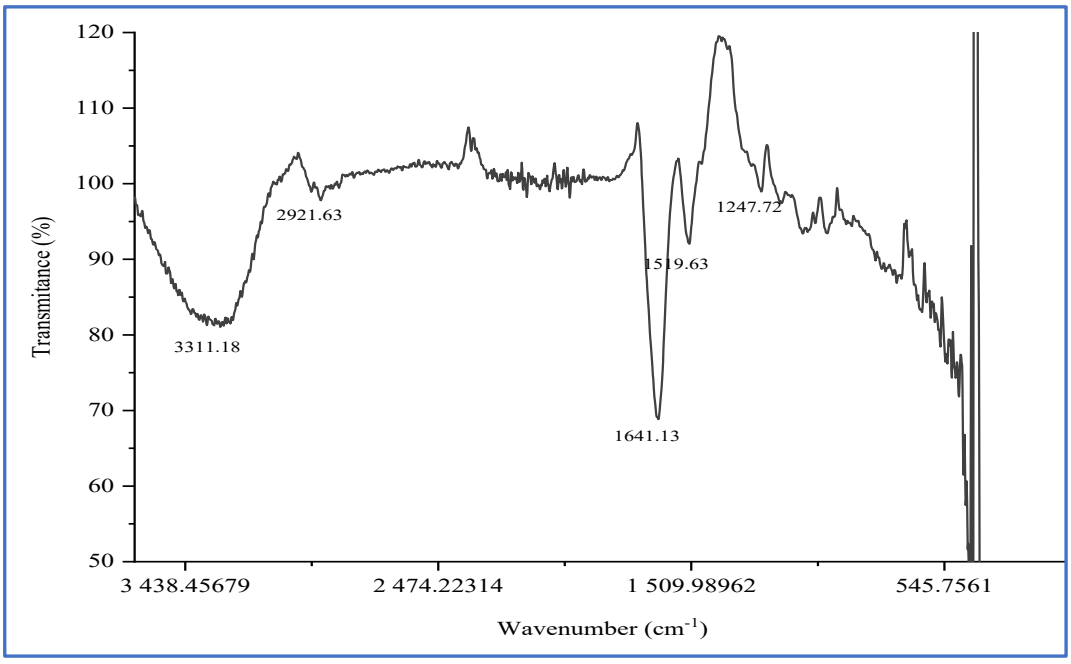

Figure 17: FTIR spectrum of collagen

Table 04: FTIR collagen peaks determination

Wavenumber (cm^{-1})	Amid	Band type
3311.18	Amid A	N–H
2921.63	Amid B	C–H
1641.13	Amid I	C=O
1819.63	Amid II	N–H, C–N
1247.72	Amid III	C–N, N–H

I.1.2. Biosynthesis and Characterization of ZnO NPs-BV

I.1.2.1. UV-Vis Spectroscopy of ZnO NPs-BV

Figure 18 shows the UV-Visible absorption spectrum of ZnO NPs-BV, with absorption peaks at 252, 258, and 260 nm within the 250-270 nm range.

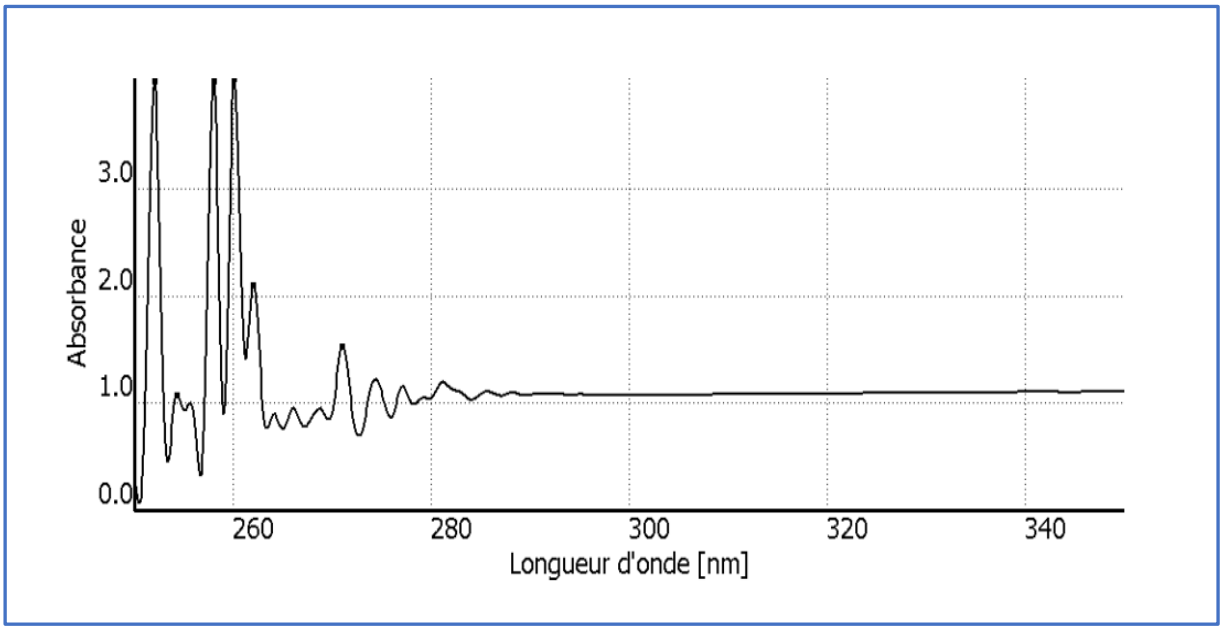

Figure 18: UV-Vis spectra of ZnO NPs-BV

I.1.2.2. FT-IR Spectroscopy of ZnO NPs-BV

Figure 19 shows the FTIR spectrum of (ZnO NPs-BV), with characteristic peaks at 3309.25, 2929.34, 1652.70, 1538.92, 1226.51, 1091.51, and 480.19 cm^{-1}.

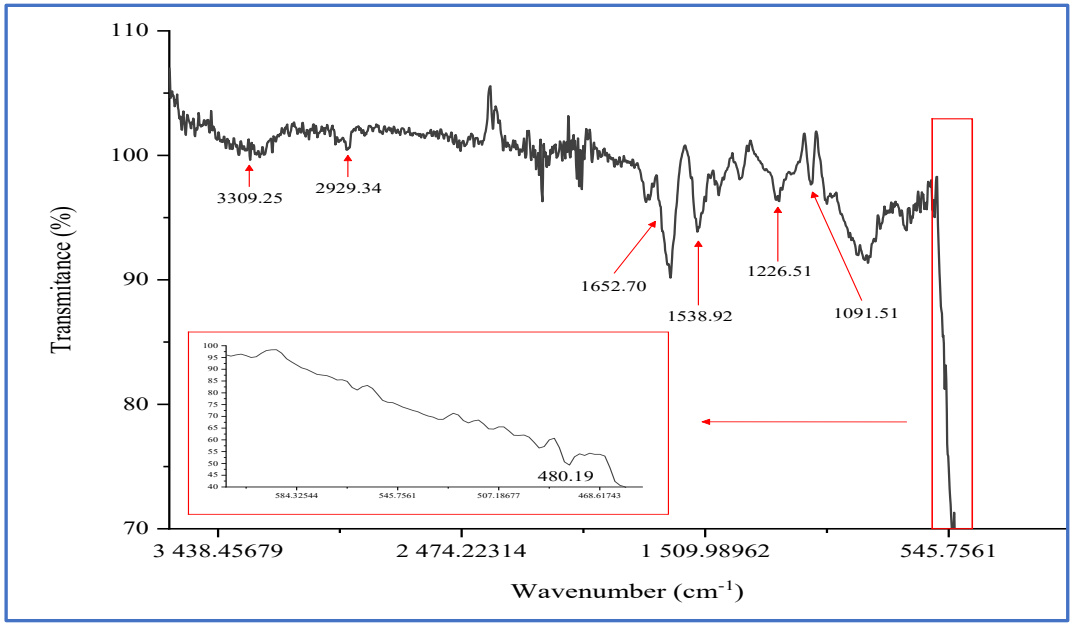

Figure 19: FTIR spectrum of ZnO NPs-BV

Table 05: FTIR ZnO NPs-BV peaks determination

Wavenumber (cm^{-1})	Band type
3309.25	O–H / N–H (proteins, biomolecules)
2929.34	C–H stretching
1652.70	Amide I (C=O, proteins)
1538.92	Amide II (N–H banding)
1226.51	C–N / Amide III
1091.51	C–O / C–N
480.19	Zn–O (ZnO nanoparticle formation)

I.1.2.3. SEM and EDX Study of ZnO NPs-BV

In **Figure 20**, the scanning electron microscopy (SEM) image illustrates the surface morphological characteristics of the nanoparticles. A structure composed of aggregated clusters was observed. In contrast, **Figure B** presents the Energy Dispersive X-ray (EDX) analysis results, which reflect the elemental composition of the sample. The results clearly confirmed the presence of zinc and oxygen, consistent with the formation of zinc oxide nanoparticles. Additionally, the EDX data revealed the presence of carbon, indicating traces of organic components associated with the surface of the nanoparticles (**Table 1**).

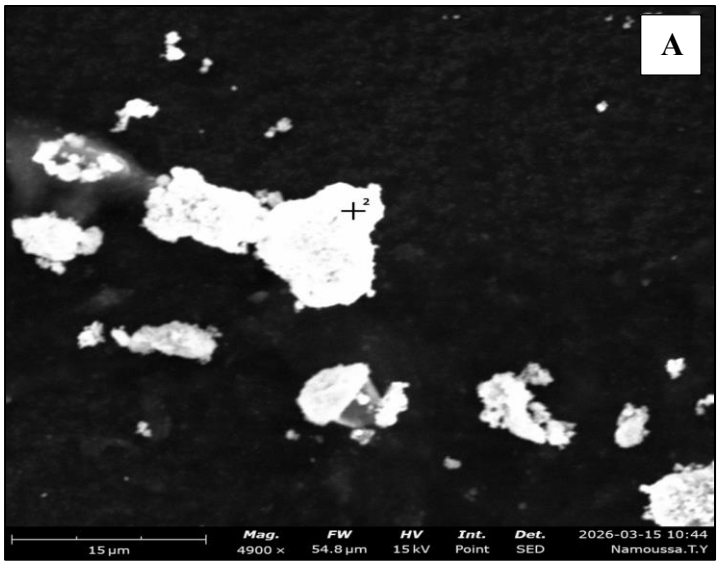

B

Element Symbol	Atomic Conc.	Weight Conc.
Zn	35.61	74.55
C	59.02	22.70
O	5.37	2.75

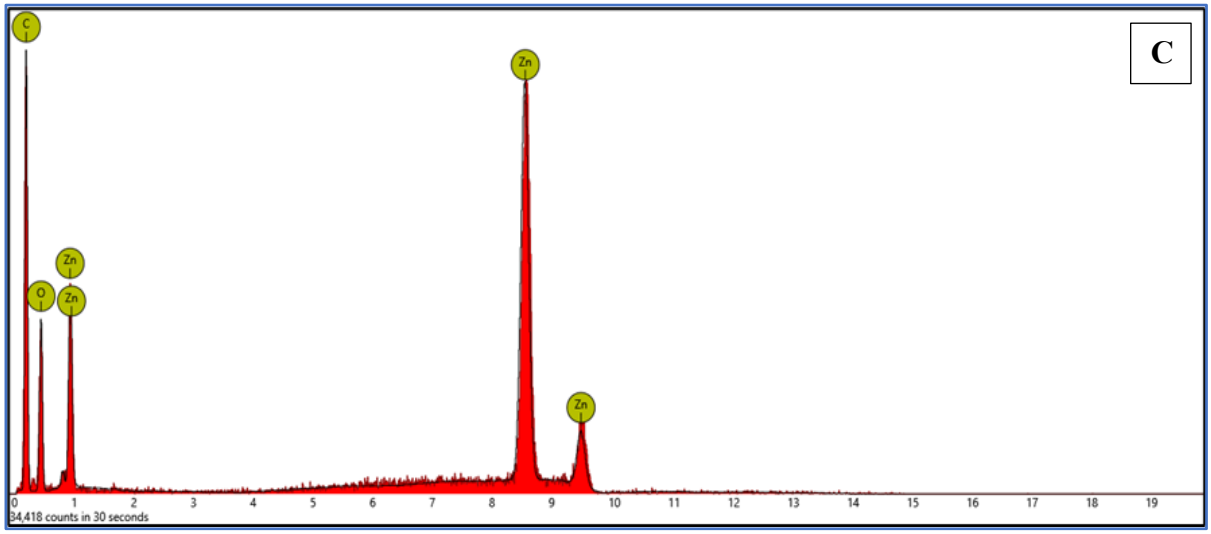

Figure 20: (**A**) SEM image and (**C**), **(B)** EDX spectrum of ZnO NPs-BV

I.1.2.4. DRX Study of ZnO NPs-BV

According to the XRD data that matched the JCPDS card Nº 01-079-0207 database, the chemical formula of the zinc oxide nanoparticles was ZnO, and their crystallite structure was hexagonal. The lattice parameters were a = b = 3.26 Å ≠ c = 5.21 Å, with a crystallite size (D) of 33.4 nm. The diffraction angles corresponded to the (100), (002), (101), (102), (110), (103), (200), (112), (201), (004) and (202) h, k, and l crystallite planes, respectively, with peaks at 31.69°, 34.35°, 36.18°, 47.47°, 56.48°, 62.74°, 66.29°, 67.88°, 69.03°, 72.52° and 76.87° (**Figure 21**).

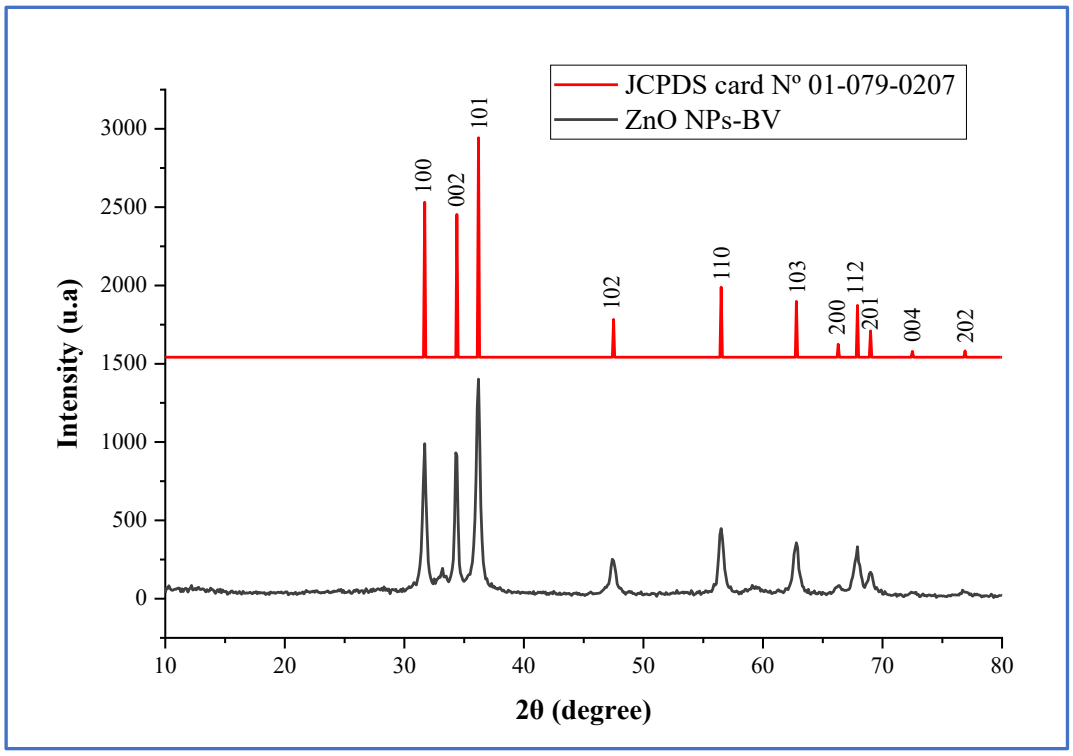

Figure 21: XRD patterns of ZnO NPs-BV

I.1.3. Protein Determination (Protein Immobilization)

Figure 22 shows that the immobilization yield (IY) of bee venom onto ZnO NPs-BV was 42.6%.

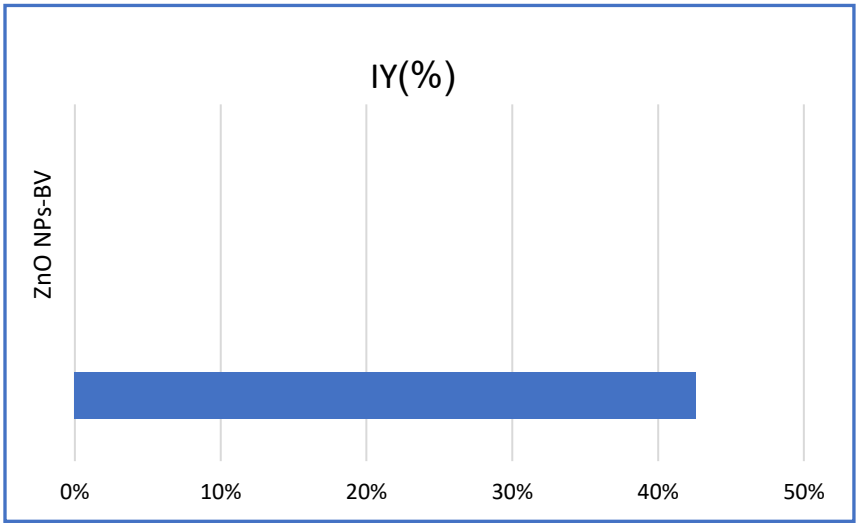

Figure 22: Immobilization yield of ZnO NPs-BV

I.2. In-vitro Study of Zinc Oxide Nanoparticles-Bee Venom (ZnO NPs-BV)

I.2.1. Biological Applications of ZnO NPs-BV

I.2.1.1. *Anti-Inflammatory Activity*

I.2.1.1.1. BSA Anti-Denaturation Assay

As shown in **Figure 23**, zinc oxide nanoparticles ZnO NPs-BV exhibited considerable anti-inflammatory activity.

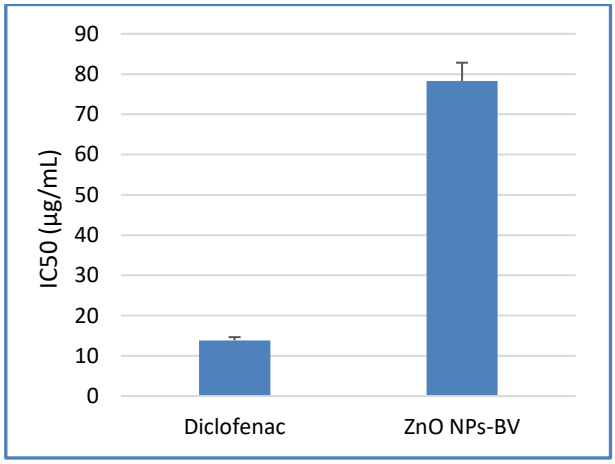

Figure 23: IC_{50} values of anti-denaturation assay of diclofenac® and ZnO NPs-BV

I.2.1.1.2. RBC Membrane Stabilization Assay

Figure 24 shows that the prepared bee venom-coated zinc oxide nanoparticles (ZnO NPs-BV) possess high anti-inflammatory activity.

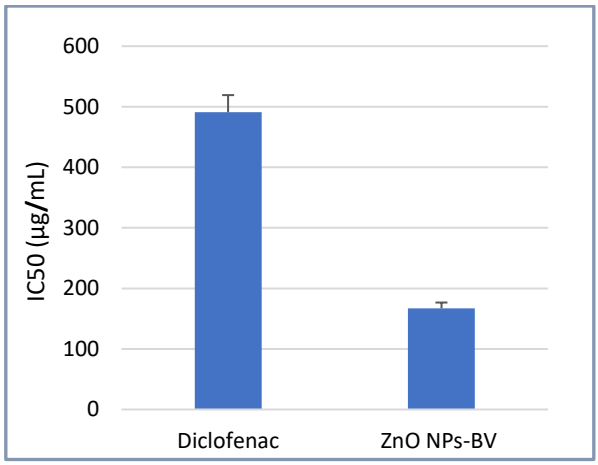

Figure 24: IC_{50} values of RBC membrane stabilization assay of diclofenac® and ZnO NPs-BV

I.2.1.2. Antioxidant Activity

I.2.1.2.1. DPPH Free-Radical Scavenging Activity

The sample shows a clear ability to inhibit DPPH radicals, indicating that it possesses measurable antioxidant activity **(Figure 25)**.

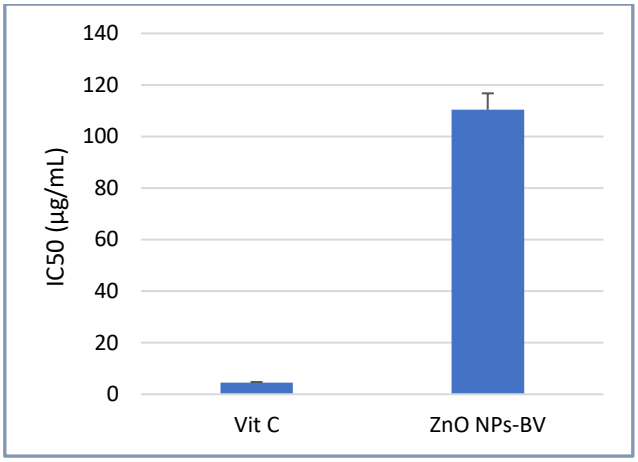

Figure 25: IC_{50} values of DPPH scavenging activity of Vit C and ZnO NPs-BV

I.2.1.2.2. Ferric Reducing Antioxidant Power FRAP

As demonstrated in **Figure 26,** the zinc oxide nanoparticles ZnO NPs-BV had a reasonable antioxidant activity.

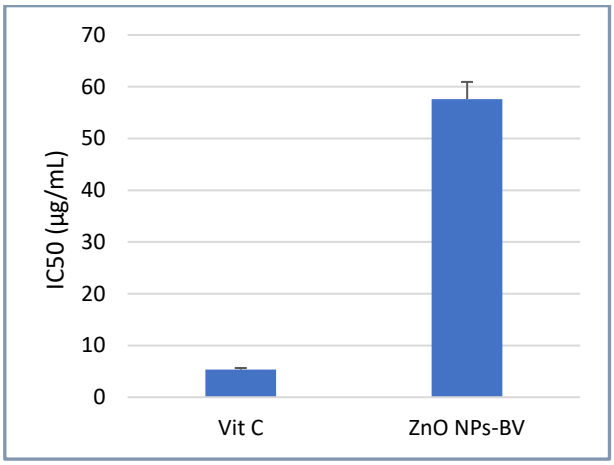

Figure 26: IC_{50} values of FRAP of Vit C and ZnO NPs-BV

I.2.1.3. Sun Protection Factor (SPF) Test

As shown in **Figure 27**, ZnO NPs-BV exhibited notable photoprotective properties, with a performance comparable to that of a commercial sunscreen formulation.

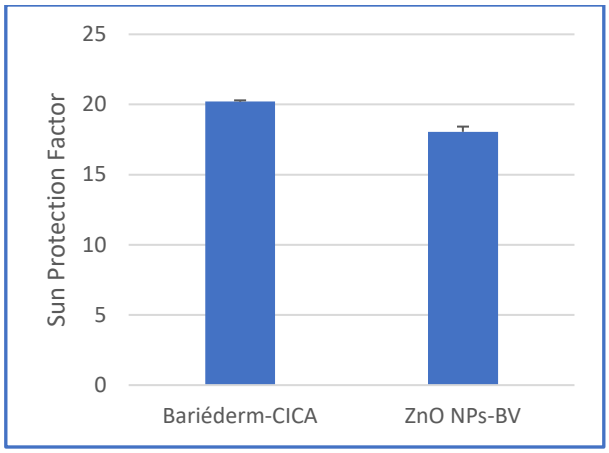

Figure 27: Sun protection factor values of bariéderm-CICA and ZnO NPs-BV

I.2.1.4. Antibacterial Activity (Disk Diffusion Assay)

The results showed antibacterial activity that varied depending on the concentration and bacterial strain. For *Pseudomonas aeruginosa*, the largest inhibition zone diameter (16 mm) was recorded at a concentration of 40 mg/mL, with a gradual decrease to 14, 13, and 8 mm at concentrations of 20, 10, and 5 mg/mL, respectively, indicating a clear direct relationship between concentration and antibacterial activity. *Escherichia coli*, on the other hand, exhibited relative resistance, with weak inhibition zones (7 and 6.5 mm) recorded at concentrations of 40 and 20 mg/mL, respectively, while no effect was observed at lower concentrations, suggesting a low susceptibility of this strain to the studied sample. For *Staphylococcus aureus*, moderate activity was observed, with the zone of inhibition diameter reaching 10 mm at a concentration of 40 mg/mL, gradually decreasing to 9, 8.5, and 7 mm at lower concentrations, further confirming the dose-dependent effect. In comparison with other antibiotics, Gentamicin demonstrated considerable activity against all strains, with zone of inhibition diameters ranging from 16 to 17.5 mm, reflecting its broad spectrum. In contrast, Ampicillin exhibited selective activity, showing no effect against *Pseudomonas aeruginosa*, while being effective against *Escherichia coli* (16 mm) and more effective against *Staphylococcus aureus* (35 mm). In general, these results show that the sample has a dose-dependent antibacterial activity, with a clear difference in the susceptibility of the strains, with *Escherichia coli* being the most resistant, while both *Staphylococcus aureus* and *Pseudomonas aeruginosa* showed greater susceptibility, especially at high concentrations (**Figure 28)**.

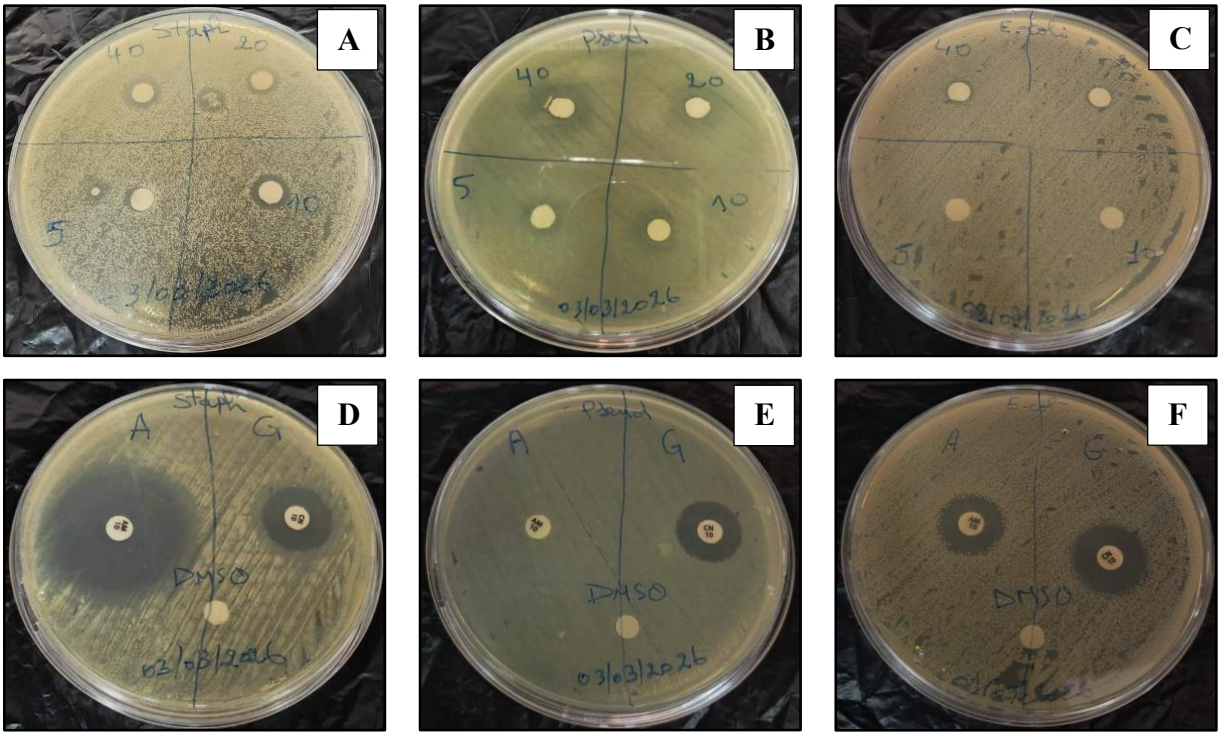

Figure 28: Zone of inhibition produced by ZnO NPs-BV (A-C), and antibiotics (D-F) against different strains tested

Table 06: Zone of inhibition against different strains tested

		Pseudomonas aeruginosa	***Escherichia coli***	***Staphylococcus aureus***
		Gram$^-$		**Gram$^+$**
		ATCC 27853	**ATCC 25922**	**ATCC 25923**
Treatments	**Concentration (mg/mL)**	**Inhibition zone (mm)**		
ZnO NPs-BV	**05**	8±0.462	0±0	7±0.404
	10	13±0.751	0±0	8.5±0.491
	20	14±0.808	6.5±0.375	9±0.52
	40	16±0.924	7±0.404	10±0.577
Antibiotic	**Gentamicin**	16±0.924	17.5±1.01	17.5±1.01
	Ampicillin	0±0	16±0.924	35±2.02
Negative control	**DMSO**	0±0	0±0	0±0

I.3. *In Vivo* Study Zinc Oxide Nanoparticles-Bee Venom (ZnO NPs-BV)

I.3.1. Wound Area Measurement

The photographic images of the wounds showed progressive improvement in wound healing in the treated groups compared with the untreated group. The ZnO NPs-BV-treated group exhibited faster wound closure, improved tissue regeneration, and hair growth, particularly during the final days of the experiment, which is consistent with the wound measurement results (**Figure 29)**.

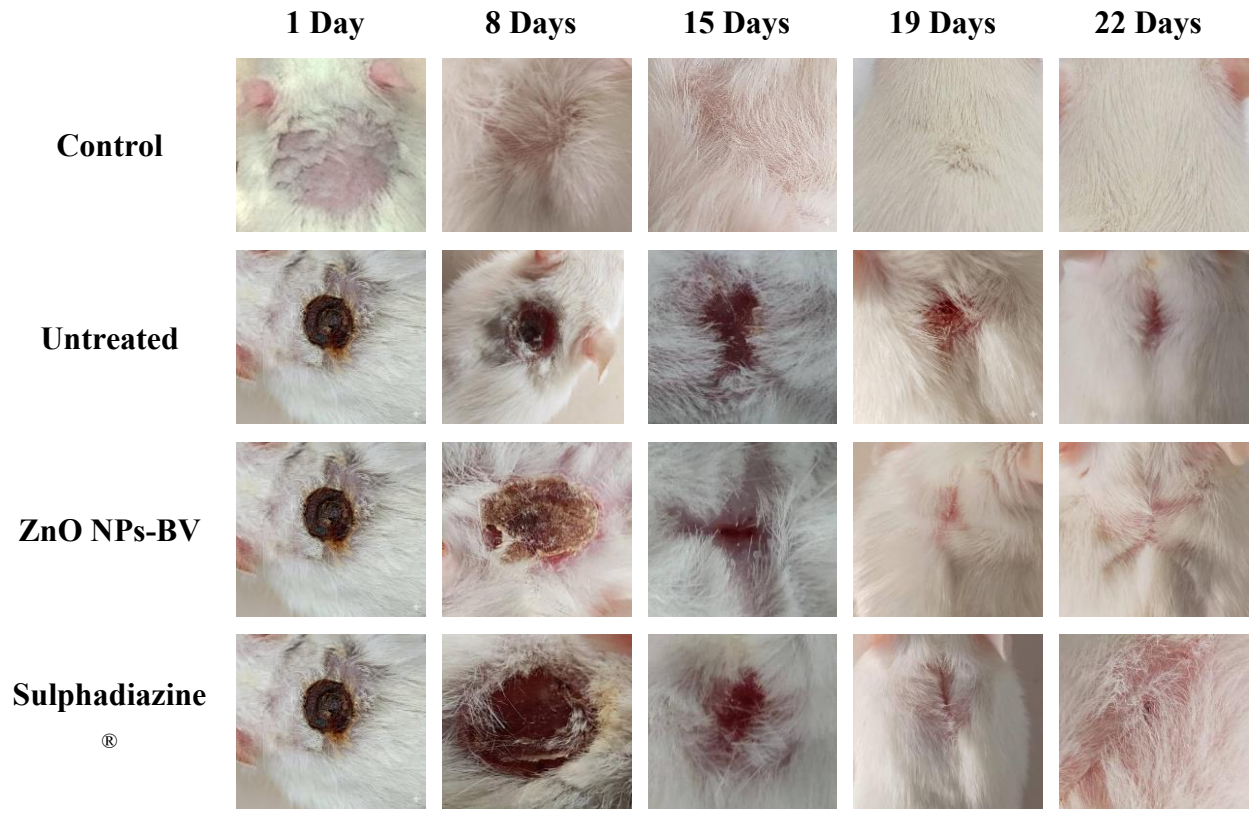

Figure 29: Macroscopic evaluation of burn injury on rats

The graph in **(Figure 30)** shows the change in wound area during the experimental period for the studied groups compared to the untreated group. We observe a significant increase ($p>0.01$) for the ZnO NPs-BV-treated group on day 8, with varying significant decreases on the remaining days for the same group ($p<0.05$) on day 19 and ($p<0.001$) on days 15 and 22. As for the sulfadiazine group, there is no significant difference throughout the experimental period.

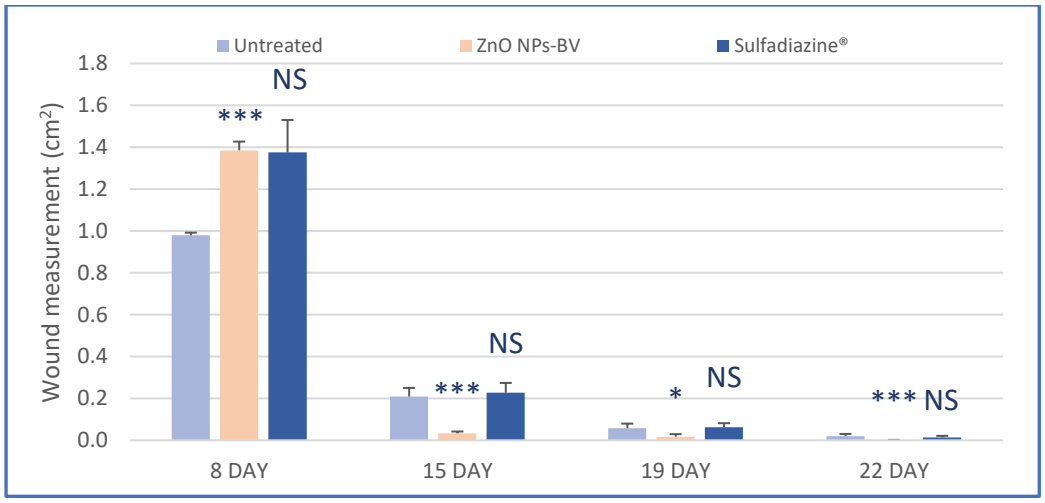

Figure 30: Wound measurement at different time points during healing

Data are expressed as mean ± SD (n=5).

* p<0.05, *** p<0.001: significantly different from control group.

NS: No significance difference.

I.3.2. Relative Organs Weight

The relative organs weight was summarized in **(Table 07)** for the different experimental groups (control, untreated, ZnO NPs-BV, and sulfadiazine®). The results showed that, when comparing the control group with both the untreated group and the treated groups, no significant differences were observed in liver weight, and similarly, comparisons between the treated groups (ZnO NPs-BV and sulfadiazine) and the untreated group also revealed no significant changes in liver weight. Regarding spleen weight, no significant difference was observed between the ZnO NPs-BV group and the untreated group, whereas a significant decrease was recorded in the sulfadiazine group compared to the untreated group ($p < 0.001$). Overall, the treatments did not induce noticeable effects on the relative weights of the studied organs, except for the decrease observed in spleen weight in the sulfadiazine group.

Table 07: Relative organs weight for control and experimental groups

Relative Organs Weight (%)	Control	Untreatment	ZnO NPs-BV	Sulphadiazine®
Liver	4,44±0,127	4,4826±0,0324^{NS}	4,225±0,114$^{NS NS}$	4,368±0,162$^{NS NS}$
Spleen	0,00255±0,00008	0,00247±0,00005^{NS}	0,00215±0,00016$^{NS NS}$	0,00208±0,00006^{***c}

Data are expressed as mean ± SD (n=5).

*** p<0.001: significantly different from control group.

[c] p<0.001: significantly different from untreated group.

NS: No significance difference.

I.3.3. Hematological Parameters

I.3.3.1. Leucocyte Line Markers

The results presented in **(Table 08)** showed a significant increase in white blood cell count in the untreated group compared to the control group (p<0.01), whereas only a slight increase was observed in the Sulfadiazine® and ZnO NPs-BV groups (p>0.05), with a marked decrease recorded in the ZnO NPs-BV group compared to the untreated group (p<0.01). In addition, neutrophil levels increased in all groups compared to the control group, while the decrease was slight in the ZnO NPs-BV group (p>0.05) and more pronounced in the Sulfadiazine® group (p<0.01) compared to the untreated group. Regarding lymphocytes, their level increased significantly in the untreated group compared to the control group (p<0.001), whereas no significant difference was observed in the Sulfadiazine® and ZnO NPs-BV groups (p>0.05), with a marked reduction in both groups compared to the untreated group (p<0.01). As for monocytes, a significant increase was observed in the Sulfadiazine® and untreated groups (p<0.01), while a greater increase was recorded in the ZnO NPs-BV group (p<0.001), with no significant difference compared to the untreated group (p>0.05).

Table 08: Leukocytes line markers level in control and experimental groups

Parameter	Control	Untreated	ZnO NPs-BV	Sulfadiazine®
WBC $10^3/mm^3$	6.953±0.417	8.3±0.298**	6.933±0.301 NS b	6.963 ±0.379NS a
Neutrophiles $10^3/mm^3$	1.537±0.0741	1.667±0.142NS	1.650±0.117NS NS	1.500±0.0258NS b
Lymphocytes $10^3/mm^3$	4.467±0.295	5.767±0.142***	4.267±0.231NS b	4±0.246NS b
Monocytes $10^3/mm^3$	0.5467±0.0374	0.825±47.4**	0.875±0.0303*** NS	0.800±0.0516**NS

Data are expressed as mean ± SD (n=5).

** p<0.01, *** p<0.001: significantly different from control group.

[a] p<0.05,[b] p<0.01: significantly different from untreated group.

NS: No significance difference.

I.3.3.2. Erythrocyte Line Markers

The study results indicated varying hematological changes among the groups. Red blood cell counts decreased significantly in the untreated and Sulfadiazine® groups compared to the control group ($p<0.01$), while the decrease was slight in the ZnO NPs-BV group ($p>0.05$). Compared to the untreated group, no significant differences were observed in the treated groups ($p>0.05$). Conversely, hemoglobin levels increased significantly in the ZnO NPs-BV group compared to the control and untreated groups ($p<0.01$ and $p<0.001$, respectively), whereas the increase was slight in the other groups ($p>0.05$), with a significant increase observed in the Sulfadiazine® group compared to the untreated group ($p<0.01$). Hematocrit also showed a significant decrease in both the untreated and Sulfadiazine® groups compared to the control group ($p<0.01$), and a lower decrease in the ZnO NPs-BV group ($p<0.05$), while it increased compared to the untreated group in both the Sulfadiazine® group ($p<0.01$) and the ZnO NPs-BV group ($p<0.05$). Regarding the MCV index, a slight increase was observed in the ZnO NPs-BV and Sulfadiazine® groups ($p>0.05$), whereas a significant increase was recorded in the untreated group ($p<0.01$), with no significant differences compared to the untreated group ($p>0.05$). In addition, both MCH and MCHC increased significantly compared to the control group ($p<0.001$), with a slight significant decrease in the MCHC index observed in both the Sulfadiazine® group ($p<0.01$) and the ZnO NPs-BV group compared to the untreated group. Meanwhile, the RDW index decreased in all groups compared to the control group, with a more significant decrease observed in the Sulfadiazine® and untreated groups ($p<0.001$), and a less pronounced decrease in the ZnO NPs-BV group ($p<0.01$). Finally, the platelet index increased in the untreated group ($p<0.001$), was lower in the ZnO NPs-BV group ($p>0.05$), and decreased in the Sulfadiazine® group, with a decrease compared to the untreated group observed in both the Sulfadiazine® group ($p<0.01$) and the ZnO NPs-BV group ($p>0.05$) **(Table 09)**.

Table 09: Erythrocytes line markers level in control and experimental groups

Parameter	Control	Untreated	ZnO NPs-BV	Sulfadiazine®
RBC $10^6/mm^3$	8.353±0.102	6.877±0.155**	7.832±0.387$^{NS\ NS}$	7.024±0.126^{**NS}
Hemoglobine g/L	14.45±0.065	14.367±0.127^{NS}	15.825±0.244$^{**\ b}$	14.640±0.08$^{NS\ a}$
Hematocrite %	43.450±0.476	35.925±0.534***	39.67±1.43$^{*\ a}$	36.820±0.196$^{***\ b}$

M.C.V fl	51.17±0.505	52.933±0.415**	52.15±0.581NS NS	51.78±0.741 NSNS
M. C. H pg	17.233±0.116	20.833±0.283***	21.320±0.74**NS	20.920±0.355***NS
M. C. H. C g/dl	32.667±0.054	40.1±0.169***	40.46±1.06**NS	39.820±0.0.079***b
RDW %	15.767±0.284	13.175±0.168***	12.980±1.549**NS	12.940±0.247***NS
Platelets	908.33±0.79	980.5±4.78***	914.3±19.1NS b	841±56.9NSNS

Data are expressed as mean ± SD (n=5).

* p<0.05, ** p<0.01, *** p<0.001: significantly different from control group.

[a] p<0.05, [b] p<0.01: significantly different from untreated group.

NS: No significance difference.

I.3.4. Biochemical Parameters

I.3.4.1. Iron

Iron levels showed significant deascrease in untreated group (p<0.01) compared with control group. The ZnO NPs-BV group exhibited significant deascrease in iron levels compared to the control group (p<0.01). In contrast, the sulfadiazine group showed no significant differences compared to either the control group or the untreated group. **(Figure 31)**

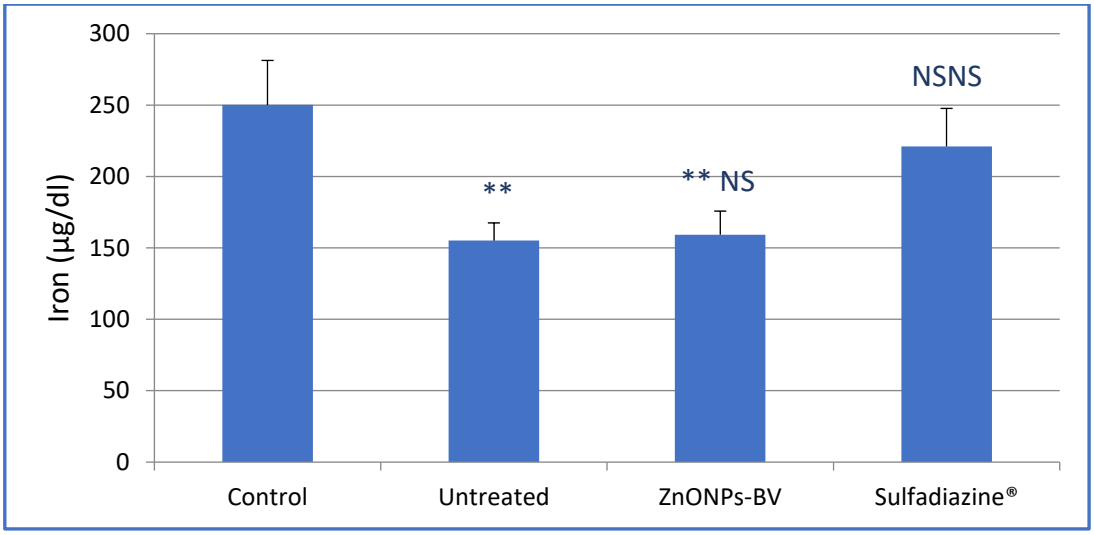

Figure 31: Serum iron levels across experimental groups

Data are expressed as mean ± SD (n=5).

** p<0.01: significantly different from control group.

NS: No significance difference.

I.3.4.2. Albumin

Albumin levels showed significant variations among the studied groups, with the untreated group exhibiting a significant decrease compared to the control group ($p<0.01$), reflecting the impact of the untreated condition on this parameter. In contrast, the ZnO NPs-BV group showed no significant difference compared to the control group, while a significant difference was observed compared to the untreated group ($p<0.01$). The sulfadiazine group showed the same pattern, with no significant difference compared to the control group, and a significant difference compared to the untreated group ($p<0.01$) **(Figure 32)**.

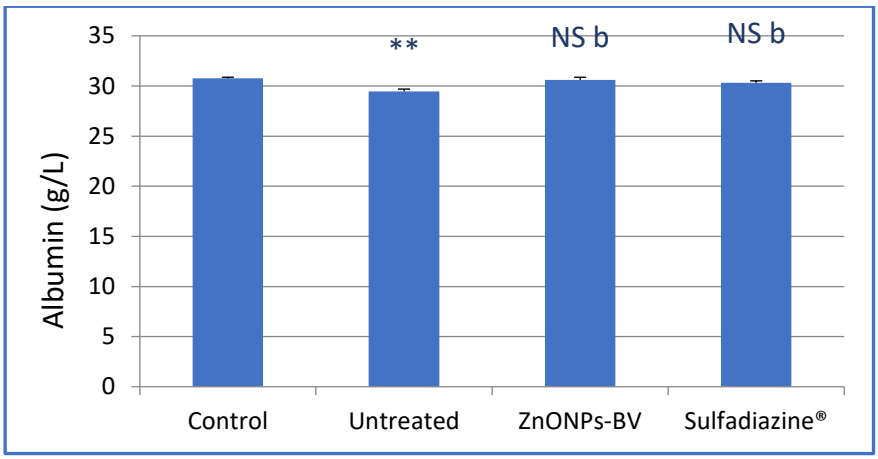

Figure 32: Serum albumin levels across experimental groups

Data are expressed as mean ± SD (n=5).

** $p<0.01$: significantly different from control group.

b $p<0.01$: significantly different from untreated group.

NS: No significance difference.

I.3.4.3. Blood Glucose

Blood glucose levels showed significant variations among the studied groups, with the untreated group exhibiting a significant increase compared to the control group ($p<0.01$). In contrast, both the ZnO NPs-BV group and the sulfadiazine group showed no significant difference compared to the control group, while both exhibited a significant difference compared to the untreated group, at ($p<0.01$) for the ZnO NPs-BV group and ($p<0.01$) for the sulfadiazine group **(Figure 33)**.

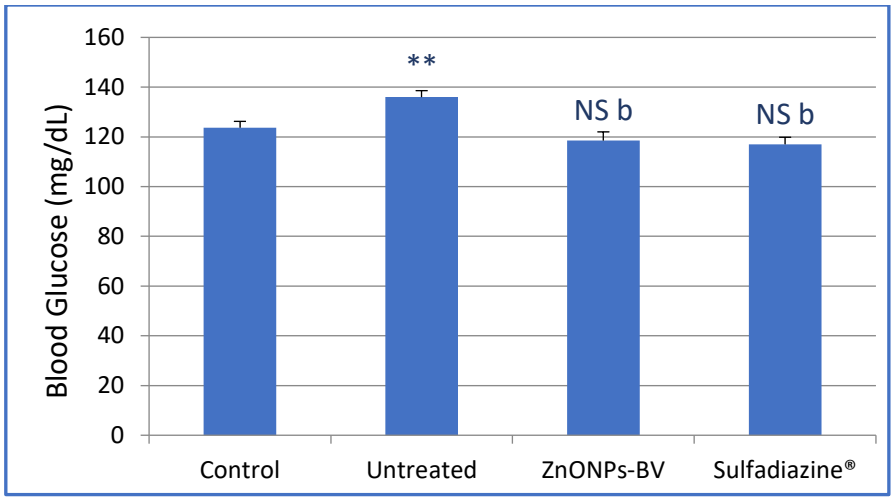

Figure 33: Blood glucose levels across experimental groups

Data are expressed as mean ± SD (n=5).

** $p<0.01$: significantly different from control group.

b $p<0.01$: significantly different from untreated group.

NS: No significance difference.

I.3.5. Oxidative Stress Parameters

I.3.5.1. Malondialdehyde (MDA) Levels

After comparison of MDA levels with the control groups, the results revealed a significant increase in the spleen and skin ($p<0.001$) and in the liver ($p<0.01$) in the untreated group. The ZnO NPs-BV group also showed a significant increase in the skin ($p<0.001$), accompanied by a significant decrease in the liver ($p<0.05$). Finally, sulfadiazine group exhibited significant increases in the liver ($p<0.01$). On the other hand, compared with untreated group, the data demonstrated a significant decrease in all organs, including the liver, spleen ($p<0.001$), in both ZnO NPs-BV and sulfadiazine groups, Except for skin ($p<0.05$) in sulfadiazine group. **(Figure 34).**

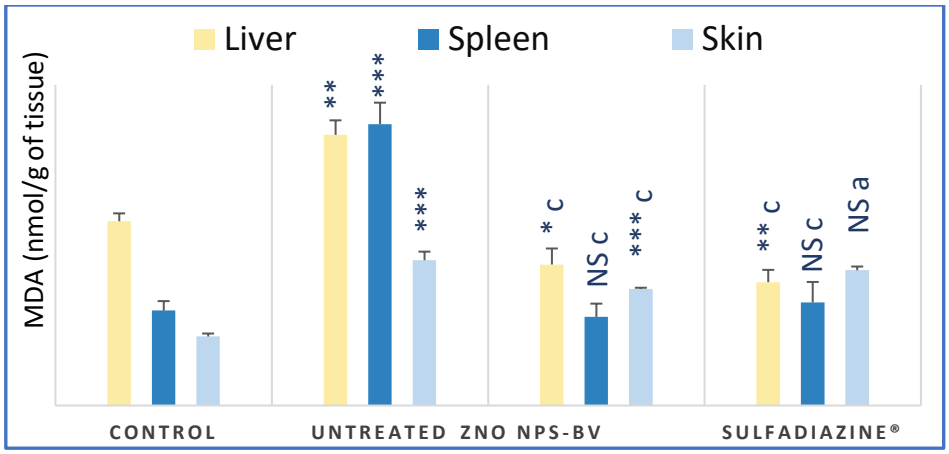

Figure 34: MDA levels in control and experimental groups

Data are expressed as mean ± SD (n=5).

* p<0.05, ** p<0.01, *** p<0.001: significantly different from control group. NS: No significance difference.

a p<0.05, c p<0.001: significantly different from untreated group.

I.3.5.2. Reduced Glutathione (GSH) Levels

Compared with control group, GSH activity in the liver and spleen showed a significant decrease (p<0.001) in the untreated group. Similarly, a significant reduction in GSH activity was recorded in liver and spleen (p<0.001), as well as in the skin (p<0.05), in the ZnO NPs-BV group. Moreover, sulfadiazine group exhibited a significant decrease in all examined organs: liver and skin (p<0.001) and spleen (p<0.01). Furthermore, compared with untreated group, the ZnO NPs-BV group showed a significant decrease in the skin (p<0.05), while sulfadiazine group demonstrated a significant decrease in liver (p<0.01) and skin (p<0.001), together with a significant increase in the spleen (p<0.01) **(Figure 35).**

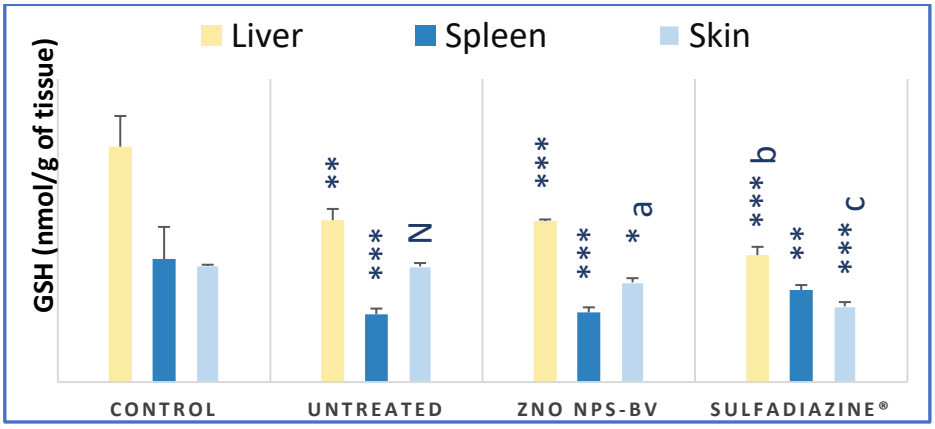

Figure 35: GSH levels in control and experimental groups

Data are expressed as mean ± SD (n=5).

* p<0.05, ** p<0.01, *** p<0.001: significantly different from control group.

a p<0.05, b p<0.01, c p<0.001: significantly different from untreated group.

NS: No significance difference.

II.3.5.3. Superoxide Dismutase (SOD) Activity

The results of SOD levels in the different tissues presented in **(Figure 36)** showed that, compared with the control group, the untreated group exhibited a highly significant increase in SOD levels in the skin (p<0.001), along with a significant decrease in the liver (p<0.001) and spleen (p<0.01). In the ZnO NPs-BV group, a significant increase was observed in liver (p<0.01). In contrast, sulfadiazine group showed a significant increase in the liver (p<0.01) and a significant increase in the skin (p<0.05). Compared with the untreated group, a significant increase in SOD levels was observed in the liver (p<0.001), together with a significant decrease in the skin (p<0.001) in the ZnO NPs-BV group. A similar pattern was also recorded in sulfadiazine group.

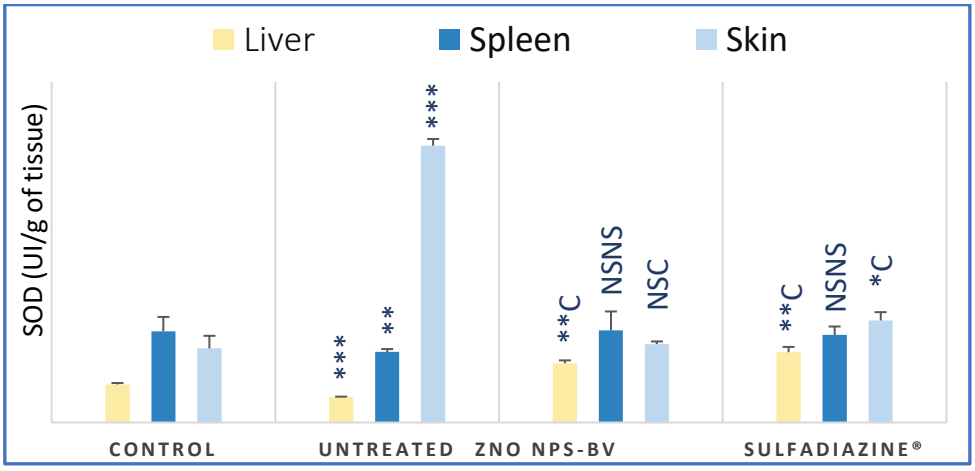

Figure 36: SOD levels in control and experimental groups

Data are expressed as mean ± SD (n=5).

* p<0.05, ** p<0.01, *** p<0.001: significantly different from control group.

c p<0.001: significantly different from untreated group.

NS: No significance difference.

I.3.6. Histological Study

I.3.6.1. Photomicrographs of Spleen Section

(**Figure 37)** illustrates histological sections of the spleen in all experimental groups stained with hematoxylin and eosin (H&E) at two different magnifications (×10 and ×40), three weeks after burn induction. Histological examination of the control group revealed a normal splenic architecture, with well-preserved tissue organization and a clear distinction between the white pulp and red pulp, reflecting the integrity of the splenic structure and its normal physiological functions.In contrast, burn injury induced marked histological alterations in the untreated group, characterized by evident disruption of both the white and red pulp architecture, along with the presence of edematous areas and cell-free spaces. These findings indicate significant impairment of splenic histoarchitecture and immune response as a consequence of burn-associated inflammatory stress. On the other hand, the groups treated with ZnO NPs-BV and sulfadiazine exhibited a histological appearance closely resembling that of the control group, where the structural integrity of both white and red pulp, as well as the marginal zone, was largely preserved. A clear restoration of normal splenic architectural organization was observed, reflecting improved tissue integrity and recovery of the organ's immunological homeostasis.

	(A): 10 x 10	**(B): 40 x 10**
Control	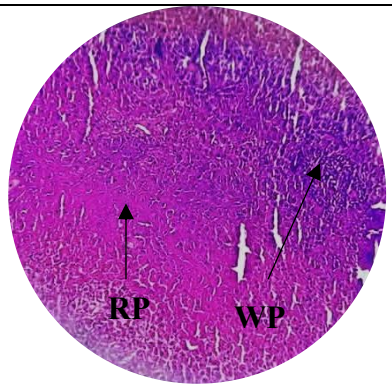	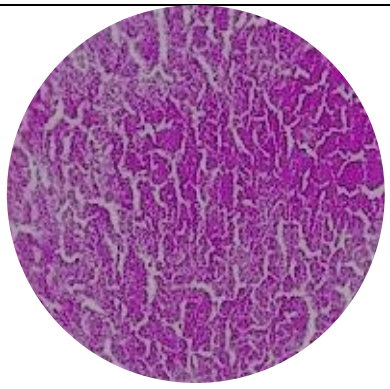

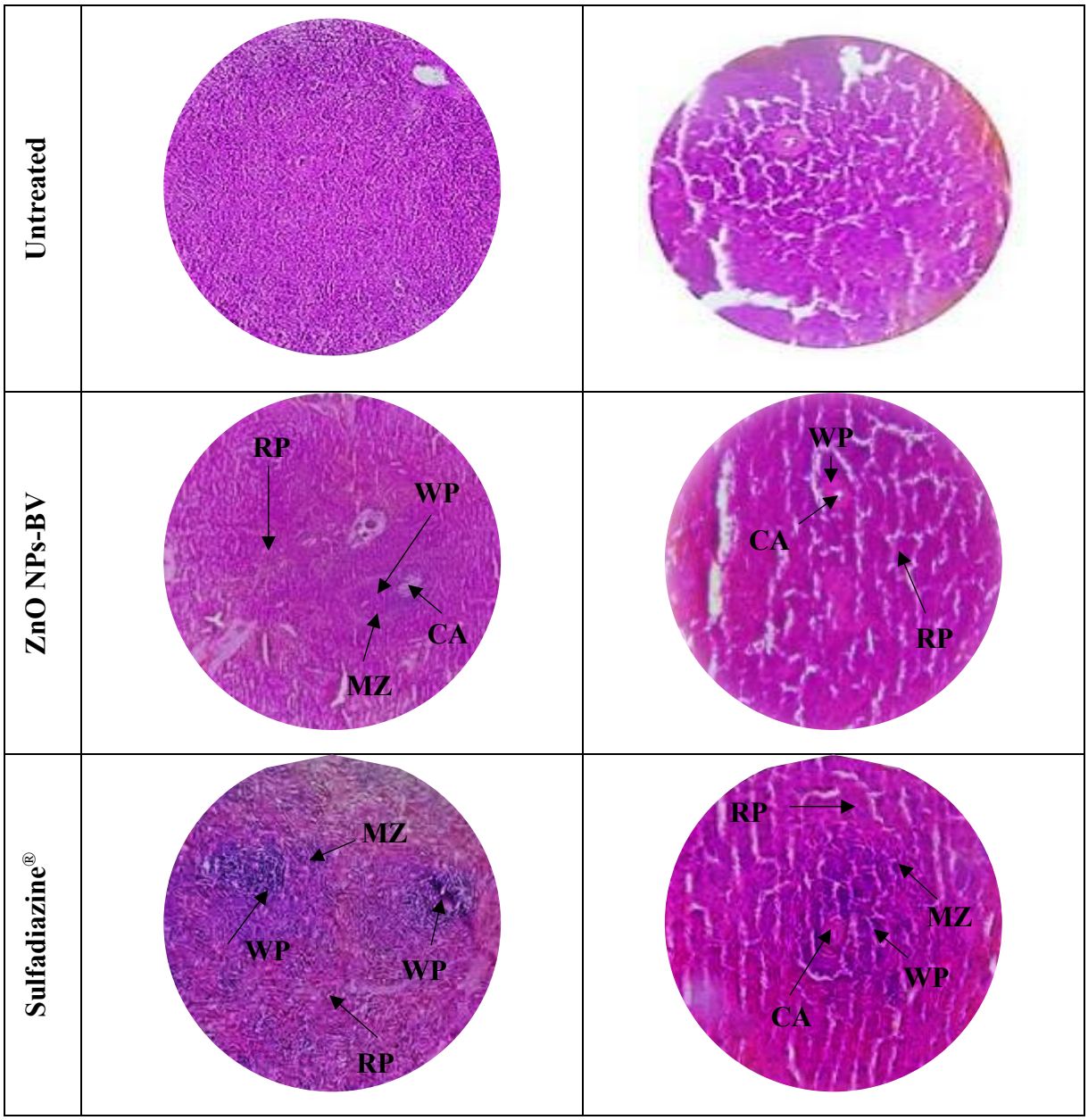

Figure 37: Histological photomicrographs of spleen section of all experimental groups stained with hematoxylin and eosin (H&E), (A): x 40 and (B): x 100

RP: Red pulp, **WP:** White pulp, **CA:** Central Arteriole, **MZ:** Marginal Zone

I.3.6.2. Photomicrographs of Skin Section

The figure shows histological sections of the skin in all experimental groups stained with hematoxylin and eosin (H&E) at two different magnifications (×10 and ×40). The control group showed a normal skin histoarchitecture, with intact and well-organized epidermal layers exhibiting clear stratification, and a well-structured dermis containing regularly arranged collagen fibers and

normal skin appendages. In contrast, the untreated burn group displayed pronounced histological alterations, including disruption and disorganization of the epidermal layer, degeneration of dermal collagen fibers, as well as marked inflammatory cell infiltration and vascular congestion, reflecting the direct histopathological impact of burn injury. Conversely, the group treated with ZnO NPs-BV showed significant histological improvement, characterized by re-epithelialization and substantial restoration of dermal architecture, along with a marked reduction in inflammatory infiltration and reorganization of collagen fibers. Notably, the tissue appearance in this group closely resembled that of the control group, indicating the efficacy of the treatment in accelerating tissue regeneration and restoring both structural and functional integrity of the skin following burn injury. Similarly, the sulfadiazine-treated group exhibited notable improvement in skin histology, with better epidermal organization and clear progression of tissue repair processes, confirming the beneficial role of the applied treatments in promoting burn wound healing **(Figure 38).**

	(A): 10 x 10	**(B): 40 x 10**
Control	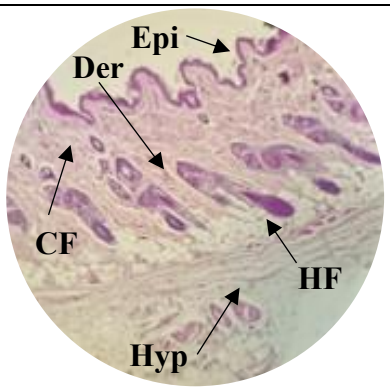	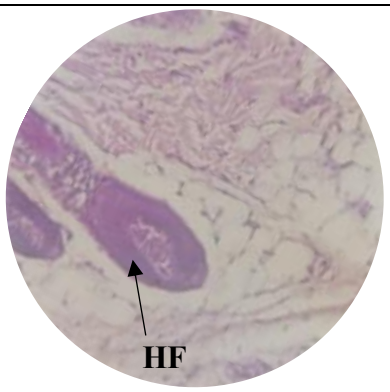
Untreated	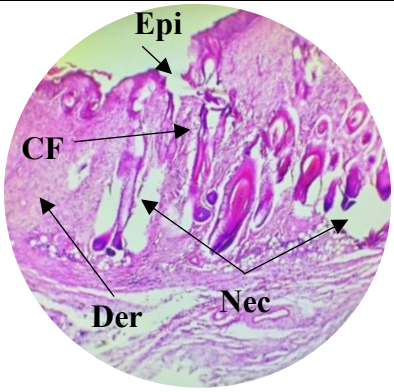	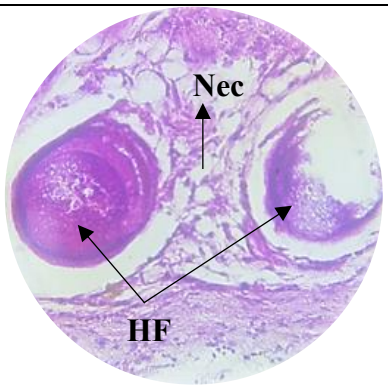

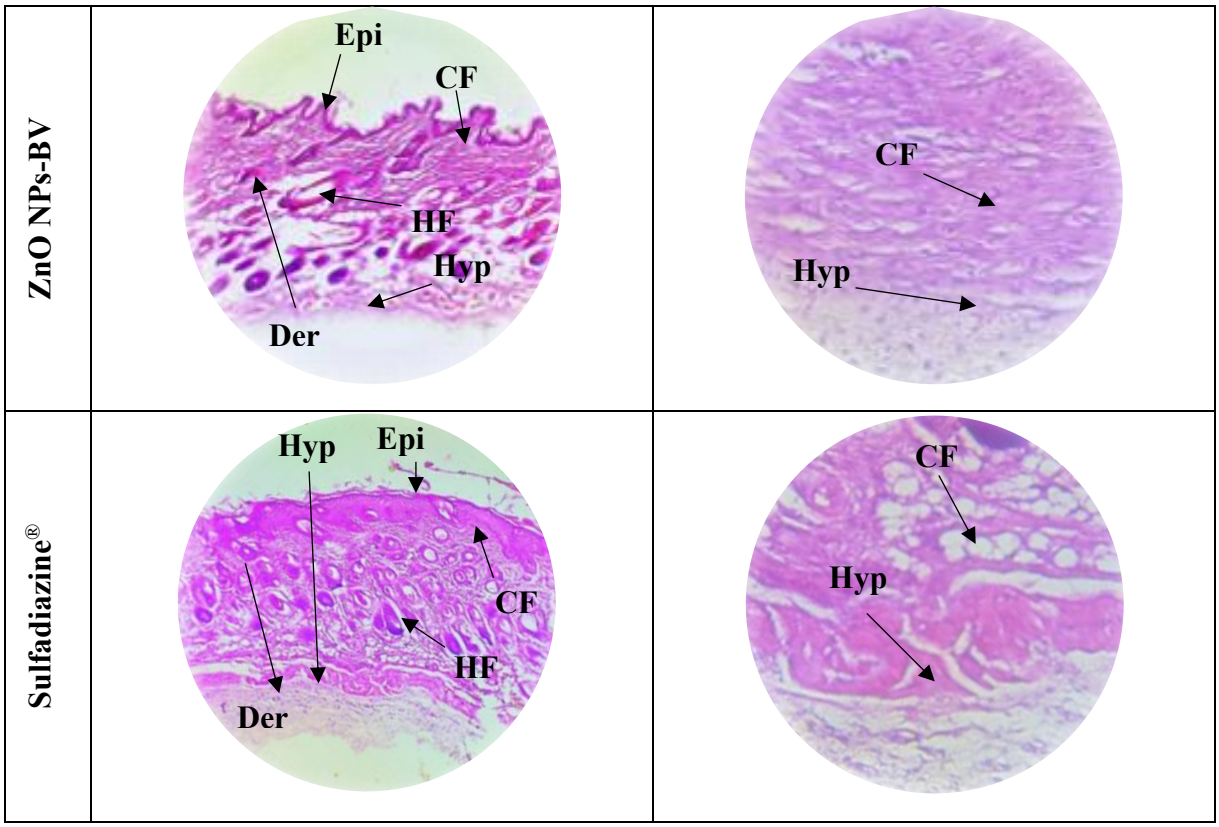

Figure 38: Histological photomicrographs of skin section of all experimental groups stained with hematoxylin and eosin (H&E), (A): x 40 and (B): x 100

Epi: Epidermis, **Der:** Dermis, **Hyp:** Hypodermis, **HF:** Hair follicle, **CF:** Collagen fibers, **Nec**: Necrosis

II. Discussion

Bee venom is considered a promising bioactive substance with multiple therapeutic properties, as studies indicate its ability to regulate the inflammatory response by affecting human neutrophil functions under *in vitro* conditions, in addition to demonstrating anti-inflammatory activity in animal models, highlighting its key role in modulating inflammatory pathways (Chabane et al., 2025). Building on these properties, it also plays an important role in accelerating wound and burn healing by reducing inflammation, promoting cell proliferation and regeneration, enhancing angiogenesis, and increasing collagen deposition, which collectively contributes to effective tissue reconstruction and improved overall healing quality (Sadek et al., 2024). In this context, the use of nanotechnology represents a significant advancement in enhancing these therapeutic effects, as it improves the stability of bee venom active components and protects them from degradation, ensuring the persistence of their biological activity for longer periods. It also enhances its anti-inflammatory effects by improving interaction with cellular mechanisms involved in the inflammatory response, while also suggesting a potential supportive role in antibacterial activity. Moreover, nanocarrier systems enable precise control over the delivery and sustained release of the active compound, ultimately leading to improved therapeutic efficiency compared to the conventional form of bee venom (Qanash et al., 2025).

II.1. Characterization of Collagen

The extracted collagen exhibited a pure white color and a viscous, gel-like consistency, with a pH value of 5.87, reflecting physicochemical properties typically associated with acid extraction methods that preserve the native nature of collagen while providing a mildly acidic environment. These results are consistent with those reported by Hussin (2012), who found that collagen extracted from striped catfish skin (*Pangasianodon hypophthalmus*) using an acid-based method showed a light color and acidic nature, with a lower pH value of 4.69. This difference can be attributed to variations in extraction conditions such as acid concentration, processing time, and washing steps, all of which directly influence the final pH of the collagen extract.

Using UV-Vis spectroscopy, the absorption spectrum showed several peaks at 228, 241, 244, 250, and 262 nm. The peak at 228 nm in collagen extracted from chicken feet is consistent with the findings of Nalinanon et al. (2011), who recorded an absorption peak at 230 nm for collagen extracted from the skin of the ornamental eel. This absorption, according to Ashraf et al. (2024), is attributed to the presence of amino acids such as glycine, hydroxyproline, and proline, which play

a crucial role in determining the molecular structure of proteins. Naderi Garaghshlag et al. (2019) also noted that collagen extracted from the rutile frizzi cotum exhibits an absorption peak at 240 nm, which is similar to the peaks recorded in this study at 241 and 244 nm. Furthermore, the peak at 250 nm is consistent with that reported by Ashraf et al. (2024) (251 nm), which was attributed to the presence of sensitive chromophores. Finally, the emergence of absorption in the 260–290 nm range, as demonstrated by Ali et al. (2017), indicates the presence of aromatic amino acids such as tyrosine, tryptophan, and phenylalanine, which is consistent with the peak recorded at 262 nm in collagen extracted from chicken feet.

FTIR spectroscopy analysis of collagen revealed the presence of amide bands A, B, I, II, and III sequentially, which are characteristic of fibrous protein structure. According to Uğurlu et al. (2023), the amide band A is typically associated with the stretching vibrations of the N–H group, with the free vibration of this group appearing in the range of 3400–3440 cm^{-1}. However, the occurrence of this band at 3311 cm^{-1} in this study suggests the presence of hydrogen bonds, which aligns with Gharagheshlagh et al. (2020) reporting a shift in frequencies toward lower values when these bonds form. The amide band B is associated with the asymmetric vibration of the aliphatic C–H group, in addition to the contribution of the NH_3^+ group, and typically appears between 2850 and 2950 cm^{-1}. In this study, it was recorded at 2921 cm^{-1}, which is within the reference range. The amide I band, which is most important in determining the secondary structure of the protein, is primarily attributed to carbonyl (C=O) stretching vibrations and is typically found between 1600 and 1700 cm^{-1}. It was observed at 1641 cm^{-1}, which is consistent with standard values. The amide II band, on the other hand, results from N–H bending vibrations coupled with C–N stretching and is typically located between 1500 and 1600 cm^{-1}. In this study, it was found at 1519 cm^{-1}, which is consistent with the findings of He et al. (2019). The amide III band, which is associated with the overlap of C–N stretching vibrations with N–H deformation, is an important indicator of the integrity of the triple helix structure of collagen, and was recorded at 1247 cm^{-1}, in line with the results of Uğurlu et al. (2023). Based on these results, the infrared spectrum confirms that the collagen extracted from chicken feet retains its natural triple-helix structure.

II.2. Characterization of ZnO NPs-BV

The UV–Visible absorption spectrum of zinc oxide nanoparticles (ZnO NPs) synthesized using bee venom and collagen showed an absorption range in the 250–270 nm region, with distinct peaks at 252, 258, and 260 nm. These results confirm the formation of ZnO nanoparticles coated

with bioactive molecules, which contributed to their stabilization and improved surface properties. In comparison with previous studies, ZnO nanoparticles synthesized using pomegranate peel extract exhibited an absorption peak at 257 nm, while conventional ZnO nanoparticles showed a peak at 270 nm. This shift toward shorter wavelengths is associated with reduced particle size and enhanced stability due to the presence of phytochemical capping agents (Kapare et al., 2025). The observed peak at 258 nm in the present study, compared to conventional ZnO, similarly indicates a blue shift, reflecting improved surface capping, reduced crystallite size, and strong interactions between bee venom–collagen components and the nanoparticle surface. These interactions further enhance nanoparticle stability and their optical properties.

The formation of zinc oxide nanoparticles (ZnO NPs) in this system was confirmed by the appearance of a characteristic FTIR band at 480.19 cm^{-1}, attributed to Zn–O stretching vibrations, indicating successful nanoparticle synthesis. The FTIR spectra also exhibited absorption bands at 3309.25 cm^{-1} and 2929.34 cm^{-1}, corresponding to O–H, N–H, and C–H stretching vibrations, reflecting the presence of proteinaceous and organic components derived from collagen and bee venom. Furthermore, peaks observed at 1652.70 cm^{-1} and 1538.92 cm^{-1} were assigned to the Amide I and Amide II regions, while bands at 1226.51 cm^{-1} and 1091.51 cm^{-1}, related to C–N and C–O vibrations, confirmed the presence of biomolecules and peptides attached to the nanoparticle surface, acting as biological reducing and stabilizing agents. These findings are supported by Hou et al. (2022), who reported a characteristic Zn–O peak at approximately 450 cm^{-1}, close to the value obtained in the present study, along with bands at 2925 cm^{-1}, 1640 cm^{-1}, and 1548 cm^{-1} associated with organic functional groups and the Amide I and II regions, highlighting the role of biomolecules in nanoparticle capping and stabilization. Similarly, Naseer et al. (2020) reported absorption bands within 683–500 cm^{-1} attributed to Zn–O vibrations, together with bands at 1600–1510 cm^{-1} corresponding to Amide I and II, and bands within 1400–1000 cm^{-1} assigned to C–N vibrations and amine groups. These values are consistent with the bands observed in our study at 1226.51 and 1091.51 cm^{-1}, suggesting strong interactions between biomolecules and the ZnO surface leading to the formation of a stabilizing biological capping layer that prevents nanoparticle aggregation and enhances structural stability. Additionally, these results agree with those reported by Sangeetha et al. (2011) for biologically synthesized ZnO nanoparticles, where similar peaks were observed at 2932 cm^{-1} (C–H stretching), 1640 cm^{-1} (Amide I), and 1540 cm^{-1} (Amide II), closely matching the peaks recorded in our study at 2929.34, 1652.70, and 1538.92 cm^{-1} thereby

confirming the involvement of protein functional groups in nanoparticle formation and stabilization.

The scanning electron microscopy (SEM) results showed that the nanoparticles prepared using collagen and bee venom formed clear aggregates or clusters, a common phenomenon in nanoparticle synthesis as reported by Alprol et al. (2024). Similarly, Karam and Abdulrahman (2022) indicated that green-synthesized zinc oxide nanoparticles tend to agglomerate due to their high surface energy and interaction with environmental conditions, leading to heterogeneous cluster formation. Regarding elemental composition, energy-dispersive X-ray spectroscopy (EDX) was used to determine the purity and constituents of the zinc oxide nanoparticle samples, revealing that zinc and oxygen were the main elements present, with zinc accounting for 74.55% by weight and oxygen for 2.75%, values consistent with Hou et al. (2022) regarding zinc abundance, while the low oxygen content aligns with Somani et al. (2025) and is attributed to synthesis conditions and reaction parameters. Furthermore, EDX analysis detected a carbon content of 22.70%, attributed to residual organic compounds from bee venom such as proteins and peptides, particularly melittin, which are likely responsible for coating the nanoparticle surface and contributing to their stabilization; this observation is supported by Huq et al. (2023) and Alprol et al. (2024), who highlighted the role of organic constituents in surface modification of nanoparticles.

The X-ray diffraction (XRD) analysis confirmed the successful synthesis of zinc oxide nanoparticles, where their chemical composition was identified as ZnO with a hexagonal crystalline structure, in agreement with the JCPDS card No. 01-079-0207. The XRD pattern revealed a set of characteristic diffraction peaks at 31.69° (100), 34.35° (002), 36.18° (101), 47.47° (102), 56.48° (110), 62.74° (103), 66.29° (200), 67.88° (112), 69.03° (201), 72.52° (004), and 76.87° (202), confirming the hexagonal crystal structure with lattice parameters of a = b = 3.26 Å and c = 5.21 Å. These findings are consistent with those reported by (Tiwari et al., 2024). The synthesized ZnO nanoparticles in this study exhibited a crystallite size (D) of 33.4 nm, which falls within the typical range of zinc oxide nanoparticles. This result is further supported by previous studies, where smaller crystallite sizes of approximately 13.58 nm (El-Khawaga et al., 2025) and larger values around 38 nm (El-Zahed et al., 2024) have been reported.

Regarding protein content determination, bee venom-loaded zinc oxide nanoparticles (ZnO NPs-BV) exhibited a high protein percentage, with an immobilization yield (IY) of 42.6%,

indicating the successful and efficient immobilization of proteins onto the surface of the nanoparticles.

II.3. *In vitro* Study of ZnO NPs-BV

The anti-inflammatory activity was evaluated *in vitro* using protein denaturation inhibition and red blood cell membrane stabilization assays. The results demonstrated a significant anti-inflammatory effect of zinc oxide nanoparticles loaded with bee venom (ZnO NPs-BV) compared to diclofenac. These findings are consistent with those reported by El Mehdi et al. (2021), who confirmed that the anti-inflammatory properties of bee venom are well established through both *in vitro* and *in vivo* studies. Furthermore, Rozik et al. (2024) highlighted the potential application of these effects in the treatment of various inflammatory diseases, including intestinal schistosomiasis. In addition, Hassan et al. (2021) demonstrated that bee venom reduces inflammation and hepatic fibrosis. The observed effects can be attributed to melittin, the principal active component of bee venom, which exerts its action by inhibiting Toll-like receptors (TLRs) and suppressing the nuclear factor kappa-B (NF-κB), a key regulator of inflammatory responses. It also downregulates the expression of pro-inflammatory cytokines. Moreover, loading bee venom and its active component melittin onto nanoparticles enhances their therapeutic efficacy, as reported by Khalil et al. (2021). Al-Darwesh et al. (2024) demonstrated that zinc oxide nanoparticles represent a promising drug delivery system with intrinsic anti-inflammatory properties. Additionally, these nanoparticles have been widely employed as effective drug carriers for the treatment of various diseases (El-Saadony et al., 2024). Furthermore, nanoparticles have been shown to protect therapeutic agents from degradation, improve their solubility, prolong their circulation time in the bloodstream, and enhance their permeability across biological membranes. They also enable targeted delivery and controlled drug release (Prieložná et al., 2024). These findings suggest that combining the biological properties of bee venom with nanotechnology can significantly enhance its anti-inflammatory potential.

The overall results indicate that bee venom loaded onto zinc oxide nanoparticles (ZnO NPs-BV) exhibits a clear antioxidant activity, as evidenced by its ability to scavenge free radicals and demonstrate considerable reducing power compared to standard compounds, indicating the effectiveness of the antioxidant activity in the nano-formulation. Bee venom contains bioactive components such as melittin, PLA2, and apamin, which contribute to its antioxidant activity by inhibiting lipid peroxidation and enhancing the activity of antioxidant enzymes such as SOD, GST,

and GPx. It also reduces oxidative stress markers such as MDA and TBARS while increasing total antioxidant capacity (TAC), confirming its protective role against reactive oxygen species (ROS) (Mheich et al., 2026). However, these peptides may be unstable under physiological conditions, which limits their effectiveness in free form. ZnO-based nanocomposites provide a synergistic platform for improving biological performance. This synergy results from the interaction between the ZnO core, released Zn^{2+} ions, and the loaded bioactive material, leading to improved regulation of reactive oxygen species and enhanced biological activity compared to individual components (Gomaa et al., 2024). Accordingly, loading bee venom onto ZnO may enhance its antioxidant activity by improving stability, protecting peptides from degradation, and increasing cellular uptake. A study by Nasrallah et al. (2018) demonstrated that curcumin-loaded ZnO nanoparticles maintained their antioxidant activity, as confirmed by the DPPH assay, while showing improved stability and pH-dependent release. These findings suggest that loading natural compounds onto ZnO does not reduce their bioactivity but may enhance it through protection against degradation and improved bioavailability. Similarly, studies by Patra et al. (2018) and Craig (2022) have shown that nanodelivery systems improve the efficiency of bioactive compounds by enhancing solubility, stability, and bioavailability, while protecting active molecules from degradation and increasing targeted delivery and cellular uptake, thereby supporting the preservation or enhancement of biological activity and the effectiveness of nanotherapeutic systems. Overall, these findings indicate that loading bee venom onto ZnO does not reduce its antioxidant activity; rather, it enhances it through synergistic effects, improved stability, enhanced cellular delivery, and stronger regulation of oxidative stress.

The evaluation of the Sun Protection Factor (SPF) revealed that the developed formulation (ZnO NPs-BV) achieved an SPF value of 18, indicating good efficacy in protecting against ultraviolet (UV) radiation. This result is consistent with the findings reported by Elbrolesy et al. (2023), who demonstrated that zinc oxide nanoparticles with SPF values exceeding 15 are considered effective in UV protection. Thus, the SPF value obtained in the present study (18) is in agreement with these reports (Elbrolesy et al., 2023), further supporting the effectiveness of these nanoparticles in sunscreen applications. The effectiveness of zinc oxide nanoparticles (ZnO NPs) can be attributed to their ability to provide broad-spectrum protection through absorption, reflection, and scattering of UV radiation. In addition, the small particle size enhances their distribution over the skin surface and improves the uniformity of coverage, thereby increasing photoprotective efficiency (Ghorbani et al., 2025). Several previous studies have confirmed these

properties, reporting that formulations based on ZnO NPs exhibit considerable SPF values and high efficacy in UV protection (Kapare et al., 2025; Azeez et al., 2024; Maryani et al., 2024). Regarding bee venom, its role can be interpreted as a functional additive that improves the behavior of ZnO NPs within the formulation. Irede et al. (2024) reported that coating or stabilizing nanoparticles with suitable materials enhances their homogeneous dispersion and improves their UV-blocking efficiency. Accordingly, it is plausible that the components of bee venom contributed to reducing nanoparticle agglomeration and improving their distribution, thereby supporting the observed photoprotective performance (Irede et al., 2024). Overall, the results indicate that loading ZnO NPs with bee venom does not compromise their optical properties in UV protection; rather, it may enhance their effectiveness.

The antibacterial activity was evaluated using the disk diffusion method (Chetehouna et al., 2023). The study results demonstrated that bee venom exhibits antibacterial activity against both *Pseudomonas aeruginosa* and *Staphylococcus spp*. across a broad range of concentrations. In contrast, its effect against *Escherichia coli* was limited, as significant antibacterial activity was observed only at higher concentrations. Fadel et al. (2018) also reported that bee venom exhibits antibacterial activity against various bacterial strains, including *E. coli, S. aureus, and P. aeruginosa*, with variations in efficacy depending on the bacterial species as well as the concentration of the venom used. Furthermore, Tanuğur and Kekeçoğlu (2021) showed that phospholipase A2 possesses antibacterial properties and serves as an important defense component in the body. It exerts its effect by disrupting the bacterial cell membrane due to its lipolytic and allergenic nature. Considering the correlation between reduced microbial load and increased levels of this enzyme, it can be inferred that the antibacterial efficacy of bee venom is largely attributed to the presence of phospholipase A2. Notably, in comparison with the present study, Mandal et al. (2022) reported that zinc oxide nanoparticles (ZnO NPs) act as effective nanocarriers due to their large surface area and biocompatibility. This property explains their ability to load proteins as well as drugs, as demonstrated in studies by Ezzat et al. (2025) and Lebaka et al. (2025). Qanash et al. (2025) also reported that combining the BV compound with nanoparticles significantly enhanced the antibacterial efficacy.

II.4. *In Vivo* Study of ZnO NPs-BV

The effect of bee venom-loaded zinc oxide nanoparticle ointment (ZnO NPs-BV) on burn wound healing was evaluated. Periodic measurements and digital images of the burn area showed

a gradual improvement in the healing process in the groups treated with ZnO NPs-BV and sulfadiazine. The ZnO NPs-BV group achieved near-complete wound closure by day 22, with a marked improvement in tissue regeneration and hair growth compared to the untreated group, indicating enhanced tissue regeneration and restoration of skin structure. Measurements of wound area also confirmed a clear improvement in the ZnO NPs-BV-treated group compared to the untreated group on day 22. This effect may be attributed to the ability of bee venom to stimulate collagen production (Abacı & Orhan, 2022), in addition to its anti-inflammatory properties at the burn site (Denk et al., 2024). Bee venom is also known for its antioxidant, antimicrobial, and analgesic properties, which enhance damaged tissue repair and contribute to accelerated burn wound healing (Al-Waili et al., 2015). Furthermore, the application of nanotechnology in burn treatment improves the therapeutic efficacy and enhances the bioavailability of the active compounds (Rashad et al., 2024). The findings of the present study are consistent with those reported by Valadi and colleagues (2024), who achieved nearly complete wound closure by day 21 using a hydrogel containing silymarin and ZnO NPs. Another study on burns treated with zinc alginate hydrogel reported a healing rate of 90.75% on day 21 (Niculescu et al., 2025).

Monitoring organ weight variation represents a fundamental approach for evaluating both pathological alterations and potential protective effects induced by experimental treatments. In the present study, the stability of relative organ weights observed in the ZnONPs-BV group indicates a favorable biological profile, with no evidence of systemic toxicity despite the well-documented systemic disturbances associated with burn injuries (Atiyeh, Gunn, & Dibo, 2008). This preservation of organ integrity suggests a robust maintenance of physiological homeostasis, likely driven by the synergistic action of bee venom's anti-inflammatory and antioxidant properties and the functional role of zinc oxide nanoparticles as an efficient delivery system that enhances stability, bioavailability, and therapeutic performance (El Mehdi et al., 2021; Khalil et al., 2021; Mheich et al., 2026). Notably, this pattern aligns with previous experimental findings reporting unchanged relative weights of major organs, including the liver, kidneys, and spleen—organs particularly vulnerable to oxidative and thermal stress—following treatment with Ginkgo biloba extract. Collectively, these converging evidence support the notion that the treatment mitigates burn-induced systemic alterations while preserving overall organ functional homeostasis (Sakarcan et al., 2005).

The untreated group exhibited a significant increase in inflammatory biomarker levels compared with the control group, whereas the treated group showed a marked reduction in these markers relative to the untreated group. White blood cells are a fundamental component of both the innate and adaptive immune systems, comprising granulocytes such as neutrophils, as well as monocytes and lymphocytes, including B and T lymphocytes, which perform diverse immune functions that may be either stimulatory or regulatory in nature (Brenner et al., 2014). Lymphocyte count is considered an important auxiliary diagnostic parameter, as it undergoes significant changes in systemic inflammatory conditions and various diseases (Boulaares et al., 2020; Boulaares & Derouiche, 2021). Several immune cells contribute to the wound-healing process following burn injuries, where they perform key functions through the secretion of cytokines and chemokines, most notably TNF-α, IL-6, IL-1β, and IL-10 produced by monocytes (Akir et al., 2004). Monocytes are also capable of antigen presentation and T-cell activation via HLA-DR molecules; however, the expression of these molecules is reduced in burn patients, particularly in cases of sepsis (Devine et al., 2018). Neutrophils are among the first cells to migrate to the burn site, where they rely on phagocytosis, production of reactive oxygen species, and antimicrobial proteases to eliminate pathogens (Strudwick et al., 2017), although burn injuries may impair their chemotactic ability (Strudwick et al., 2017; Devine et al., 2018). On the other hand, lymphocytes are key components of adaptive immunity involved in the burn response, and thermal injury induces multiple functional alterations in these cells, including suppression of their activity (Korzeniowski et al., 2022). These immune disturbances during burn wound healing may weaken the immune system and increase susceptibility to infections, thereby prolonging recovery time, which highlights the importance of understanding immune mechanisms in burn patients (Akir et al., 2004). Bee venom contains at least four compounds with anti-inflammatory properties, including melittin, apamin, adolapin, and phospholipase A2 (Bava et al., 2023). Among these, melittin is the most prominent, exhibiting strong anti-inflammatory effects by interacting with active enzymes, thereby reducing the production and release of pro-inflammatory cytokines such as IL-6, IL-1β, and TNF-α (Khalil et al., 2021). Nanoparticles also contribute to improving pharmacological properties by modulating drug release profiles, enhancing diffusion, bioavailability, and solubility, as well as modifying immune responses, leading to improved drug administration, reduced toxicity and side effects, enhanced therapeutic efficacy, and prolonged shelf life (Khafaga et al., 2021).

The study demonstrated clear hematological alterations among the experimental groups, with a marked decrease in red blood cell count, hemoglobin levels, and hematocrit observed in the

untreated group compared with the control group, whereas these alterations were less pronounced in the treated group, which showed a notable improvement in hemoglobin levels. In addition, a relative increase was observed in erythrocyte indices (MCV, MCH, and MCHC) across the different groups, accompanied by a decrease in the RDW index. The results also revealed elevated platelet-related parameters in the untreated group, whereas a clear improvement in these indices was recorded in the treated group, findings that are consistent with Sen et al., 2019, who reported early characteristic hematological alterations in patients with severe burns, particularly in complete blood count parameters, including a progressive decline in hemoglobin and hematocrit levels during the first week post-injury, a decrease that is often more closely associated with reduced red blood cell count than with hemoglobin loss itself. This reduction in erythrocytes during the early days after severe burns is attributed to multiple pathological mechanisms associated with the injury, including hemolysis, a process characterized by early loss of red blood cell membrane integrity leading to the release of intracellular contents, particularly hemoglobin, into the extracellular environment (Dimitrov et al., 2023). The exacerbation of inflammatory responses and activation of innate immune cells involves multiple mechanisms, including activation of Toll-like receptors TLR2 and TLR4, increased oxidative stress, and membrane damage, where heme contributes to the oxidation of low-density lipoprotein (LDL), thereby activating these receptors and amplifying inflammatory responses (Bekkering et al., 2014; Mancek-Keber et al., 2015). Moreover, free heme promotes hydroxyl radical formation via iron-dependent Fenton reactions and enhances lipid peroxidation, leading to increased membrane damage, elevated permeability, and ultimately cell death (Mancek-Keber et al., 2015). Platelets also play an important role in linking innate and adaptive immune responses by releasing pro-inflammatory mediators from their granules upon activation, thereby promoting immune cell recruitment and activation even at distant inflammatory sites (Voudoukis et al., 2014). The observed effects in the ZnONPs_BV-treated group may be attributed to melittin, the principal active component of bee venom, which exerts anti-inflammatory effects through inhibition of Toll-like receptors and suppression of NF-κB signaling (Hassan et al., 2021). Bee venom also contains protease inhibitors with anti-inflammatory properties that reduce inflammatory reactions and contribute to hemostasis (Eze et al., 2016). Zinc plays a fundamental role in erythropoiesis by supporting growth hormone and IGF-1 activity, regulating GATA-1 transcription factor, inhibiting caspase-3-mediated apoptosis, and protecting red blood cells from oxidative stress, thereby prolonging their lifespan (Takahashi et al., 2024). In its nanoform, zinc enhances cellular uptake, bioavailability, solubility, and tissue penetration, thereby improving its

overall therapeutic efficacy in supporting erythropoiesis, reducing oxidative stress, and promoting tissue regeneration and wound healing (Agarwal et al., 2019).

The present study demonstrated that ZnO NPs-BV significantly increased iron levels compared with the untreated group, supporting previous evidence that links iron imbalance to impaired wound healing and suggesting that its therapeutic effect is mediated through the restoration of iron homeostasis. Wound healing is a highly coordinated and dynamic biological process that progresses through overlapping phases, beginning with hemostasis characterized by hemorrhage and fibrin clot formation, followed by inflammation, proliferation involving re-epithelialization, granulation tissue formation, and angiogenesis, and finally tissue remodeling (Reinke & Sorg, 2012), where the initial hemorrhagic phase plays a crucial role in directing subsequent regenerative responses. Iron is a key element in skin physiology and tissue repair due to its essential roles in oxygen transport, cellular metabolism, and collagen synthesis, and disturbances in iron homeostasis—particularly in conditions associated with blood loss or anemia—are strongly associated with delayed wound closure and impaired tissue regeneration (Wright et al., 2014). In addition, impaired healing in burns and diabetes is closely associated with hypoxia, which disrupts the early inflammatory phase by reducing macrophage and neutrophil recruitment, thereby slowing tissue repair, while also affecting iron utilization required for processes such as hemoglobin synthesis and collagen maturation; at the same time, hypoxia increases oxidative stress through excessive production of reactive oxygen species (ROS), including superoxide anion and hydrogen peroxide, leading to cellular damage and impaired neovascularization. In this context, bee venom has been reported to improve the wound microenvironment by reducing ROS production in immune cells and alleviating oxidative stress within damaged tissues, thereby restoring redox balance and cellular homeostasis (Kurek-Górecka et al., 2021), which helps preserve iron homeostasis by limiting iron-related oxidative reactions and enhancing tissue repair efficiency. In addition, zinc oxide nanoparticles may enhance the therapeutic effect of bee venom in wound healing by strengthening its antioxidant and anti-inflammatory properties (Qanash et al., 2025). This synergistic action improves the wound microenvironment, thereby positively influencing iron homeostasis by facilitating its utilization in oxygen transport, collagen synthesis, and angiogenesis, ultimately enhancing tissue repair efficiency and accelerating wound healing.

The present study showed a marked decrease in serum albumin levels in the untreated group compared with the control group, while an increase was observed in the ZnO NPs-BV-treated group. Serum albumin is the most abundant plasma protein and plays a fundamental role in maintaining colloidal osmotic pressure and physiological homeostasis, in addition to serving as a carrier for various endogenous and exogenous molecules in the circulation (Rothschild et al., 1988). Burn injury induces a severe systemic inflammatory response mediated by pro-inflammatory cytokines such as IL-6, IL-1, and TNF-α, which activate the hepatic acute-phase response, leading to a shift in protein synthesis toward positive acute-phase proteins such as C-reactive protein and fibrinogen, while suppressing albumin as a negative acute-phase protein. This hypoalbuminemia is further aggravated by increased vascular permeability and fluid resuscitation–induced hemodilution, indicating that reduced serum albumin primarily reflects the severity of the inflammatory state (Ishida et al., 2014). In this context, bee venom exerts strong anti-inflammatory and immunomodulatory effects by downregulating pro-inflammatory cytokines (IL-6, IL-1β, TNF-α) and upregulating anti-inflammatory mediators such as IL-10, thereby improving hepatic function and contributing to the restoration of serum albumin levels through attenuation of oxidative stress and lipid peroxidation (ElAdham et al., 2022). Additionally, zinc oxide nanoparticles (ZnO NPs) may potentiate these therapeutic effects through a dual mechanism, acting both as nanocarriers that enhance the stability, bioavailability, and targeted delivery of bee venom bioactive components, and as intrinsic anti-inflammatory agents that suppress IL-6, TNF-α, and COX-2 expression, thereby reducing inflammatory and oxidative stress; consequently, this synergistic interaction may lead to improved liver function and a more pronounced restoration of serum albumin levels in the ZnO NPs-BV-treated group (Agarwal & Shanmugam, 2020).

The present study demonstrated a marked increase in blood glucose levels in the untreated burn group compared with the control group, reflecting a state of metabolic stress induced by burn injury. Burn injury is a strong trigger of the hypermetabolic response, characterized by marked activation of stress hormones such as catecholamines, cortisol, and glucagon. This hormonal surge leads to an increased basal metabolic rate, elevated energy expenditure, and enhanced protein and lipid catabolism. Consequently, significant disturbances in glucose homeostasis occur, including increased hepatic glucose production, reduced peripheral glucose utilization, and the development of insulin resistance, resulting in persistent hyperglycemia during the acute post-burn phase. Although this metabolic response initially serves as an adaptive mechanism to provide energy required for inflammation and tissue repair, its prolonged persistence may contribute to chronic

metabolic imbalance and delayed recovery (Williams et al., 2009). In contrast, treatment with zinc oxide nanoparticles loaded with bee venom (ZnO NPs-BV) resulted in a marked reduction in blood glucose levels, reflecting an improvement in metabolic balance. This effect can be attributed to the role of bee venom in modulating key metabolic and hormonal pathways involved in glucose regulation, including effects on insulin-related activity and stress-associated hormonal responses. Furthermore, the nanocarrier system (ZnO NPs) enhances the efficacy of bee venom by improving its bioavailability, stability, and absorption, thereby increasing its therapeutic efficiency. In addition, nano-sized zinc contributes to improving insulin sensitivity and supporting glucose metabolism through its antioxidant and anti-inflammatory properties, which help reduce oxidative stress associated with glucose dysregulation (Jayawardena et al., 2012).

Malondialdehyde (MDA), a secondary product of lipid peroxidation, is considered one of the most important biomarkers used to evaluate oxidative stress in various biological samples (Wang et al., 2021). It also contributes to the stimulation of pro-inflammatory cytokine production (Mueangson et al., 2023). The results of our study showed a highly significant increase in MDA levels in burned rats compared with the control group, which is consistent with the findings reported by Babu & Babu (2018), reflecting the aggravation of lipid peroxidation and consequently tissue and cellular damage (Chen et al., 2025). When the ZnO NPs-BV group was compared with the untreated group, a decrease in MDA levels was observed, which was also confirmed by the study of Elshater et al., and this reduction may be attributed to the antioxidant activity of bee venom (Elshater et al., 2014). Similar findings were also recorded in sulfadiazine group, in agreement with the study conducted by Dwivedi et al., which demonstrated that MDA levels decreased in the sulfadiazine group compared with the untreated group after 14 days of burn treatment (Dwivedi et al., 2010).

Glutathione (GSH) acts as a major defense mechanism against oxidative stress (Denk et al., 2024), playing a crucial role in protecting cells from oxidative damage and maintaining the cellular redox balance (Basil Ribeiro, 2023). Our results demonstrated a significant decrease in the activity of this enzyme in the liver, spleen, and skin tissues of burned rats compared with the healthy groups. These findings are consistent with those reported by Beiraghi-Toosi et al. (2018), who suggested that the reduction in GSH levels following burns is attributed to its increased consumption in response to oxidative stress, as it functions to protect proteins and cellular structures from irreversible oxidative damage.

Superoxide dismutase (SOD) is considered one of the most important antioxidant enzymes, as it contributes to protection against oxidative stress by eliminating harmful free radicals (Abdulgafor et al., 2018). Our results showed a significant decrease in the activity of this enzyme in the liver and spleen in the untreated group, which is consistent with the findings of Saitoh et al., who attributed this decrease to the excessive consumption of the enzyme as a result of its intensive activation under oxidative stress conditions (Saitoh et al., 2001). In contrast, the skin exhibited a highly significant increase in this enzyme, which is inconsistent with the findings reported by Fang et al. (Fang et al., 2017). This may be explained by its ability to convert the superoxide radical ($O2^{\cdot}-$) into hydrogen peroxide (H2O2) in order to reduce oxidative stress (Wang et al., 2021).When comparing the ZnO NPs-BV group with the untreated group, a significant increase in SOD levels was observed, suggesting that this treatment contributed to enhancing the antioxidant response and improving the ability of tissues to cope with burn-induced oxidative stress (Elshater et al., 2014).

Zinc contributes to the enhancement of antioxidant defense systems and the reduction of oxidative stress. Superoxide dismutase (SOD) is considered one of the most important antioxidant enzymes responsible for protecting cells against reactive oxygen species, as zinc acts as a cofactor for the SOD1 enzyme, which is involved in scavenging free radicals within the cytoplasm and in the extracellular environment (Cheng & Chen, 2021).

The histological results of the spleen showed that burns induced marked architectural disturbances of the organ, particularly in both the white and red pulp, accompanied by edema and the presence of acellular spaces in the untreated group. The white pulp remained atrophic, with a noticeable reduction in lymphocyte numbers, especially B lymphocytes, which is consistent with the findings of Maekawa et al. (2002). Fukuzuka et al. (2000) also reported an early splenic response to burns characterized by a significant increase in apoptosis among lymphocytes, particularly T and B cells. In contrast, the groups treated with ZnO NPs-BV and sulfadiazine showed a significant improvement in splenic histology, with a restoration of the organization of both white and red pulp, approaching the normal architecture compared to the control group, which is in agreement with the 24-day post-burn results reported by Maekawa et al. (2002). Another study attributed these effects to bee venom, which possesses anti-inflammatory properties and contributes to the regulation and improvement of the immune response (Hassan et al., 2021).

Similarly, the histological findings of the skin revealed clear differences between the experimental groups, where the control group exhibited a normal skin structure with well-organized epidermal and dermal layers, whereas the untreated burned group showed severe tissue damage characterized by epidermal disruption, degradation of collagen fibers, and marked inflammatory infiltration with vascular congestion, consistent with Abdel-Gawad et al. (2021), who reported that burns induce inflammation and cellular damage through increased reactive oxygen species, leading to breakdown of the structural components of the tissue and delayed wound healing. On the other hand, the treated groups demonstrated significant tissue regeneration, particularly the ZnO NPs-BV group, which showed near-complete restoration of skin architecture with reduced inflammation and improved collagen fiber organization. This effect may be attributed to the ability of bee venom to stimulate collagen production (Abacı & Orhan, 2022), in addition to its anti-inflammatory, antioxidant, and antimicrobial properties that enhance tissue repair and accelerate burn wound healing (Denk et al., 2024; Al-Waili et al., 2015). Furthermore, zinc, as a key component of many enzymes involved in cell division, maturation, and migration, plays an important role in wound healing (Khalid et al., 2017), while nanoparticles enhance therapeutic efficiency through improved cellular penetration and targeted delivery to inflamed tissues (Agarwal et al., 2019).

Conclsion & Perspectives

Conclusion

The results of this study demonstrated the successful extraction of collagen from chicken leg skin, which was confirmed using ultraviolet–visible (UV–Vis) spectroscopy and Fourier transform infrared (FTIR) spectroscopy. Furthermore, the extracted collagen proved effective in the biosynthesis of bee venom-loaded zinc oxide nanoparticles (ZnO NPs-BV), which exhibited distinctive structural and physicochemical properties. These were confirmed through multiple characterization techniques, including UV-Vis spectroscopy, FTIR spectroscopy, X-ray diffraction (XRD), as well as scanning electron microscopy (SEM) coupled with energy-dispersive X-ray spectroscopy (EDX).

The *in vitro* analysis of ZnO NPs-BV revealed multiple biological activities, including antioxidant, anti-inflammatory, antibacterial, and sunscreen properties, highlighting their potential as promising biomaterials for medical applications, particularly in burn treatment and wound healing promotion.

The stability of relative organ weights after ZnO NPs-BV treatment indicated the absence of systemic toxicity, supporting the biosafety of the nanotherapeutic approach alongside its therapeutic efficacy.

Hematological analysis showed clear differences between the untreated group and the ZnO NPs-BV-treated groups, where the treatment reduced inflammatory markers and improved red blood cell counts along with other related hematological parameters, reflecting its role in reducing inflammation and enhancing the biological response during burn healing.

Biochemical analysis demonstrated that ZnO NPs-BV treatment improved metabolic parameters by restoring albumin and blood glucose levels close to those of the control group, with a moderate improvement in iron levels, indicating its role in restoring metabolic balance and reducing biochemical disturbances.

The current findings also revealed that ZnO NPs-BV improved the overall antioxidant status by reducing oxidative stress markers in tissues, suggesting a protective role against burn-induced oxidative damage in Wistar rats.

Histological examination, particularly in the skin, confirmed that ZnO NPs-BV treatment significantly improved tissue architecture and restored the organization of skin layers closer to

normal structure, along with noticeable improvement in spleen tissue, reflecting its role in enhancing tissue repair following burns.

Overall, these findings highlight the promising therapeutic and preventive potential of ZnO NPs-BV in medical and pharmaceutical applications.

Perspectives

- Evaluation of the long-term biosafety and toxicity of ZnO NPs-BV on vital organs such as the liver, kidneys, and spleen.
- Development of topical formulations with enhanced stability and prolonged therapeutic efficacy to improve the clinical application of ZnO NPs-BV.
- Investigation of the antifungal activity of ZnO NPs-BV against pathogenic fungal species associated with wound and burn infections.
- Assessment of the stability of ZnO NPs-BV under different storage conditions and its impact on therapeutic effectiveness.
- Evaluation of the therapeutic efficacy of ZnO NPs-BV in comparison with conventional treatments used for burn healing.
- Investigation of the potential use of ZnO NPs-BV in the treatment of chronic wounds and other skin inflammatory disorders.
- Development of advanced pharmaceutical formulations, such as bioactive hydrogels and ZnO NPs-BV-loaded wound dressings.

Bibliographical References

Abacı, N., & Orhan, İ. E. (2022). Bee venom and its biological effects. Current Perspectives on Medicinal and Aromatic Plants, 5(1), 86-105.

Abazari, M., Ghaffari, A., Rashidzadeh, H., Badeleh, S. M., & Maleki, Y. (2022). A systematic review on classification, identification, and healing process of burn wound healing. The international journal of lower extremity wounds, 21(1), 18-30.

Abbas, R., Luo, J., Qi, X., Naz, A., Khan, I. A., Liu, H., ... & Wei, J. (2024). Silver nanoparticles: Synthesis, structure, properties and applications. Nanomaterials, 14(17), 1425.

Abdel-Gawad, D. R. I., Moselhy, W. A., Ahmed, R. R., Al-Muzafar, H. M., Amin, K. A., Amin, M. M., El-Nahass, E. S., & Abdou, K. A. H. (2021). Therapeutic effect of mesenchymal stem cells on histopathological, immunohistochemical, and molecular analysis in second-grade burn model. Stem Cell Research & Therapy, 12, 308.

Abdelrahaman, D., Shanab, O., Abdeen, A., Abdelkader, A., Elazab, K. M., Kouriem, H., ... & Mostafa, L. (2025). Bee venom ameliorates gentamicin-induced kidney injury by restoring renal aquaporins and enhancing antioxidant and anti-inflammatory activities in rats. Frontiers in pharmacology, 16, 1525529.

Abdulgafor, A. B., Owain, M. S., Hasan, M. S., Hussein, M. A., Aboud, Q. M., & Al-Zobaie, A. J. (2018). Liver, kidney function tests and oxidative damage during and after treatment of Salmonella typhimurium infection in experimental local rabbits. International Journal of Pharmaceutical Quality Assurance, 9(5-6).

Afetor, M., Bosoka, S. A., Abanga, W. A., Zeng, V., Tamal, C. S., Issahaku, G. R., ... & Kubio, C. (2024). Cases of burns reported to health facilities in the Volta region of Ghana, 2019–2023. Burns Open, 8(4), 100373.

Agarwal, H., & Shanmugam, V. (2020). A review on anti-inflammatory activity of green synthesized zinc oxide nanoparticle: Mechanism-based approach. Bioorganic Chemistry, 94, 103423.

Agarwal, H., Nakara, A., & Shanmugam, V. K. (2019). Anti-inflammatory mechanism of various metal and metal oxide nanoparticles synthesized using plant extracts: A review Biomedicine & Pharmacotherapy, 109, 2561-2572. doi: 10.1016/j.biopha.2018.11.116

Ahire, S. A., Bachhav, A. A., Pawar, T. B., Jagdale, B. S., Patil, A. V., & Koli, P. B. (2022). The Augmentation of nanotechnology era: A concise review on fundamental concepts of nanotechnology and applications in material science and technology. Results in Chemistry, 4, 100633. doi: 10.1016/j.rechem.2022.100633.

Ajaz, M., Rasool, W., & Mahmood, A. (2024). Comprehensive Review of Nanotechnology: Innovations and Multidisciplinary Applications. Futuristic Biotechnology, 4(01).

Akinyemi, K. O., Al-Khafaji, N. S. K., Al-Alaq, F. T., Fakorede, C. O., Al-Dahmoshi, H. O. M., Iwalokun, B. A., Akpabio, I., Alkafaas, S. S., & Saki, M. (2022). Extended-spectrum Beta-lactamases encoding genes among Salmonella enterica serovar Typhi isolates in patients with typhoid fever from four academic medical centers Lagos, Nigeria. Revista de Investigación Clínica, 74(5), 287-295.

Al-Darwesh, M. Y., Ibrahim, S. S., & Mohammed, M. A. (2024). A review on plant extract mediated green synthesis of zinc oxide nanoparticles and their biomedical applications. Results in chemistry, 7, 101368.

Al-Harbi, N., & Abd-Elrahman, N. K. (2025). Physical methods for preparation of nanomaterials, their characterization and applications: a review. Journal of Umm Al-Qura University for Applied Sciences, 11(2), 356-377.

Ali, A.M.M., Benjakul, S., Kishimura, H. (2017). Molecular characteristics of acid and pepsin soluble collagens from the scales of golden carp (Probarbus jullieni). Emirates Journal of Food and Agriculture, 29(6), 450-457.

Alprol, A. E., Eleryan, A., Abouelwafa, A., Gad, A. M., & Hamad, T. M. (2024). Green synthesis of zinc oxide nanoparticles using Padina pavonica extract for efficient photocatalytic removal of methylene blue. Scientific Reports, 14(1), 32160.

Alshammari, B. H., Lashin, M. M., Mahmood, M. A., Al-Mubaddel, F. S., Ilyas, N., Rahman, N., ... & Khan, R. (2023). Organic and inorganic nanomaterials: fabrication, properties and applications. RSC advances, 13(20), 13735-13785.

Alshammari, R. A., Qaisi, H. M., Alshammari, M. Z. H., Awaji, N. A. A., Aljawan, M. M. A., Alrashidy, I. M. E., ... & Hakami, M. M. M. (2024). Burns: Biochemical Aspects, Pathophysiology, Classification, Treatment, and Nursing Care.

Al-Shehaby, N., Elshoky, H. A., Zidan, M., Salaheldin, T. A., Gaber, M. H., Ali, M. A., & El-Sayed, N. M. (2025). *In vitro* localization of modified zinc oxide nanoparticles showing selective anticancer effects against colorectal carcinoma using biophysical techniques. Scientific Reports, 15(1), 16811.

Altammar, K. A. (2023). A review on nanoparticles: characteristics, synthesis, applications, and challenges. Frontiers in microbiology, 14, 1155622.

Álvarez-Chimal, R., García-Pérez, V. I., Álvarez-Pérez, M. A., Tavera-Hernández, R., Reyes-Carmona, L., Martínez-Hernández, M., & Arenas-Alatorre, J. Á. (2022). Influence of the particle size on the antibacterial activity of green synthesized zinc oxide nanoparticles using Dysphania ambrosioides extract, supported by molecular docking analysis. Arabian Journal of Chemistry, 15(6), 103804.

Al-Waili, N., Hozzein, W. N., Badr, G., Al-Ghamdi, A., Al-Waili, H., Salom, K., & Al-Waili, T. (2015). Propolis and bee venom in diabetic wounds; a potential approach that warrants clinical investigation. African Journal of Traditional, Complementary and Alternative Medicines, 12(6), 1-11.

Ambika, S., & Sundrarajan, M. (2015). Green biosynthesis of ZnO nanoparticles using Vitex negundo L. extract: Spectroscopic investigation of interaction between ZnO nanoparticles and human serum albumin. Journal of Photochemistry and Photobiology B: Biology, 149, 143-148.

Andrusiewicz, A., Khimuk, S., Mijas, D., Shmorhun, B., & Nowicka, D. (2025). Molecular Mechanisms in the Etiopathology of Rosacea—Systematic Review. International Journal of Molecular Sciences, 26(23), 11292.

Anjum, S., Hashim, M., Malik, S. A., Khan, M., Lorenzo, J. M., Abbasi, B. H., & Hano, C. (2021). Recent advances in zinc oxide nanoparticles (ZnO NPs) for cancer diagnosis, target drug delivery, and treatment. Cancers, 13(18), 4570.

Ansari, M., Ahmed, S., Abbasi, A., Khan, M. T., Subhan, M., Bukhari, N. A., . . . Abdelsalam, N. R. (2023). Plant mediated fabrication of silver nanoparticles, process optimization, and impact on tomato plant. Scientific reports, 13(1), 18048.

Antony Jose, S., et al. (2025). Wear- and corrosion-resistant coatings for extreme environments: Advances, challenges, and future perspectives. Coatings, 15(8), 878.

Aouadi, A., Hamada Saud, D., Rebiai, A., Achouri, A., Benabdesselam, S., Mohamed Abd El-Mordy, F., ... & Messaoudi, M. (2024). Introducing the antibacterial and photocatalytic degradation potentials of biosynthesized chitosan, chitosan–ZnO, and chitosan–ZnO/PVP nanoparticles. Scientific Reports, 14(1), 14753.

Apalla, Z., Lallas, A., Sotiriou, E., Lazaridou, E., & Ioannides, D. (2017). Epidemiological trends in skin cancer. Dermatology practical & conceptual, 7(2), 1.

Apalla, Z., Nashan, D., Weller, R. B., & Castellsagué, X. (2017). Skin cancer: epidemiology, disease burden, pathophysiology, diagnosis, and therapeutic approaches. Dermatology and therapy, 7(Suppl 1), 5-19.

Aristizabal-Torres, M. A., Bruce, C. J., Caruso, M. A., Wieczorek, M. A., Pacheco-Spann, L. M., Carter, R. E., ... & Hall, M. R. (2025). Allergic contact dermatitis revisited: A comprehensive review. Jaad Reviews, 4, 92-103.

Asharaf, F., & Rajan, R. (2024). Bioconversion of eel skin waste into valuable collagen: Isolation, spectral characterization, and biocompatibility assessment. Waste and Biomass Valorization, 15, 4773-4783.

Ashour, M. A., & Abd-Elhalim, B. T. (2024). Biosynthesis and biocompatibility evaluation of zinc oxide nanoparticles prepared using Priestia megaterium bacteria. Scientific Reports, 14(1), 4147.

Azam, S., Taj, M. K., Taj, I., Khan, S., Khan, M. A., Ali, S. A., ... & Shah, S. J. (2024). The burn wound injury its causes and management. Journal of Population Therapeutics and Clinical Pharmacology, 31(6), 2596-2512.

Azeez, H. H., Gozeh, B. A., Azeez, H. H., & Slewa, L. (2024). The Effect of Green Synthesis ZnO NPs on Sun Protection Factor of Sunblock Lotion. Rafidain Journal of Science, 33, 137-47.

B

Babu, R. J., & Babu, M. (2018). Oxidative stress in major thermal burns: Its implications and significance. Indian Journal of Burns, 26(1), 38-43.

Bains, V., Sharma, P., Budhalakoti, B., & Sharma, S. (2025). Nanomaterials at the forefront: Classification, fabrication techniques, and cross-sector applications. Zeitschrift für Physikalische Chemie, 239(10).

Baker, P., Huang, C., Radi, R., Moll, S. B., Jules, E., & Arbiser, J. L. (2023). Skin Barrier Function: The Interplay of Physical, Chemical, and Immunologic Properties. Cells, 12(23), 2745.

Balaji, R., Duraisamy, R., & Kumar, M. P. (2019). Complications of diabetes mellitus: A review. Drug Invention Today, 12(1).

Basil Ribeiro, M. (2023). Glutathione: the master antioxidant. Ozone Therapy Global Journal, 13(1), 175-197.

Bava, R., Castagna, F., Musella, V., Lupia, C., Palma, E., & Britti, D. (2023). Therapeutic use of bee venom and potential applications in veterinary medicine. Veterinary Sciences, 10(2), 119.

Bava, R., Castagna, F., Palma, E., Ceniti, C., Millea, M., Lupia, C., ... & Musella, V. (2023). Prevalence of Varroa destructor in honeybee (Apis mellifera) farms and varroosis control practices in Southern Italy. Microorganisms, 11(5), 1228.

Beauchamp, C., & Fridovich, I. (1971). Superoxide dismutase: improved assays and an assay applicable to acrylamide gels. Analytical biochemistry, 44(1), 276-287. doi: 10.1016/0003-2697(71)90370-8

Beiraghi-Toosi, A., Askarian, R., Haghighi, F. S., Safarian, M., Kalantari, F., & Hashemy, S. I. (2018). Burn-induced oxidative stress and serum glutathione depletion; a cross sectional study. Emergency, 6(1), e54.

Bekkering S, Quintin J, Joosten LA, van der Meer JW, Netea MG, Riksen NP. Oxidized low-density lipoprotein induces long-term proinflammatory cytokine production and foam cell formation via epigenetic reprogramming of monocytes. Arterioscler Thromb Vasc Biol. 2014;34:1731–1738. doi: 10.1161/ATVBAHA.114.303887

Bernal, E., & Arnoldo, B. D. (2018). Electrical injuries. In Total burn care (pp. 396-402). Elsevier.

Bhatia, N., Kaur, G., Soni, V., Kataria, J., & Dhawan, R. K. (2016). Evaluation of the wound healing potential of isoquercetin-based cream on scald burn injury in rats. Burns & trauma, 4.

Biswas, R., Alam, M., Sarkar, A., Haque, M. I., Hasan, M. M., & Hoque, M. (2022). Application of nanotechnology in food: processing, preservation, packaging and safety assessment. Heliyon, 8(11), e11795.

Bloch, I. (2021). Modeling imprecise and bipolar algebraic and topological relations using morphological dilations. Mathematical morphology-theory and applications, 5(1), 1-20

Boulaares, I., & Derouiche, S. (2021). Effect of Garlic and Onions Extract Enriched with Honey Treatment on the Lipid Profile, Biochemical and Hematological Biomarker Status in Healthy Women. Pharmaceutical and Biosciences Journal, 9(1), 22-27.

Boulaares, I., Derouiche, S., & Guemari, I. Y. (2024). Protective effect of ObE against Doxorubicin-Induced immunosuppression and Cardiotoxicity in Rats. Research Journal of Pharmacy and Technology, 17(4), 1839-1843. doi: 10.52711/0974-360X.2024.00292

Boulaares, I., Derouiche, S., & Niemann, J. (2024). HPLC-Q-TOF-MS analysis of phenolic compounds, *in vitro* biological activities and *in vivo* acute toxicity evaluation of Ocimum basilicum L. Fresenius Environmental Bulletin, 33(2), 73-82.

Boulaares, I., Guemari, I. Y., & Derouiche, S. (2020). Analysis of Some Hematological and Biochemical Markers in Women Cancer Patients Receiving Doxorubicine Chemotherapy. Pharmaceutical and Biosciences Journal, 8(1), 29-34

Bradford MM. (1976). A rapid and sensitive method for the quantitation of microgram quantities of protein utilizing the principle of protein-dye binding. Academic press, 72 (57), 248-254.

Brenner, D. R., Scherer, D., Muir, K., Schildkraut, J., Boffetta, P., Spitz, M. R., ... & Hung, R. J. (2014). A review of the application of inflammatory biomarkers in epidemiologic cancer research. Cancer Epidemiology, Biomarkers & Prevention, 23(9), 1729-1751.

Brito, S., Baek, M., & Bin, B. H. (2024). Skin structure, physiology, and pathology in topical and transdermal drug delivery. Pharmaceutics, 16(11), 1403.

C

Carpena, M., Nuñez-Estevez, B., Soria-Lopez, A., & Simal-Gandara, J. (2020). Bee venom: an updating review of its bioactive molecules and its health applications. Nutrients, 12(11), 3360.

Chabane, M.-D., Bedouhene, S., Belambri, S.-A., Senani, N., Rekeb, T., Ladj, K., Ksouri, R., Dang, P. M.-C., & El-Benna, J. (2025). Bee venom modulates human neutrophil inflammatory functions *in vitro* and exerts an anti-inflammatory effect *in vivo* in rats. Inflammopharmacology, 33(7), 3933–3946.

Chandraprabha, M., Krishna, R. H., Samrat, K., Pradeepa, K., Patil, N. C., & Sasikumar, M. (2022). Biogenic collagen-nano zno composite membrane as potential wound dressing material: structural characterization, antibacterial studies and *in vivo* wound healing studies. Journal of Inorganic and Organometallic Polymers and Materials, 32(9), 3429-3444. doi: 10.1007/s10904-022-02351-8

Chandrasekaran, S., Anusuya, S., & Anbazhagan, V. (2022). Anticancer, anti-diabetic, antimicrobial activity of zinc oxide nanoparticles: A comparative analysis. Journal of Molecular Structure, 1263, 133139.

Chemingui, H., Moulahi, A., Missaoui, T., Al-Marri, A. H., & Hafiane, A. (2022). Green synthesis of ZnO nanoparticles using Hibiscus sabdariffa and evaluation of antioxidant activity. Environmental Technology.

Chen, J., Guo, Y., Zhang, X., Liu, J., Gong, P., Su, Z., et al. (2023). Emerging nanoparticles in food: sources, application, and safety. J. Agricult. Food Chem. 71, 3564–3582.

Chen, J., Liu, C., Yang, Y., Gong, X., & Qian, H. (2025). The stratum corneum barrier: Impaired function in relation to associated lipids and proteins. Tissue Barriers, 13(2), 2361197.

Chen, R., Xu, H., Li, X., Dong, J., Wang, S., Hao, J., & Liang, G. (2025). Role of oxidative stress in post-burn wound healing. Burns & Trauma, 13, tkaf040.

Cheng, Y., & Chen, H. (2021). Aberrance of zinc metalloenzymes-induced human diseases and its potential mechanisms. Nutrients 13 (12).

Chetehouna, S., Atoussi, O., & Derouiche, S. (2020). Biological activity and toxicological profile of zinc oxide nanoparticles synthesized by Portulaca oleracea (L) leaves extract. Adv Nanomed Nanotechnol Res, 2(2), 125-133.

Chetehouna, S., Derouiche, S., & Réggami, Y. (2023). Green synthesis of SeNPs using Sonchus maritimus based nanosized metal oxides for *in vitro* biological applications and *in vivo* acute toxicity evaluation. Kragujevac Journal of Science, 45, 65-78.

Christensen, R. E., & Jafferany, M. (2023). Psychiatric and psychologic aspects of chronic skin diseases. Clinics in Dermatology, 41(1), 75-81.

Colebrook, A. J., & Pradhan, S. (2025). Guideline review of NICE impetigo: antimicrobial prescribing NG153. Archives of Disease in Childhood-Education and Practice, 110(5), 240-242.

Czyżowska, A., & Barbasz, A. (2022). A review: zinc oxide nanoparticles–friends or enemies?. International journal of environmental health research, 32(4), 885-901.

D

Denk, B., Yaprakci, V., Dayi, B., Sevimli, A., Stevanović, J., Glavinić, U., & Stanimirović, Z. (2024). Exploring the therapeutic potential of bee venom components in wound healing: a comprehensive evaluation of morphometric, biochemical, and histopathological markers. Acta Veterinaria-Beograd, 74(3), 347-366.

Devi, A., Sangeeta, Kumar, N. R., & Kaur, J. (2016).Honey bee venom and its composition: Focusing on different Apis species – A review.Journal of Basic and Applied Engineering Research, 3(1), 96–98.

Devine, R.; Diltz, Z.; Hall, M.W.; Thakkar, R.K. The systemic immune response to pediatric thermal injury. Int. J. Burn. Trauma2018, 8, 6–16akir, B.; Ye ˘gen, B.Ç. Systemic Responses to Burn Injury. Turk. J. Med Sci. 2004, 34, 215–226.

Dhupa, N. (2020). Burn injury. In The veterinary ICU book (pp. 973-981). CRC Press.

Diab T, Alkafaas SS, Shalaby TI, Hessien M. Paclitaxel nanoparticles induce apoptosis and regulate TXR1, CYP3A4 and CYP2C8 in breast cancer and hepatoma cells. Anticancer Agents Med Chem. 2020

Díez-Pascual, A. M. (2021). Carbon-based nanomaterials. International Journal of Molecular Sciences, 22(14), 7726.

Dimitrov, J. D., Roumenina, L. T., Perrella, G., & Rayes, J. (2023). Basic mechanisms of hemolysis-associated thrombo-inflammation and immune dysregulation. Arteriosclerosis, Thrombosis, and Vascular Biology, 43, 1349-1361.

Djouadi, A., & Derouiche, S. (2021). Spinach mediated synthesis of zinc oxide nanoparticles: Characterization, *in vitro* biological activities study and *in vivo* acute toxicity evaluation. Current Research in Green and Sustainable Chemistry, 4, 100214.

Dkhil, M. A., Diab, M. S., Aljawdah, H. M., Murshed, M., Hafiz, T. A., Al-Quraishy, S., & Bauomy, A. A. (2020). Neuro-biochemical changes induced by zinc oxide nanoparticles. Saudi Journal of Biological Sciences, 27(10), 2863-2867.

Drahansky, M., Dolezel, M., Urbanek, J., Brezinova, E., & Kim, T. H. (2012). Influence of skin diseases on fingerprint recognition. BioMed Research International, 2012(1), 626148.

Duda, G. N., Geissler, S., Checa, S., Tsitsilonis, S., Petersen, A., and Schmidt-Bleek, K. (2023). The decisive early phase of bone regeneration. Nat. Rev. Rheumatol. 19 (2),78–95.

Dwivedi, V. K., Chaudhary, M., Ahmad, A., Soni, A., & Naithani, V. (2010). Comparative efficacy of ampucare and silver sulfadiazine against burn wound rat. J Appl Sci Res, 6(6), 674-682.

E

El Mehdi, I., Falcão, S. I., Boujraf, S., Mustapha, H., Campos, M. G., & Vilas-Boas, M. (2022). Analytical methods for honeybee venom characterization. Journal of advanced pharmaceutical technology & research, 13(3), 154-160.

El Mehdi, I., Falcão, S. I., Harandou, M., Boujraf, S., Calhelha, R. C., Ferreira, I. C., ... & Vilas-Boas, M. (2021). Chemical, cytotoxic, and anti-inflammatory assessment of honey bee venom from Apis mellifera intermissa. Antibiotics, 10(12), 1514.

El-Aassar, M. R., Ibrahim, O. M., & Al-Oanzi, Z. H. (2021). Biotechnological applications of polymeric nanofiber platforms loaded with diverse bioactive materials. Polymers, 13(21), 3734.

El Adham, E. K., Hassan, A. I., & Dawoud, M. M. A. (2022). Evaluating the role of propolis and bee venom on the oxidative stress induced by gamma rays in rats. Scientific Reports, 12, 2656.

Elankathirselvan, K., Praveen, K., & Al-Ansari, M. M. (2024). Synthesis and characterization of Pyrus communis fruit extract synthesized ZnO NPs and assessed their anti-diabetic and anti-microbial potential. Environmental Research, 258, 119450.

Elbrolesy, A., Abdou, Y., Elhussiny, F. A., & Morsy, R. (2023). Novel green synthesis of UV-sunscreen ZnO nanoparticles using solanum lycopersicum fruit extract and evaluation of their antibacterial and anticancer activity. Journal of Inorganic and Organometallic Polymers and Materials, 33(12), 3750-3759.

Elhanafy, A. I., Mousa, A. M., & Kamal, A. M. (2023). Immunomodulatory, anti-inflammatory and antioxidant activities of bee venom in doe rabbits under high ambient temperature. J Anim Health Prod, 11(1), 82-89.

El-Khawaga, A. M., Elsayed, M. A., Gobara, M., Suliman, A. A., Hashem, A. H., Zaher, A. A., ... & Salem, S. S. (2025). Green synthesized ZnO nanoparticles by Saccharomyces cerevisiae and their antibacterial activity and photocatalytic degradation. Biomass Conversion and Biorefinery, 15(2), 2673-2684.

El-Moslamy, S. H., Yahia, I., Zahran, H., & Kamoun, E. A. (2023). Novel biosynthesis of MnO NPs using Mycoendophyte: industrial bioprocessing strategies and scaling-up production with its evaluation as anti-phytopathogenic agents. Scientific reports, 13(1),2052

El-Refai, H. A., Saleh, A. M., Mohamed, S. I., Aboul Naser, A. F., Zaki, R. A., Gomaa, S. K., & Hamed, M. A. (2024). Biosynthesis of zinc oxide nanoparticles using Bacillus paramycoides for *in vitro* biological activities and *in* ® assessment against hepatorenal injury induced by CCl4 in rats. Applied Biochemistry and Biotechnology, 196(9), 5953-5973.

El-Saadony, M. T., Fang, G., Yan, S., Alkafaas, S. S., El Nasharty, M. A., Khedr, S. A., ... & AbuQamar, S. F. (2024). Green synthesis of zinc oxide nanoparticles: preparation, characterization, and biomedical applications-a review. International journal of nanomedicine, 12889-12937.

Elshater, A. E. A., Mohi Eldin, M. M., Salman, M., & Kasem, N. R. (2014). The curative effect of Bee Venom and Propolis on oxidative stress induced by γ-irradiation on blood and tissues

of rats. Egyptian Academic Journal of Biological Sciences. C, Physiology and Molecular Biology, 6(1), 53-69.

Elsilk, S. E., El-Shenody, R. A., Afifi, S. S., & Abo-Shanab, W. A. (2024). Green-synthesized zinc oxide nanoparticles by Enterobacter sp.: unveiling characterization, antimicrobial potency, and alleviation of copper stress in Vicia faba (L.) plants. BMC Plant Biology, 24(1), 474.

El-Zahed, M. M., Abou-Dobara, M. I., El-Khodary, M. M., & Mousa, M. M. (2024). Antimicrobial activity and nanoremediation of heavy metals using biosynthesized CS/GO/ZnO nanocomposite by Bacillus subtilis ATCC 6633 alone or immobilized in a macroporous cryogel. Microbial cell factories, 23(1), 278.

Elzein, B. (2024). Nano Revolution: "Tiny tech, big impact: How nanotechnology is driving SDGs progress". College of Engineering, University of Business and Technology, Jeddah, Saudi Arabia; Global Council for Tolerance and Peace, Valetta, Malta.

Erdoğan, P. M., Bilgili-Tetikoğlu, F., Çelik-Uzuner, S., Yıldız, O., Kolayli, S., & Mossialos, D. (2025). Therapeutic bioactivity exerted by the Apis mellifera bee venom and its major protein melittin: a scoping review. Molecules, 30(19), 4003.

Erdoğan, Ü., & Özsoy, Y. (2025). Cochleate novel drug delivery system. İstanbul Journal of Pharmacy, 55(1), 86–94.

Eren, B., Gunduz, M. K., Kaymak, G., Berikten, D., & Bahsi, Z. B. (2024). Therapeutic Potential of Sol–Gel ZnO Nanocrystals: Anticancer, Antioxidant, and Antimicrobial Tri-Action. ACS omega, 9(13), 14818-14829.

Eze, O. B., Nwodo, O. F., & Ogugua, V. N. (2016). Therapeutic effect of honey bee venom. Proteins (enzymes), 1(2).

Ezzat, N., Emadeldien, N., Ali, M. K., Fahd, S., Shebl, S., Elshishiny, M., ... & Elzayat, E. M. (2025). *In vitro* evaluation of zinc oxide-metformin folic acid nanocomposite as a targeted drug delivery system for cancer therapy. Asian Pacific journal of cancer prevention: APJCP, 26(2), 443.

F

Fadl, A. E. W. (2018). Antibacterial and antibiofilm effects of bee venom from (Apis mellifera) on multidrug-resistant bacteria (MDRB). Al-Azhar Journal of Pharmaceutical Sciences, 58(2), 60-80.

Fang, Q., Guo, S., Zhou, H., Han, R., Wu, P., & Han, C. (2017). Astaxanthin protects against early burn-wound progression in rats by attenuating oxidative stress-induced inflammation and mitochondria-related apoptosis. Scientific reports, 7(1), 41440.

Farahani, M., Rajabi Delivand, M. H., Abednia, A., & Tajdini, G. (2025). Carbon-Based, Organic, and Metallic Nanoparticles: Biomedical Applications and Environmental Insights. J. Mater. Environ. Sci., 16 (9), 1595, 1608.

Flohr, C. Hay, R. Putting the Burden of Skin Diseases on the Global Map Br. J. Dermatol 2021, 184, 189-190.

Fouda, A., Saied, E., Eid, A. M., Kouadri, F., Alemam, A. M., Hamza, M. F., ... & Hassan, S. E. D. (2023). Green synthesis of zinc oxide nanoparticles using an aqueous extract of Punica granatum for antimicrobial and catalytic activity. Journal of Functional Biomaterials, 14(4), 205.

Fukuzuka, K., Edwards III, C. K., Clare-Salzler, M., Copeland III, E. M., Moldawer, L. L., & Mozingo, D. W. (2000). Glucocorticoid and Fas ligand induced mucosal lymphocyte apoptosis after burn injury. Journal of Trauma and Acute Care Surgery, 49(4), 710-716.

G

Gacto-Sanchez, P. (2017). Surgical treatment and management of the severely burn patient: review and update. Medicina Intensiva (English Edition), 41(6), 356-364.

Gajski, G., Leonova, E., & Sjakste, N. (2024). Bee venom: composition and anticancer properties. Toxins, 16(3), 117.

Gaur, J., Vikrant, K., Kim, K. H., Kumar, S., Pal, M., Badru, R., ... & Momoh, J. (2023). Photocatalytic degradation of Congo red dye using zinc oxide nanoparticles prepared using Carica papaya leaf extract. Materials Today Sustainability, 22, 100339.

Gavilán, H., Serrano, M. B., & Cabanelas, J. C. (2023). Nanomaterials and their synthesis for a sustainable future (Vol. 149, pp. 233–310). Materials Research Forum LLC.

Gerasymchuk, M., Robinson, G. I., Vardinska, N., Ayedun, S. A., Alozie, S. C., Robinson, J. W., ... & Kovalchuk, I. (2023). Sex-Dependent Skin Aging and Rejuvenation Strategies. Dermato, 3(3), 196-223.

Gharagheshlagh, S.N., Fatemi, M.J., Jamili, S., Sharifi, A.M., & Nourani MR (2020). Isolation and characterization of acid-soluble collagen from the skin of Rutilus Frisii Kutum (Kamensky) of the Caspian Sea. Iranian Journal of Fisheries Sciences, 19(2), 768-779. doi: 10.22092/ijfs.2019.118957.

Ghorbani, M. G., Ghazitabar, A., Gholami, F., Naderi, M., & Haghshenas, D. F. (2025). Investigating the Effect of Zinc Oxide Nanoparticles on the Absorption of Ultraviolet Radiation for Enhancing the Efficacy of Sunscreen Products. Progress in Color, Colorants and Coatings, 19(1), 47-65.

Gomaa, I., Aleid, G., EL-Moslamy, S. H., AlShammari, A., Al-Marshedy, S., Alshammary, F., Gharkan, J., Abdel-Hameed, R., & Kamoun, E. A. (2024). Synergistic efficacy of ZnO quantum dots, Ag NPs, and nitazoxanide composite against multidrug-resistant human pathogens as new trend of revolutionizing antimicrobial treatment. Discover Nano, 19, 164.

Grinn-Gofroń, A., Kołodziejczak, M., Hrynkiewicz, R., Lewandowski, F., Bębnowska, D., Adamski, C., & Niedźwiedzka-Rystwej, P. (2025). Antimicrobial potential of bee-derived products: Insights into honey, propolis and bee venom. Pathogens, 14(8), 780.

Guan, X., Xing, S., & Liu, Y. (2024). Engineered cell membrane-camouflaged nanomaterials for biomedical applications. Nanomaterials, 14(5), 413.

Guha, S., Ferrie, R. P., Ghimire, J., Ventura, C. R., Wu, E., Sun, L., ... & Wimley, W. C. (2021). Applications and evolution of melittin, the quintessential membrane active peptide. Biochemical pharmacology, 193, 114769.

H

Hameed, H., Waheed, A., Sharif, M. S., Saleem, M., Afreen, A., Tariq, M., ... & Mahmoud, R. M. (2023). Green synthesis of zinc oxide (ZnO) nanoparticles from green algae and their assessment in various biological applications. Micromachines, 14(5), 928.

Hartman-Adams, H., Banvard, C., & Juckett, G. (2014). Impetigo: diagnosis and treatment. American family physician, 90(4), 229-235.

Hassan, S. A., Alazragi, R. S., & Salem, N. A. (2021). Potential therapeutic effect of bee venom on cisplatin-induced hepatotoxicity. J. Pharm. Res. Int, 33, 200-210.

He, L., Lan, W., Wang, Y., Ahmed, S., & Liu, Y. (2019). Extraction and characterization of self-assembled collagen isolated from grass carp and crucian carp. Foods, 8(9), 396.

Helmy, Y. A., Taha-Abdelaziz, K., Hawwas, H. A. E., Ghosh, S., AlKafaas, S. S., Moawad, M. M. M., Saied, E. M., Kassem, I. I., & Mawad, A. M. M. (2023). Antimicrobial resistance and recent alternatives to antibiotics for the control of bacterial pathogens with an emphasis on foodborne pathogens. Antibiotics, 12(3), 456.

Hong, J., Lu, X., Deng, Z., Xiao, S., Yuan, B., & Yang, K. (2019). How melittin inserts into cell membrane: conformational changes, inter-peptide cooperation, and disturbance on the membrane. Molecules, 24(9), 1775.

Hosseini, M., Koehler, K. R., & Shafiee, A. (2022). Biofabrication of human skin with its appendages. Advanced Healthcare Materials, 11, e2201626

Hossen, M. S., Shapla, U. M., Gan, S. H., & Khalil, M. I. (2016). Impact of bee venom enzymes on diseases and immune responses. Molecules, 22(1), 25.

Hou, T., Sana, S. S., Li, H., Wang, X., Wang, Q., Boya, V. K. N., Vadde, R., Kumar, R., Kumbhakar, D. V., Zhang, Z., & Mamidi, N. (2022). Development of plant protein derived triangular shaped nano zinc oxide particles with inherent antibacterial and neurotoxicity properties. Pharmaceutics, 14(10), 2155.

Huq, M. A., Apu, M. A. I., Ashrafudoulla, M., Rahman, M. M., Parvez, M. A. K., Balusamy, S. R., ... & Rahman, M. S. (2023). Bioactive ZnO nanoparticles: Biosynthesis, characterization and potential antimicrobial applications. Pharmaceutics, 15(11), 2634.

I

Imath, M., Giri, J., Mohammad, F., & Ragavendran, C. (2025). Eco-friendly synthesis of ZnO nanoparticles fabricated using Fioria vitifolia L. and their biomedical potentials. Microbial pathogenesis, 199, 107139.

Irede, E. L., Awoyemi, R. F., Owolabi, B., Aworinde, O. R., Kajola, R. O., Hazeez, A., ... & Ifijen, I. H. (2024). Cutting-edge developments in zinc oxide nanoparticles: synthesis and applications for enhanced antimicrobial and UV protection in healthcare solutions. RSC advances, 14(29), 20992-21034.

Ishida, S., Hashimoto, I., Seike, T., Abe, Y., Nakaya, Y., & Nakanishi, H. (2014). Serum albumin levels correlate with inflammation rather than nutrition supply in burn patients: A retrospective study. The Journal of Medical Investigation, 61, 361–367.

Isidorov, V., Zalewski, A., Zambrowski, G., & Swiecicka, I. (2023). Chemical composition and antimicrobial properties of honey bee venom. Molecules, 28(10), 4135.

Islam, F., Shohag, S., Uddin, M. J., Islam, M. R., Nafady, M. H., Akter, A., et al. (2022). Exploring the journey of zinc oxide nanoparticles (ZnO-NPs) toward biomedical applications. Materials 15:2160. doi: 10.3390/ma15062160

Ismail, I. B., Bhat, Y. J., & ul Islam, M. S. (2025). Treatment advances in vitiligo: an updated review. Dermatology practical & conceptual, 15(1), 4600.

J

Jaafar, F. S., & Albushabaa, S. H. H. (2025). General study of honey bee venom Apis mellifera: A review. Journal of Applied Health Sciences and Medicine, 5(1), 12–18.

Jadoun, S., Arif, R., Jangid, N. K., & Meena, R. K. (2020). Green synthesis of nanoparticles using plant extracts: a review. Environmental Chemistry Letters, 19(1), 355–374.

Jayawardena, R., Ranasinghe, P., Galappatthy, P., Malkanthi, R., Constantine, G., & Katulanda, P. (2012). Effects of zinc supplementation on diabetes mellitus: A systematic review and meta-analysis. Diabetology & Metabolic Syndrome, 4, 13.

Jiang, Z., et al. (2022). Progress in laser ablation and biological synthesis processes: "Top-down" and "bottom-up" approaches for the green synthesis of Au/Ag nanoparticles. International Journal of Molecular Sciences, 23, 14658.

Joge, R. R., Kathane, P. U., & Joshi, S. H. (2022). Vitiligo: a narrative review. Cureus, 14(9).

John, J. (2025). Cutting-edge nanoparticle innovations in biomedical science: Synthesis, applications, challenges, and future prospects. Journal of Nanotechnology and Nanomaterials, 6(1), 43–66.

Jørgensen, L. B., Sørensen, J. A., Jemec, G. B., & Yderstræde, K. B. (2016). Methods to assess area and volume of wounds–a systematic review. International wound journal, 13(4), 540-553.

Joudeh, N., & Linke, D. (2022). Nanoparticle classification, physicochemical properties, characterization, and applications: a comprehensive review for biologists. Journal of nanobiotechnology, 20(1), 262.

K

Kabir, D. (2025). Green Synthesis of Nanoparticles Using Plant Extracts and Biopolymers. Journal of Applied Science and Environmental Studies, 8(4), 316-339.

Kalaba, M. H., El-Sherbiny, G. M., Ewais, E. A., Darwesh, O. M., & Moghannem, S. A. (2024). Green synthesis of zinc oxide nanoparticles (ZnO-NPs) by Streptomyces baarnensis and its active metabolite (Ka): a promising combination against multidrug-resistant ESKAPE pathogens and cytotoxicity. BMC microbiology, 24(1), 254.

Kapare, H. S., Bhosale, M., Karwa, P., Kulkarni, D., Bhole, R., & Labhade, S. (2025). Phyto-assisted synthesis and investigation of zinc oxide nanoparticles for their anti-aging, sun protection and antibacterial activity. Cosmetics, 12, 238.

Karam, S. T., & Abdulrahman, A. F. (2022, August). Green synthesis and characterization of ZnO nanoparticles by using thyme plant leaf extract. In Photonics (Vol. 9, No. 8, p. 594). Multidisciplinary Digital Publishing Institute.

Karmaker, N., Maraz, K. M., Islam, F., Haque, M. M., Razzak, M., Mollah, M., ... & Khan, R. A. (2021). Fundamental characteristics and application of radiation. GSC Advanced Research and Reviews, 7(1), 064-072.

Kasolang, S., Adlina, W. A., Rahman, N. A., & Nik, N. R. (2020). Common skin disorders: a review. Jurnal Tribologi, 25(April), 59-82.

Katt, B., & Coyle, R. (2021). 4 Thermal Burns, Chemical Burns, and Frostbite. Review of Hand Surgery, E-Book, 76.

Khafaga, D. S., El-Khawaga, A. M., Elfattah Mohammed, R. A., & Abdelhakim, H. K. (2023). Green synthesis of nano-based drug delivery systems developed for hepatocellular carcinoma treatment: a review. Molecular biology reports, 50(12), 10351-10364.

Khalid, A., Khan, R., Ul-Islam, M., Khan, T., & Wahid, F. (2017). Bacterial cellulose-zinc oxide nanocomposites as a novel dressing system for burn wounds. Carbohydrate polymers, 164, 214-221.

Khalil, A., Elesawy, B. H., Ali, T. M., & Ahmed, O. M. (2021). Bee venom: From venom to drug. Molecules, 26(16), 4941.

Khan, D. A. (2016). Hypersensitivity and immunologic reactions to biologics: opportunities for the allergist. Annals of Allergy, Asthma & Immunology, 117(2), 115-120.

Khan, I., Saeed, K., & Khan, I. (2022). Metal oxide nanoparticles and their applications. Arabian Journal of Chemistry, 15(2), 103–120. urnal of molecular sciences, 24(4), 3749.

Khan, W. S., Asmatulu, E., & Asmatulu, R. (2025). Nanotechnology emerging trends, markets and concerns. In Nanotechnology safety (pp. 1-21). Elsevier.

Korzeniowski, T., Mertowska, P., Mertowski, S., Podgajna, M., Grywalska, E., Strużyna, J., & Torres, K. (2022). The role of the immune system in pediatric burns: a systematic review. Journal of Clinical Medicine, 11, 2262.

Ku, Y. H., Kang, J. H., & Lee, H. (2020). Effect of bee venom on an experimental cellular model of Alzheimer's disease. The American Journal of Chinese Medicine, 48(08), 1803-1819.

Kuehlmann, B., Bonham, C. A., Zucal, I., Prantl, L., & Gurtner, G. C. (2020). Mechano transduction in wound healing and fibrosis. Journal of Clinical Medicine, 9(5), 1423.

Kumar, R., Lee, D., Ağbulut, Ü., et al. (2024). Different energy storage techniques: Recent advancements, applications, limitations, and efficient utilization of sustainable energy. Journal of Thermal Analysis and Calorimetry, 149, 1895–1933.

Kurek-Górecka, A., Komosinska-Vassev, K., Rzepecka-Stojko, A., & Olczyk, P. (2021). Bee venom in wound healing. Molecules, 26, 148.

L

Lada, G., Chinoy, H., Heal, C., Warren, R. B., Talbot, P. S., & Kleyn, C. E. (2022). Depression and suicidality in patients with psoriasis and the role of psoriatic arthritis: a cross-sectional study in a tertiary setting. Journal of the Academy of Consultation-Liaison Psychiatry, 63(4), 372-383.

Ladhani, H. A., Yowler, C. J., & Claridge, J. A. (2021). Burn wound colonization, infection, and sepsis. Surgical infections, 22(1), 44-48.

Layton, A. M., Bettoli, V., Delore, V., Puentes, E., & Tan, J. K. (2025). The Burden of Acne Vulgaris on Health-Related Quality of Life and Psychosocial Well-Being Domains: A Systematic Review. American Journal of Clinical Dermatology, 1-31.

Lebaka, V. R., Ravi, P., Reddy, M. C., Thummala, C., & Mandal, T. K. (2025). Zinc oxide nanoparticles in modern science and technology: multifunctional roles in healthcare, environmental remediation, and industry. Nanomaterials, 15(10), 754.

Li, S., Tan, H. Y., Wang, N., Zhang, Z. J., Lao, L., Wong, C. W., & Feng, Y. (2015). The role of oxidative stress and antioxidants in liver diseases. International journal of molecular sciences, 16(11), 26087-26124.

Liu, J., Ren, Z. H., Qiang, H., Wu, J., Shen, M., Zhang, L., & Lyu, J. (2020). Trends in the incidence of diabetes mellitus: results from the Global Burden of Disease Study 2017 and implications for diabetes mellitus prevention. BMC public health, 20(1), 1415.

Lopez Venditti, E. D., Crespo Andrada, K. F., Bustos, P. S., Maldonado Torales, M., Manrrique Hughes, I., Paraje, M. G., & Guiñazú, N. (2025). Antibacterial, antifungal, and antibiofilm activities of biogenic zinc nanoparticles against pathogenic microorganisms. Frontiers in Cellular and Infection Microbiology, 15, 1545119.

Lopez-Ojeda, W., Pandey, A., Alhajj, M., & Oakley, A. M. (2022). Anatomy, skin (integument). In StatPearls [internet]. StatPearls P

Lotfollahi, Z. (2024). The anatomy, physiology and function of all skin layers and the impact of ageing on the skin. Wound Practice and Research, 32(1), 6–10

M

Ma, X., Tian, Y., Yang, R., Wang, H., Allahou, L. W., Chang, J., ... & Poma, A. (2024). Nanotechnology in healthcare, and its safety and environmental risks. Journal of nanobiotechnology, 22(1), 715.

Madhvapathy, S. R., Arafa, H. M., Patel, M., Winograd, J., Kong, J., Zhu, J., ... & Rogers, J. A. (2022). Advanced thermal sensing techniques for characterizing the physical properties of skin. Applied Physics Reviews, 9(4).

Maekawa, T., Kajihara, H., Okabayashi, K., Otani, M., & Yuge, O. (2002). Impairment of splenic B and T lymphocytes in the early period after severe thermal injury: immunohistochemical and electron microscopic analysis. Burns, 28(4), 329-339.

Mahajan, M., Kumar, S., Gaur, J., Kaushal, S., Dalal, J., Singh, G., ... & Ahlawat, D. S. (2025). Green synthesis of ZnO nanoparticles using Justicia adhatoda for photocatalytic degradation of malachite green and reduction of 4-nitrophenol. RSC advances, 15(4), 2958-2980.

Malik, S., Muhammad, K., & Waheed, Y. (2023). Nanotechnology: A revolution in modern industry. Molecules, 28(2), 661.

Mancek-Keber M, Frank-Bertoncelj M, Hafner-Bratkovic I, Smole A, Zorko M, Pirher N, Hayer S, Kralj-Iglič V, Rozman B, Ilc N, et al. Toll-like receptor 4 senses oxidative stress mediated by the oxidation of phospholipids in extracellular vesicles. Sci Signal. 2015;8:ra60. doi: 10.1126/scisignal.2005860

Mancini, A., Inchingolo, A. M., Marinelli, G., Trilli, I., Sardano, R., Pezzolla, C., ... & Inchingolo, A. D. (2025). Topical and Systemic Therapeutic Approaches in the Treatment of Oral Herpes Simplex Virus Infection: A Systematic Review. International Journal of Molecular Sciences, 26(17), 8490.

Mandal, A. K., Katuwal, S., Tettey, F., Gupta, A., Bhattarai, S., Jaisi, S., ... & Parajuli, N. (2022). Current research on zinc oxide nanoparticles: synthesis, characterization, and biomedical applications. Nanomaterials, 12(17), 3066.

Manzoor, T., Farooq, N., Sharma, A., Shiekh, P. A., Hassan, A., Dar, L. A., ... & Ahmad, S. M. (2024). Exosomes in nanomedicine: a promising cell-free therapeutic intervention in burn wounds. Stem cell research & therapy, 15(1), 355.

Markiewicz-Gospodarek, A., Kozioł, M., Tobiasz, M., Baj, J., Radzikowska-Büchner, E., & Przekora, A. (2022). Burn wound healing: clinical complications, medical care, treatment, and dressing types: the current state of knowledge for clinical practice. International journal of environmental research and public health, 19(3), 1338.

Maryani, F., Filailla, E., & Krismastuti, F. S. H. (2024, February). Comparative studies on chemically synthesized and biosynthesized zinc oxide nanoparticles using Desmodium sp. and their potential as UV filters. In IOP Conference Series: Earth and Environmental Science (Vol. 1312, No. 1, p. 012022).

Marzano, A. V., Borghi, A., & Cugno, M. (2016). Adverse drug reactions and organ damage: the skin. European journal of internal medicine, 28, 17-24.

Mbanga, L., Mulenga, M., Mpiana, P., Bokolo, K., Mumbwa, M., & Mvingu, K. (2014). Determination of sun protection factor (SPF) of some body creams and lotions marketed in Kinshasa by ultraviolet spectrophotometry. International Journal of Advanced Research in Chemical Science 1(8), 7-13.

McKnight, G., Shah, J., & Hargest, R. (2022). Physiology of the skin. Surgery (Oxford), 40(1), 8-12.

Melnikova, N., Vorobyova, O., Balakireva, A., Malygina, D., Solovyeva, A., Belyaeva, K., Knyazev, A. (2020). The new pharmaceutical compositions of zinc oxide nanoparticles and triterpenoids for the burn treatment. Pharmaceuticals, 13(9), 207. doi: 10.3390/ph13090207

Mheich, A., et al. (2026). Bee venom bioactivity and antioxidant potential: mechanisms involving oxidative stress modulation and antioxidant enzymes.

Mirzayev, M. V. (2025). Anatomy of the skin: Structure and functions of the epidermis and dermis. International Journal of Medical Sciences, 5(03), 302–306.

Mishra, D. N., Prasad, L., & Suyal, U. (2025). Synthesis of zinc oxide nanoparticles using Trichoderma harzianum and its bio-efficacy on Alternaria brassicae. Frontiers in Microbiology, 16, 1506695.

Moghaddam, F. D., Bertani, F. R., & Tay, F. (2023). Skin Anatomy. Carrier-mediated Gene and Drug Delivery for Dermal Wound Healing, 4.

Mohammed Saied, L. H. (2022). Nanotechnology in dentistry (Bachelor of Dental Surgery project). College of Dentistry, University of Baghdad, Department of Pedodontics and Prevention.

Mosam, A., Shuping, L., Naicker, S., Maphanga, T., Tsotetsi, E., Mudau, R., ... & Singh, A. (2023). A case of antifungal-resistant ringworm infection in KwaZulu-Natal Province, South Africa, caused by Trichophyton indotineae. Public Health Bulletin South Africa, 1-7.

Mossa, A.-T. H., Swelam, E. S., & Mohafrash, S. M. (2015). Sub-chronic exposure to fipronil induced oxidative stress, biochemical and histopathological changes in the liver and kidney of male albino rats. Toxicology reports, 2, 775-784. doi: 10.1016/j.toxrep.2015.02.009

Mueangson, O., Mahittikorn, A., Anabire, N. G., Mala, W., & Kotepui, M. (2023). Increased blood Concentrations of malondialdehyde in plasmodium Infection: A Systematic Review and Meta-Analysis. Antioxidants, 12, 1502.

Mutukwa, D., Taziwa, R., & Khotseng, L. E. (2022). A review of the green synthesis of ZnO nanoparticles utilising Southern African indigenous medicinal plants. Nanomaterials, 12(19), 3456.

N

Naderi Gharagheshlagh, S., Fatemi, M.J., Jamili, S., Sharifi, A.M., Nourani, M.R. (2019). Isolation and characterization of acid-soluble collagen from the skin of Rutilus Frisii Kutum (Kamensky) of the Caspian Sea. Iranian Journal of Fisheries Sciences, doi:10.22092/ijfs.2019.118957.

Nagle, S. M., Stevens, K. A., & Wilbraham, S. C. (2023). Wound assessment. In StatPearls [Internet]. StatPearls Publishing.

Nalinanon, S., Benjakul, S., Kishimura, H., Osako, K. (2011). Type I collagen from the skin of ornate threadfin bream (Nemipterus hexodon): Characteristics and effect of pepsin hydrolysis. Food Chemistry, 125(2), 500-507.

Naseer, M., Aslam, B., Iqbal, J., Khan, M. Y., Khan, S. A., & Shah, S. S. A. (2020). Green synthesis of zinc oxide nanoparticles using Nigella sativa seed extract and their antibacterial activity. Journal of Materials Research and Technology, 9(3), 4252–4261.

Naser, S. S., Ghosh, B., Simnani, F. Z., Singh, D., Choudhury, A., Nandi, A., ... & Verma, S. K. (2023). Emerging trends in the application of green synthesized biocompatible ZnO nanoparticles for translational paradigm in cancer therapy. Journal of Nanotheranostics, 4(3), 248-279.

Nasrallah, O., El Kurdi, R., & Mouslmani, M. (2018). Doping of ZnO nanoparticles with curcumin: pH-dependent release and DPPH scavenging activity of curcumin in nanocomposites.

Nassar, M. I. (2022). Bee venom: Antitumor activity and its therapeutic applications. In Bee products and their applications in the food and pharmaceutical industries (pp. 369–390). Academic Press.

Niculescu, A. G., Bîrcă, A. C., Mogoşanu, G. D., Rădulescu, M., Holban, A. M., Manuc, D., ... & Mogoantă, L. (2025). Zinc Alginate Hydrogel-Coated Wound Dressings: Fabrication, Characterization, and Evaluation of Anti-Infective and *In Vivo* Performance. Gels, 11(6), 427.

Nielson, C. B., Duethman, N. C., Howard, J. M., Moncure, M., & Wood, J. G. (2017). Burns: pathophysiology of systemic complications and current management. Journal of Burn Care & Research, 38(1), e469-e481.

Obagi, Z. A. I. D. A. L., Damiani, G., Grada, A., & Falanga, V. I. N. C. E. N. T. (2019). Principles of wound dressings: a review. Surg. Technol. Int, 35(5), 0-57.

Ong, W. Y., Farooqui, T., Kokotos, G., & Farooqui, A. A. (2015). Synthetic and natural inhibitors of phospholipases A2: their importance for understanding and treatment of neurological disorders. ACS chemical neuroscience, 6(6), 814-831.

₱

Parveen, F., Kadam, P., Mujawar, A., Sannakki, B., Patole, S., Wu, Z., Kallel, M., & Pathan, H. (2025). Silver nanoparticles in plasmonic solar cells: A review. ES Materials and Manufacturing, 28, Article 1548.

Patra, J. K., Das, G., Fraceto, L. F., et al. (2018). Nanotechnology-based drug delivery systems: Recent developments and future prospects. [5] Craig, M. (2022). Employing synergistic strategies to advance nanomedicine. AZoNano.

Pelizzo, G., Calcaterra, V., Canonica, C. P. M., Magenes, V. C., Marinaro, M., Durante, E., Cordaro, E., & Zuccotti, G. (2025). Burns in Early Childhood: Age-Specific Causes, Risks, Management, and Implications—A Narrative Review. Children, 12(11), 1424.

Prajapati, R. N., Jagrati, K., Sengar, A., & Prajapati, S. K. (2024). Nanoparticles: Pioneering the future of drug delivery and beyond. World Journal of Pharmaceutical Research, 13(13), 1243-1262.

Prieložná, J., Mikušová, V., & Mikuš, P. (2024). Advances in the delivery of anticancer drugs by nanoparticles and chitosan-based nanoparticles. International journal of pharmaceutics: X, 8, 100281.

Q

Qanash et al. (2025) also reported that combining the BV compound with nanoparticles significantly enhanced the antibacterial efficacy.

Qanash, H., Bazaid, A. S., Alharbi, S. F., Binsaleh, N. K., Barnawi, H., Alharbi, B., Alsolami, A., & Almashjary, M. N. (2025). Therapeutic effects of nanocoating of apitoxin (bee venom) and polyvinyl alcohol supplemented with zinc oxide nanoparticles. Pharmaceutics, 17(2), 172.

R

Radwan, I. A., Rady, D., Ramadan, M., & El Moshy, S. (2024). Mechanism underlying the anti-diabetic potential of bee venom as compared to bone marrow mesenchymal stem cells in the diabetic rat tongue. Dental and Medical Problems, 61(1), 53-64.

Raha, S., & Ahmaruzzaman, M. (2022). ZnO nanostructured materials and their potential applications: progress, challenges and perspectives. Nanoscale advances, 4(8), 1868-1925.

Rahman, M., Islam, M., Biswas, M., & Khurshid Alam, A. (2015). *In vitro* antioxidant and free radical scavenging activity of different parts of Tabebuia pallida growing in Bangladesh. BMC research notes, 8(1), 1-9. doi: 10.1186/s13104-015-1618-6

Ramana, V., Rajeshkumar, S., & Jagadeesh, K. (2023). Review of the environmentally friendly production of zinc oxide nanoparticles and its anti-oxidant, anti-hyperlipidemic, and anti-diabetic properties. Journal of Survey in Fisheries Sciences.

Ramzan, M., Ahmed, S., Khan, F., & Ali, H. (2022). Synergistic effect of zinc oxide nanoparticles and Moringa oleifera leaf extract alleviates cadmium toxicity. Frontiers in Plant Science, 13, 900347.

Rashad, A. A., Ahmed, A., Azmy, O., & Louis, D. (2024). An overview on the application of nanotechnology in burn wound management. International Journal for Holistic Research, 1-8.

Rassaei, L., Marken, F., Sillanpää, M., Amiri, M., Cirtiu, C. M., and Sillanpää, M. (2011). Nanoparticles in electrochemical sensors for environmental monitoring. TrAC Trends Anal. Chem. 30, 1704–1715.

Rathi, M., Kamboj, S., Guarve, K., Kamboj, R., & Dass, R. (2025). Comprehensive Review on Tinea Infection Therapies: Allopathic and Herbal Approaches for Dermatophytosis. Recent Advances in Anti-Infective Drug Discovery.

Reinke, J. M., and Sorg, H. (2012). Wound repair and regeneration. Eur. Surg. Res. 49, 35–43. doi: 10.1159/000339613

Reshma, Shaik, H., Venkatesan, K., Venugopal, A., Kadeer, M., & Puppala, V. S. (2025). A review on nanomaterials: introduction, synthesis, characterization, and applications. Chemical Papers, 79(7), 4075-4085.

Roky, A. H., Islam, M. M., Ahasan, A. M. F., Mostaq, M. S., Mahmud, M. Z., Amin, M. N., & Mahmud, M. A. (2025). Overview of skin cancer types and prevalence rates across continents. Cancer pathogenesis and therapy, 3(02), 89-100.

Rostkowska, E., Poleszak, E., Wojciechowska, K., & Dos Santos Szewczyk, K. (2023). Dermatological management of aged skin. Cosmetics, 10(2), 55.physical properties of skin. Applied Physics Reviews, 9(4).

Rothschild, M. A., Oratz, M., & Schreiber, S. S. (1988). Serum albumin. Hepatology, 8(2), 385-401.

Rowan, M. P., Cancio, L. C., Elster, E. A., Burmeister, D. M., Rose, L. F., Natesan, S., ... & Chung, K. K. (2015). Burn wound healing and treatment: review and advancements. Critical care, 19(1), 243.

Roy, S., Mukherjee, P., Kundu, S., Majumder, D., Raychaudhuri, V., & Choudhury, L. (2024). Microbial infections in burn patients. Acute and Critical Care, 39(2), 214-225.

Rozik, O. I., Hussein, M. M., El-Elebiarie, A. S., & Nady, S. (2024). *In vitro* anti-inflammatory activity of bee venom melittin and phospholipase A2 on murine splenocytes

stimulated with Schistosoma mansoni antigens. Egyptian Academic Journal of Biological Sciences. C, Physiology and Molecular Biology, 16(2), 75-88.

S

Sadek, K. M., Shib, N. A., Taher, E. S., Rashed, F., Shukry, M., Atia, G. A., ... & Abdeen, A. (2024). Harnessing the power of bee venom for therapeutic and regenerative medical applications: an updated review. Frontiers in pharmacology, 15, 1412245.

Saitoh, D., Shirani, K. Z., Cioffi, W. G., Kizaki, T., Ohno, H., Okada, Y., ... & Pruitt Jr, B. A. (2001). Changes in the tissue and plasma superoxide dismutase (SOD) levels in a burned rat model. The Tohoku Journal of Experimental Medicine, 193(1), 27-36.

Sakarcan, A., Sehirli, Ö., Velioğlu-Övünç, A., Ercan, F., Erkanlı, G., Gedik, N., & Şener, G. (2005). Ginkgo biloba extract improves oxidative organ damage in a rat model of thermal trauma. Burns, 31, 1009–1014.

Salem, S. S., Hammad, E. N., Mohamed, A. A., & El-Dougdoug, W. (2022). A comprehensive review of nanomaterials: Types, synthesis, characterization, and applications. Biointerface Res. Appl. Chem, 13(1), 41

Sana, S. S., Vadde, R., Kumar, R., Arla, S. K., Somala, A. R., Rao, K. K., ... & Mamidi, N. (2023). Eco-friendly and facile production of antibacterial zinc oxide nanoparticles from Grewia flavescens (G. flavescens) leaf extract for biomedical applications. Journal of Drug Delivery Science and Technology, 80, 104186.

Sangeetha, G., Rajeshwari, S., & Venckatesh, R. (2011). Green synthesis, characterization and antimicrobial activity of zinc oxide nanoparticles using Azadirachta indica leaf extract. Materials Research Bulletin, 46(12), 2560–256.

Sen, S., Hsei, L., Tran, N., Romanowski, K., Palmieri, T., Greenhalgh, D., & Cho, K. (2019). Early clinical complete blood count changes in severe burn injuries. Burns, 45(1), 97-102.

Senthelal, S., Dydyk, A. M., & Mesfin, F. B. (2024). Ablative nerve block. In StatPearls [Internet]. StatPearls Publishing.

Shi, P., Xie, S., Yang, J., Zhang, Y., Han, S., Su, S., & Yao, H. (2022). Pharmacological effects and mechanisms of bee venom and its main components: Recent progress and perspective. Frontiers in Pharmacology, 13, 1001553.

Shnawa, B. H., Jalil, P. J., Al-Ezzi, A., Mhamedsharif, R. M., Mohammed, D. A., Biro, D. M., & Ahmed, M. H. (2024). Evaluation of antimicrobial and antioxidant activity of zinc oxide nanoparticles biosynthesized with Ziziphus spina-christi leaf extracts. Cureus, 16(1), e38105670.

Shpichka, A., Butnaru, D., Bezrukov, E. A., Sukhanov, R. B., Atala, A., Burdukovskii, V., ... & Timashev, P. (2019). Skin tissue regeneration for burn injury. Stem cell research & therapy, 10(1), 94.

Silva de França, F., & Tambourgi, D. V. (2023). Hyaluronan breakdown by snake venom hyaluronidases: From toxins delivery to immunopathology. Frontiers in immunology, 14, 1125899.

Singh, M., & Prakash, S. (2018). Burn: A clinical perspective. In Theory and applications of heat transfer in humans (Vol. 2, pp. 513–527).

Singh, R., Singh, N., Saini, B., & Rao, H. S. (2008). *In vitro* antioxidant activity of pet ether extract of black pepper. Indian Journal of Pharmacology, 40(4), 147-151. doi: 10.4103/0253-7613.43160

Somani, C., Naharwal, P., Khan, M. F., Maurya, V. K., Ansari, W. A., Ali, M. B., & Yadav, D. K. (2025). Zinc oxide nanoparticles (ZnONPs) from Manilkara hexandra leaves: biogenic synthesis, GC–MS analysis and antibacterial activity. Discover Chemistry, 2(1), 179.

Sood, R. F., & Gibran, N. S. (2020). Mechanisms of burn injury. Oxford Textbook of Plastic and Reconstructive Surgery, 129.

Sriwidodo, S., Suhandi, C., Wilar, G., & Wathoni, N. (2025). Bee venom in pharmacology: mechanistic insights from pro-inflammatory trigger to anti-inflammatory therapeutic agent. Biomedicine & Pharmacotherapy, 192, 118636.

Stela, M., Cichoń, N., Spławska, A., Szyposzyńska, M., & Bijak, M. (2024). Therapeutic potential and mechanisms of bee venom therapy: A comprehensive review of apitoxin applications and safety enhancement strategies. Pharmaceuticals, 17(9), 1211.

Strudwick, X.L.; Cowin, A.J. The Role of the Inflammatory Response in Burn Injury; IntechOpen: London, UK, 2017; ISBN 978-1-78923-131-1

Suparno, O., & Prasetyo, N. (2019). Isolation of collagen from chicken feet with hydro-extraction method and its physico-chemical characterisation. Paper presented at the IOP Conference Series: Earth and Environmental Science.

Supriya, Y., Jamparapu, P. R., Komera, S., Saravanan, S., Balakrishnan, P., & Sivamalar, S. (2025). Biomedical Applications of Bee Venom: A Natural Approach to Cancer, Infections, and Inflammatory Diseases. Journal of Pure & Applied Microbiology, 19(3).

Swain, M., Mishra, D., & Sahoo, G. (2025). A review on green synthesis of ZnO nanoparticles. Discover Applied Sciences, 7(9), 997.

Swain, S. K., Biswal, A., Patra, S., & Sahu, K. M. (2025). Carbon-based nanomaterials: an overview. Carbon Based Nanomaterials for Drug Delivery, 1-37.

Szczyglewska, P., Feliczak-Guzik, A., & Nowak, I. (2023). Nanotechnology–general aspects: A chemical reduction approach to the synthesis of nanoparticles. Molecules, 28(13), 4932.

T

Takahashi, A. (2024). Zinc supplementation enhances the hematopoietic activity of erythropoiesis-stimulating agents but not hypoxia-inducible factor–prolyl hydroxylase inhibitors. Nutrients, 16(4), 520.

Talamonti, M., Galluzzo, M., Silvaggio, D., Lombardo, P., Tartaglia, C., & Bianchi, L. (2021). Quality of life and psychological impact in patients with atopic dermatitis. Journal of clinical medicine, 10(6), 1298.

Tanuğur-Samanc, A. E., & Kekeçoğlu, M. (2021). An evaluation of the chemical content and microbiological contamination of Anatolian bee venom. PLoS One, 16(7), e0255161.

Tayyar, R., & Ho, D. (2023). Herpes simplex virus and varicella zoster virus infections in cancer patients. Viruses, 15(2), 439.

Thomas, R. E., & Thomas, B. C. (2021). Reducing biofilm infections in burn patients' wounds and biofilms on surfaces in hospitals, medical facilities and medical equipment to improve burn care: a systematic review. International journal of environmental research and public health, 18(24), 13195.

Tiwari, A. K., Jha, S., Tripathi, S. K., Shukla, R., Awasthi, R. R., Bhardwaj, A. K., ... & Dikshit, A. (2024). Spectroscopic investigations of green synthesized zinc oxide nanoparticles (ZnO NPs): antioxidant and antibacterial activity. Discover Applied Sciences, 6, 399.

Tiwari, H., Rai, N., Singh, S., Gupta, P., Verma, A., Singh, A. K., Kajal, P., Salvi, P., Singh, S. K., & Gautam, V. (2023). Recent Advances in Nanomaterials-Based Targeted Drug Delivery for Preclinical Cancer Diagnosis and Therapeutics. Pharmaceutics / Nanomedicine-focused journal (exact journal details may vary by database listing).

Tramontana M, Hansel K, Bianchi L, Sensini C, Malatesta N and Stingeni L (2023) Advancing the understanding of allergic contact dermatitis: from pathophysiology to novel therapeutic approaches. Front. Med. 10:1184289. doi: 10.3389/fmed.2023.1184289

Tusiimire, J. (2016). A study of the biological activity of bee venom and its fractions with regard to cosmetic science and immunology.

U

Uğurlu, E., Duysak, Ö., Sayın, S., Saygılı, E. İ., & Benlier, N. (2023). Isolation and Characterization of Collagen from the Invasive Sea Urchin (Diadema setosum L., 1778) in North-Eastern Mediterranean Sea, Türkiye. Kahramanmaraş Sütçü İmam Üniversitesi Tarım ve Doğa Dergisi, 26(6), 1377-1386.

Ullah, A., Aldakheel, F. M., Anjum, S. I., Raza, G., Khan, S. A., & Tlak Gajger, I. (2023). Pharmacological properties and therapeutic potential of honey bee venom. Saudi Pharmaceutical Journal, 31(1), 96–109.

V

Valadi, M., Doostan, M., Khoshnevisan, K., Doostan, M., & Maleki, H. (2024). Enhanced healing of burn wounds by multifunctional alginate-chitosan hydrogel enclosing silymarin and zinc oxide nanoparticles. Burns, 50, 2029-2044.

Vijayakumar, S., & Vaseeharan, B. (2018). Antibiofilm, anti cancer and ecotoxicity properties of collagen based ZnO nanoparticles. Advanced Powder Technology, 29(10), 2331-2345.

Voudoukis, E., Karmiris, K., & Koutroubakis, I. E. (2014). Multipotent role of platelets in inflammatory bowel diseases: a clinical approach. World Journal of Gastroenterology: WJG, 20(12), 3180. doi: 10.3748/wjg.v20.i12.3180

W

Wang, R., Li, S., Jia, H., Si, X., Lei, Y., Lyu, J., Dai, Z., & Wu, Z. (2021). Protective effects 5 of cinnamaldehyde on the inflammatory response, oxidative stress, and apoptosis in liver of salmonella typhimurium-Challenged mice. Molecules/Molecules Annual, 26, 2309.

Warby, R., & Maani, C. V. (2023). Burn classification. In StatPearls. StatPearls Publishing.

Wary, R. R., Baglari, S., Brahma, D., Gautam, U. K., Kalita, P., & Baruah, M. B. (2022). Synthesis, characterization, and photocatalytic activity of ZnO nanoparticles using water extract of waste coconut husk. Environmental Science and Pollution Research, 29(28), 42837-42848.

Weckbecker, G., & Cory, J. G. (1988). Ribonucleotide reductase activity and growth of glutathione-depleted mouse leukemia L1210 cells *in vitro*. Cancer letters, 40(3), 257-264. doi: 10.1016/0304-3835(88)90084-5

Wehbe, R., Frangieh, J., Rima, M., El Obeid, D., Sabatier, J. M., & Fajloun, Z. (2019). Bee venom: Overview of main compounds and bioactivities for therapeutic interests. Molecules, 24(16), 2997.

Weng, T., Wu, P., Zhang, W., Zheng, Y., Li, Q., Jin, R., Chen, H., You, C., Guo, S., Han, C., & Wang, X. (2020). Regeneration of skin appendages and nerves: Current status and further challenges. Journal of Translational Medicine, 18, 53.

Williams, F. N., Herndon, D. N., & Jeschke, M. G. (2009). The hypermetabolic response to burn injury and interventions to modify this response. Clinics in Plastic Surgery, 36(4), 583–596.

Wright, J. A., Richards, T., & Srai, S. K. S. (2014). The role of iron in the skin and cutaneous wound healing. Frontiers in Pharmacology, 5, 156.

Wu, G. (2017). The mechanisms of rubber abrasion (Doctoral dissertation, Queen Mary University of London).

X

Xu, Y. (2018). A DIGESTIVE PHOSPHOLIPASE A2 IN MIDGUTS OF WORKER HONEY BEES, APIS MELLIFERA: SIGNIFICANCE IN LIPID NUTRITION AND HEALTH (Doctoral dissertation, University of Missouri-Columbia).

Y

Yagi, K. (1976). A simple fluorometric assay for lipoperoxide in blood plasma. Biochemical medicine, 15(2), 212-216. doi: 10.1016/0006-2944(76)90049-1

Yang, Q., Guo, J., Long, X., Pan, C., Liu, G., & Peng, J. (2023). Green synthesis of silver nanoparticles using Jasminum nudiflorum flower extract and their antifungal and antioxidant activity. Nanomaterials, 13(18), 2558.

Ying, S., Guan, Z., Ofoegbu, P. C., Clubb, P., Rico, C., He, F., et al. (2022). Green synthesis of nanoparticles: Current developments and limitations. Environmental Technology & Innovation, 26, 102336

Yousefpoor, Y., Osanloo, M., Mirzaei-Parsa, M. J., Najafabadi, M. R. H., Hashemi, S. M., & Abbasifard, M. (2022). Subcutaneous Injection of Bee Venom in Wistar Rats: effects on blood cells and biochemical parameters. Journal of pharmacopuncture, 25(3), 250.

Youssef, F. S., Ismail, S. H., Fouad, O. A., & Mohamed, G. G. (2024). Green synthesis and biomedical applications of zinc oxide nanoparticles: A review. Journal of the Egyptian Veterinary Medical Association.

Z

Zahra, Z., Habib, Z., Chung, S., and Badshah, M. A. (2020). Exposure route of TiO2 NPs from industrial applications to wastewater treatment and their impacts on the agro-environment. Nanomaterials 10:1469. doi: 10.3390/nano10081469

Zeghoud, S., Hemmami, H., Seghir, B. B., Amor, I. B., Kouadri, I., Rebiai, A., ... & Simal-Gandara, J. (2022). A review on biogenic green synthesis of ZnO nanoparticles by plant biomass and their applications. Materials Today Communications, 33, 104747.

Zemaitis, M. R., Guirguis, M., & Cindass, R. (2025). Electrical injuries. In StatPearls [Internet]. StatPearls Publishing.

Zhang, J., Yu, H., Man, M. Q., & Hu, L. (2024). Aging in the dermis: Fibroblast senescence and its significance. Aging cell, 23(2), e14054.

Żwierełło, W., Piorun, K., Skórka-Majewicz, M., Maruszewska, A., Antoniewski, J., & Gutowska, I. (2023). Burns: classification, pathophysiology, and treatment: a review. International journal of molecular sciences, 24(4), 3749.

Annex

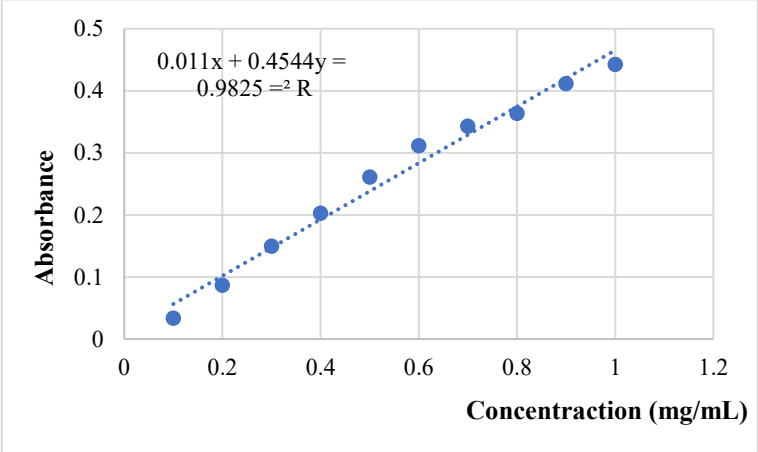

Annex 1: BSA calibration curve for protein determination

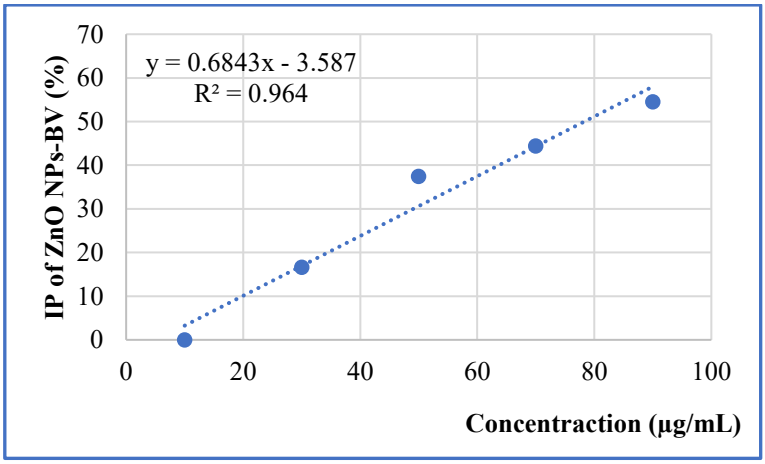

Annex 2: IP of denaturation of protein test in different concentrations of ZnO NPs-BV

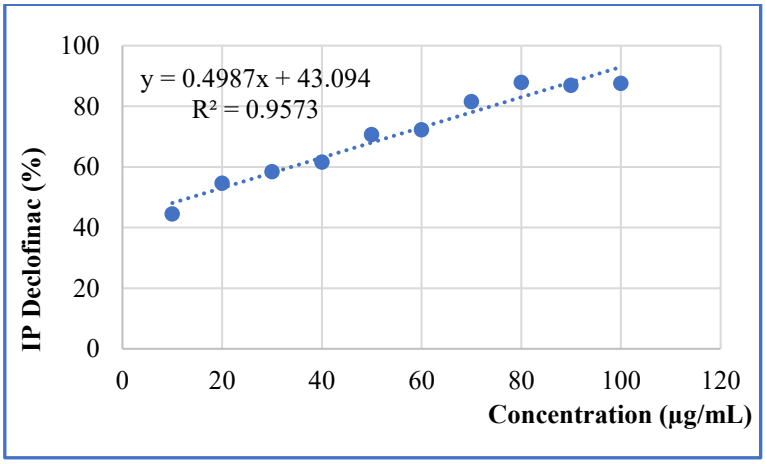

Annex 3: IP of denaturation of protein test in different concentrations of diclofenac®

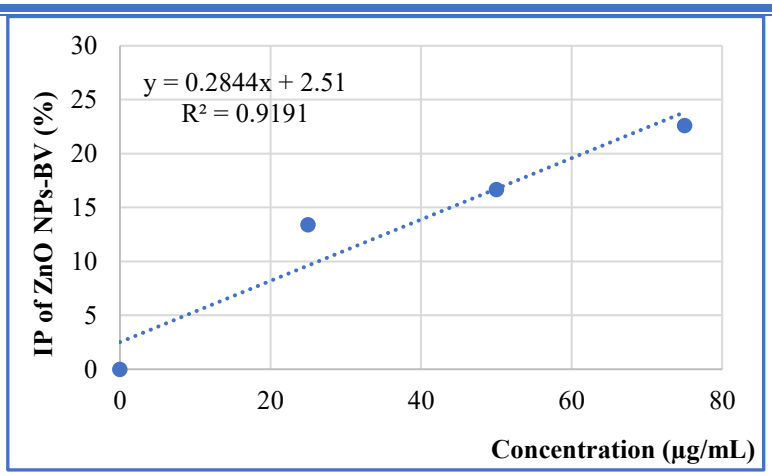

Annex 4: IP of hemolysis assay in different concentrations of ZnO NPs-BV

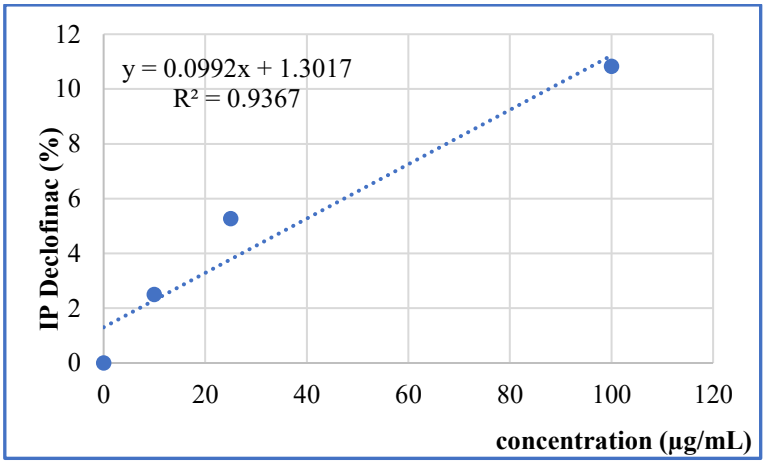

Annex 5: IP of hemolysis assay in different concentrations of Diclofenac®

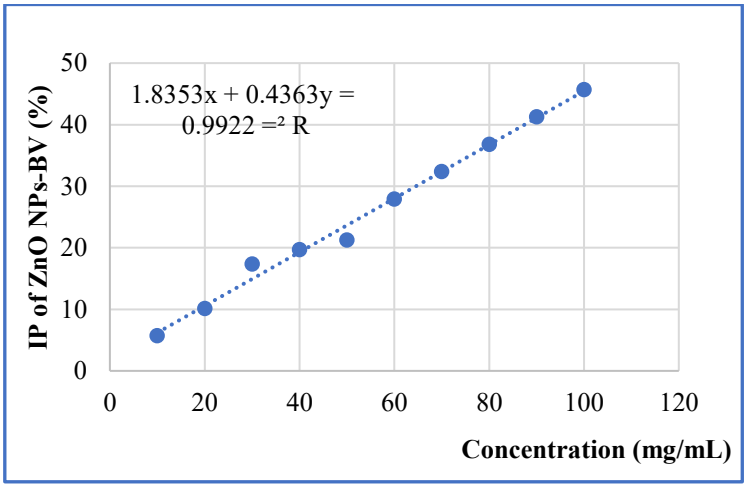

Annex 6: IP of DPPH test in different concentration of ZnO NPs-BV

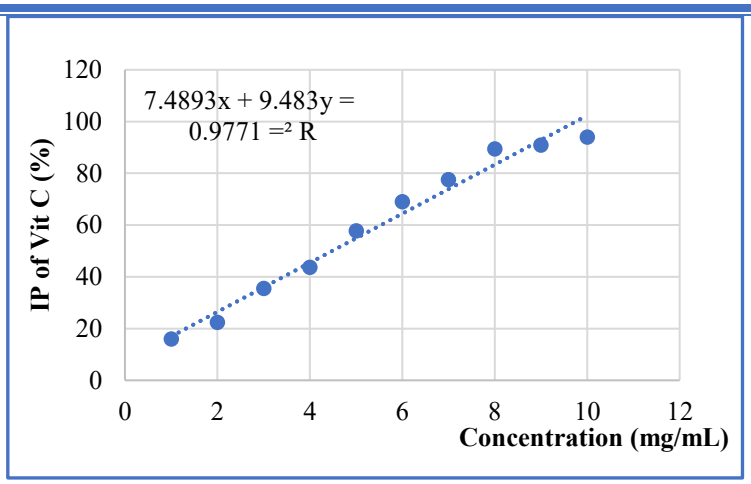

Annex 7: IP of DPPH test in different concentration of Vit C

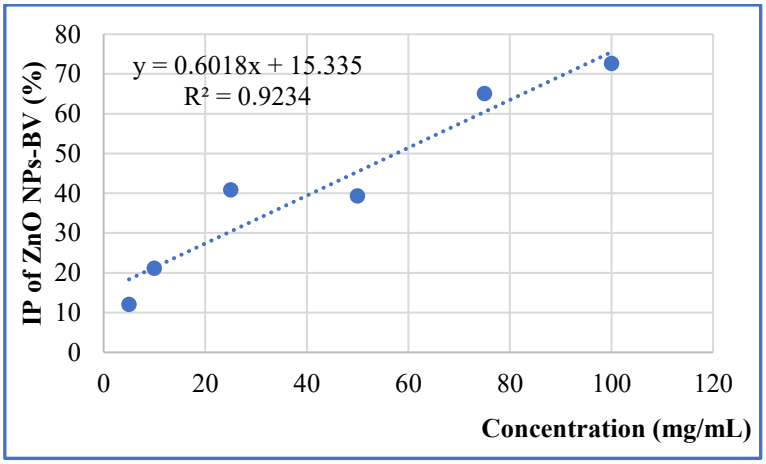

Annex 8: IP of FRAP test in different concentration of ZnO NPs-BV

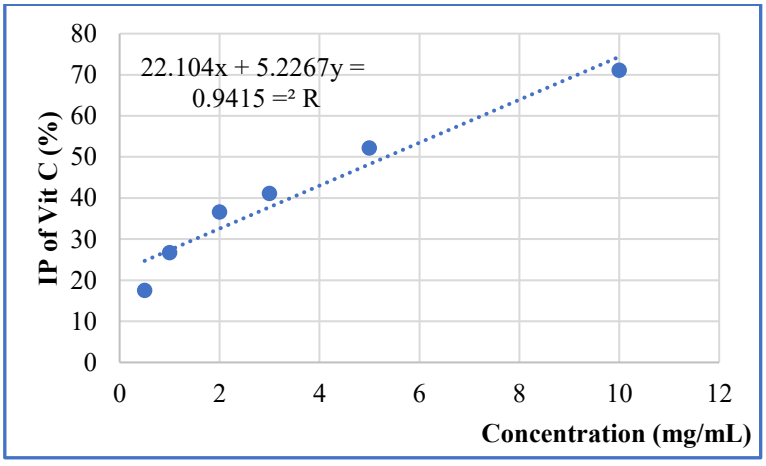

Annex 9: IP of FRAP test in different concentration of Vit C

Annex 10: A real image showing the burning tool used

Annex 11: A real image showing the experimental conditions and the burning of the rats

Annex 12: A real picture of a mouse after shaving